79N21334
19790013163

NASA
CR
159523-
v.1

NASA CONTRACTOR REPORT NASA CR-159523

(NASA-CR-159523-Vol-1) LASER POWER CONVERSION SYSTEM ANALYSIS, VOLUME 1 Final Report, 26 Sep. 1977 - 26 Sep. 1978 (Lockheed Missiles and Space Co.) 109 p HC A06/MF A01 CSCL 20E G3/36

N79-21334

Unclas
14738

LOAN COPY: RETURN TO
AFWL TECHNICAL LIBRARY
KIRTLAND AFB, N.M.

FINAL REPORT

LASER POWER CONVERSION SYSTEM ANALYSIS

VOL. I

RECEIVED
NASA STI FACILITY
ACCESS DEPT.

PREPARED UNDER CONTRACT NO. NAS3-21137
BY
LOCKHEED MISSILES & SPACE COMPANY, INC.
LOCKHEED PALO ALTO RESEARCH LABORATORY
PALO ALTO, CALIFORNIA 94304
FOR
NASA-LEWIS RESEARCH CENTER
CLEVELAND, OHIO

SEPTEMBER 1978

18 FEB 1981
Technical Library
AF Weapons
Laboratory

"Page missing from available version"

page III

ILLUSTRATIONS

Figure		Page
1	Mission model orbits	15
2	GEO satellite deployment	16
3	Space processing encounters and ranges (10 days)	18
4	Space processing encounters and range (5 days)	19
5	Space processing encounters and ranges (3 hr)	20
6	Minimum space processing encounter	21
7	Ground sites for laser transmitters	22
8	Comparison of relays in equatorial and elliptical orbits	24
9	Viewing opportunities for 8-hr orbits (4 relays)	26
10	Viewing opportunities for 6-hr orbits (5 relays)	27
11	Viewing opportunities for 4-hr orbits (8 relays)	29
12	Viewing opportunities for 3-hr orbits (12 relays)	30
13	Variation of 1-σ beam radius with number of actuators	31
14	Turbulent beam spread variation	32
15	Total beam spread variation	34
16	Range from relay to satellite	35
17	Variation of receiver optics with transmitter	37
18	Receiver/transmitter variation for candidate relay deployments	38
19	Four-relay network with Hawaii viewing (300 nmi, 0°)	39
20	Four-relay network with Hawaii viewing (300 nmi, 180°)	40
21	Four-relay network with Hawaii viewing (300 nmi, 270°)	41
22	Four-relay network with Hawaii viewing (8000 nmi, 0°)	43
23	Four-relay network with Hawaii viewing (8000 nmi, 180°)	44
24	Four-relay network with Hawaii viewing (800 nmi, 270°)	45
25	Effect of wavelength on spot diameter	46
26	Beam profiles at receiver	47

PRECEDING PAGE BLANK NOT FILMED

Figure		Page
27	Receiver efficiencies	48
28	Photovoltaic receiver and thermal control	54
29	TELEC device concept and typical weights	55
30	Converter input power requirements (Ref. 1-4)	57
31	Converter efficiency as a function of current density and barrier index (Ref. 1-4)	57
32	Effect of molecular weight on heat exchanger size	59
33	1.3 kW_e Brayton cycle schematic	60
34	Brayton cycle turbomachinery predicted efficiencies	61
35	Brayton cycle efficiency	63
36	Brayton power system specific mass	64
37	Rankine cycle power systems	67
38	20 kW_e Rankine cycle power system	68
39	Dynamic power cycle efficiency comparison (Ref. 3-1)	69
40	Overall efficiency comparison of power cycle concepts (Ref. 1-29)	70
41	Comparison of maximum work Diesel, Otto, and Brayton cycles with GP and Stirling cycles (minimum and maximum temperatures and minimum pressure held constant)	71
42	Energy exchanger/Brayton cycle power system	73
43	NiCd cell weight	76
44	Feasible storage cells	77
45	Temperature effect to cycle life	78
46	Nickel-cadmium battery optimization	79
47	Flywheel summary	81
48	Heat storage receivers	82
49	Photovoltaic (receiver-converter)/batteries	85
50	Telescope/TELEC/batteries	86
51	Topping: thermionic/batteries/bottoming: Brayton/generator	89
52	TELEC/batteries/bottoming: Brayton/generator	90
53	Receiver (heat storage)/Brayton/supply	91
54	Receiver (heat storage)/energy exchanger/Brayton/supply	93
55	Solar array weights	96

Preceding Page Blank

TABLES

Table		Page
I	Laser Power Conversion Mission Model (1995–2005)	5
II	System Efficiencies and Power Requirements	8
III	Relay Receiver Aperture Requirements	33
IV	Power Conversion Device Summary	50
V	Matrix of Potential Power Conversion Subsystems	51
VI	Brayton Power Systems	58
VII	Rankine Cycle Power Systems	66
VIII	High Efficiency Energy Exchanger/Brayton Cycle Subsystem Mass (kg)	74
IX	Real-Time Conversion to Electrical or Mechanical Energy	83
X	Real-Time Conversion to Electrical Energy Plus Bottoming Cycle With Delayed Conversion	87
XI	Energy Storage With Delayed Conversion	91
XII	Summary of Power Conversion System Evaluations	94
XIII	LPCS – Conventional Power Spacecraft (FY '77$)	95
XIV	Typical Missions	98
XV	Power Requirements – All Missions	99
XVI	Power Requirements: Missions Under 50 kW_e	99

Section 1

SUMMARY

The Laser Power Conversion Systems Analysis, Contract NAS 3-21137, is reported in two volumes. Volume I describes the analysis for orbit-to-orbit laser energy transfer and conversion to electrical energy for spacecraft use, and Volume II describes the analysis for orbit-to-ground laser energy transfer and conversion to electrical energy for consumer use on earth.

1.1 OBJECTIVES

The objectives of the orbit-to-orbit Laser Power Conversion System analysis are to identify potential missions, establish efficient system concepts, and compare the cost effectiveness of the laser concepts with conventional spacecraft electrical power subsystems.

The objectives of the orbit-to-ground Laser Power Conversion System Analysis are to develop Space Laser Power Systems to convert solar energy to laser energy, transfer the laser energy to ground sites for conversion to electrical energy, and compare the cost effectiveness of the Space Laser Power System with the Solar Power Satellite.

1.2 STUDY SCOPE

The orbit-to-orbit Laser Power Conversion Systems Analysis investigated the feasibility and utility of using remote lasers to supply electrical power to spacecraft for a variety of missions with electrical power requirements ranging from 1 to 300 kW.

The orbit-to-ground Laser Power Conversion System Analysis investigated the feasibility and cost effectiveness of converting solar energy into laser energy in space and transmitting the laser energy to earth for conversion into electrical energy with electrical power requirements on earth ranging from 100 to 10,000 MW.

1.3 STUDY RESULTS

The orbit-to-orbit Laser Power Conversion System Analysis (Vol. 1) showed that the laser system would not be competitive with current systems from either weight, cost, or development risk standpoints

The orbit-to-ground Laser Power Conversion System Analysis (Vol. 2) shows the laser system to be a viable alternate to the microwave Solar Power Satellite which can

compete economically without excessively large requirements for funding proof-of-concept. A few comparisons of interest include:

	Laser	Microwave
• Transmitter Diameter (m)	31.5	1000
• Ground Receiver Diameter (m)	31.5	~8000
• Land Requirements (Acres)	200	85,000
• Major Operational Orbit	LEO	GEO
• Development and Verification Program Cost Estimate ($B)	0.857*	46.5**

*Scaled verification from LEO with shuttle transportation.

**Boeing, Space Based Power Conversion System, NAS 8-31628, Dec 1976. This estimate includes development of HLLV, OTVs, Space Stations, etc., that are required for Verification Program.

1.4 CONCLUSIONS

- The orbit-to-orbit Laser Power Conversion System for supplying electrical power to satellites is not competitive with current spacecraft electrical power subsystems from either economic or technology standpoints.

- Orbit-to-ground Laser Power Conversion Systems are competitive with the microwave Solar Power Satellite and offer the potential of substantial cost reductions as well as a much lower "front-end" cost for proof-of-concept.

- The orbit-to-ground Laser Power Conversion Systems are worthy of much more in-depth study and optimization than were provided in this study with limited funds and schedule.

Section 2
INTRODUCTION

2.1 BACKGROUND

Recent advances in critical technologies such as lasers, large adaptive optics, pointing and tracking, photovoltaics and other energy conversion devices have opened possibilities for many laser applications in the near future. Laser energy transfer for orbit-to-orbit propulsion has been shown to have substantial potential in the Laser Rocket Systems Analysis, Contract NAS 3-20372. Laser powered rockets are more cost effective than conventional LO_2-LH_2 propulsion systems by factors ranging from 2 to 8, depending upon the mission model upon which the comparison is based. Laser applications that have been investigated in various depths range from surgical and industrial uses with miniscule power requirements to multimegawatt devices for laser-powered aircraft and rockets as well as military applications. To date, applications have been investigated on their individual feasibility and merit without consideration of the synergistic effect of multiple applications. However, it seems clear that the development of any high-energy laser (HEL) application will enhance the feasibility and merit of all other HEL applications.

2.2 STUDY DESCRIPTION

The objectives of the orbit-to-orbit Laser Power Conversion Systems Analysis are to identify promising missions and synthesize efficient systems for transmitting and converting laser-beamed energy to electrical power for satellite use, then compare the laser system(s) to conventional spacecraft electrical power subsystems relative to technology requirements, development risks, and cost. The laser systems are investigated for both space and ground locations for the transmitter.

2.2.1 Task I: Mission Model Definition

Since the beginning of the space era, a large number of experts have considered the questions surrounding electrical power in space. Satellite electrical power requirements have increased by an order of magnitude for each 5 years over the past 15 years. The accomplishment of providing satisfactory power levels for over 600 civilian and military space missions has been substantial. In general, besides the increase in power requirements, lifetimes have increased markedly and the current space undertakings, with reduced budgets, have generated a definite emphasis on low costs.

The mission model developed for this study is based on the 1995 to 2005 time frame as a reasonable period for introduction of space laser power conversion technology. Current NASA and DOD projections were surveyed to determine the power needs and orbital parameter of future spacecraft. The orbital parameters are essential so that

opportunities of energy transfer can be determined. The baseline mission model is categorized by orbit groupings with military missions included, but not identified. Communications compose the bulk of the geosynchronous category followed by earth observation and weather satellites. All satellites are considered to be improved versions of present satellites. The low earth orbit category includes a larger percentage of missions which are still in the development stage. The most demanding in terms of electrical power requirements is the weather modification mission.

Table I represents the baseline mission model which is made to be flexible by the use of activity level multipliers. The activity multipliers permit increasing, decreasing, or zeroing out specific missions so that system sensitivity can be determined.

2.2.2 Tasks II and V: Parametric Analysis: Space-Based and Ground Based Lasers

The purpose of the parametric analysis is to synthesize system concepts and evaluate the effectiveness and sensitivities of the various subsystems relative to their interactions with one another and overall system effect. From these data, an optimum system concept can be synthesized using the most advantageous subsystems for comparison with current conventional systems which supply electrical power to satellites.

Transmission Opportunities

Energy transmission opportunities is a function of the laser basing parameters and can vary from normal phasing contacts with line-of-sight between a laser transmitter and the receiving satellite to a continuous opportunity through the use of orbital relay satellites deployed to provide a continuous path between laser transmitter(s) and the receiving satellites.

Space-Based Laser Transmitter Deployment

Various orbital parameters (altitudes, inclinations, and ellipticities) were investigated to optimize encounters relative to time in sight, time between encounters, and encounter ranges. The encounter ranges are important to select applicable laser wavelength, determine pointing and tracking requirements, and to size the transmitter aperture and satellite receiver. The selected orbital parameters for the space-based laser are a sun-synchronous, circular orbit with an altitude of 6,396 km (3,460 nmi) which produces a 4-hr orbit period. This provided acceptable encounter parameters for the LEO satellites with ranges permitting laser wavelengths up to 5.0 μm with reasonable pointing and tracking and receiver sizes. Shorter wavelengths would permit a relaxation of pointing and tracking requirements and/or reduction of transmitter and/or receiver sizes.

Ground-Based Laser Transmitter Deployment

An analysis was made of weather conditions, elevations, and locations of laser transmitter sights to assure a probability of one clear sight being greater than 99%. The 99% probability is required to assure that the electrical energy could be transferred

TABLE I. LASER POWER CONVERSION MISSION MODEL (1995–2005)

MISSIONS	SPACECRAFT WEIGHT* (kg)	ORBIT	NO. OPERATIONAL AT ANY TIME DURING 10-YR. PERIOD	kW POWER	EXPECTED VALUE	ACTIVITY LEVEL MULTIPLIERS		
						CASE 1 (NOM.)	2 (HIGH)	3 (LOW)
GEOSYNCHRONOUS (MILITARY INCLUDED)								
SYN. EQUATORIAL								
• ORBITAL ANTENNA FARMS (UP TO 8-COMMUNICATIONS SATELLITES PER FARM)	6,000	90°W, 0°, 90°E, 180°W, 100W	15	20-50	(35)	1	2	1
• PERSONNEL COMMUNICATIONS	7,300	90°W	2	21		1	1	1
• TV BROADCAST	6,500	85 & 105°W	2	130		1	3	2
• DIPLOMATIC HOT LINE	1,350	90°W, 0°, 90°E, 180°W, 100°W	5	1		1	1	1
• EARTH OBSERVATION/WEATHER	1,000-10,000	90°W, 0°, 90°E, 180°W, 100°W	10	2		1	0	1
• ELECTRONIC MAIL	9,000	85°, 105°W	2	15		1	4	0
• COASTAL ANTICOLLISION PASSIVE RADAR	90,000	75°W, 120°W	2	300		1	2	0
• ASTRONOMY	4,500	155°	2	5-20	(15)	1	0	1
• ENERGY MONITOR		90°W	1	22		1	0	0
LOW EARTH ORBIT (MILITARY INCLUDED)								
100-600 NMI								
• SPACE PROCESSING		300 NMI, 28.5° INCL.	5	3-90	(35)	1	2	1
• ATMOSPHERIC TEMP. PROFILE SOUNDER	1,800	600 NMI POLAR	4	4		1	0	0
• SOLAR OBSERVATORY WEATHER MODIF. & EXPERIMENTATION		300 NMI, 55°	2	10-1000	(50)	1	2	0
• EARTH OBSERVATION SATELLITES	1,500-50,000	200 NMI-POLAR 500 NMI, 99.0°	1 4	5-100 5	(50)	1	2	1
• OCEAN CONDITION & WEATHER SATELLITE	1,500-50,000	500 NMI, 98.0°	4	5		1	2	1
600 NMI								
• TRANSPORTATION SERVICES/NAVIGATION		8,000 NMI POLAR	20-40	6		1	0	1
• WEATHER		700 NMI, 99.9°	5-10	2		1	2	0
PECULAIR MILITARY ORBITS CLASSIFIED	1,000-20,000	ELIPTICAL 287-24,500 NMI 63.5°	15	50-200 (?)		1	2	1

*LOWER WEIGHTS REPRESENT CURRENT OR NEAR TERM SATELLITE DESIGNS

as scheduled avoiding additional energy storage requirements if an opportunity of energy transfer was missed. Five laser transmitter sites (Haleakala, HA; Edwards Air Force Base, CA; Blyth, N.M.; Tucson, AZ; and El Paso, TX) are required and were selected to facilitate deployment of relay satellites to provide continuous coverage of the sites. The relays are deployed in elliptical orbits at 63.4° inclination with the apogee at about 35° north latitude to provide continuous coverage with minimum nadir angles. The ranges are such that only laser wavelengths of about 0.5 μm or less could be selected and maintain acceptable pointing and tracking and receiver parameters.

Geosynchronous Relay Deployment

Relay satellites for both the space-based and ground-based laser transmitters are deployed in a near geosynchronous orbit near groups of satellites at their various locations. This provides a view of the satellites in the area with acceptable ranges and minimizes the number of relays required.

Power Conversion Techniques

Power conversion techniques investigated include photovoltaic; thermionic; brayton, rankine, and piston cycles; thermoelectric energy converter (TELEC); energy exchanger with brayton, rankine, and piston; and MHD as well as combinations to use as much of the rejected energy as possible. Energy storage techniques included batteries, induction, flywheels, and heat with various materials.

Receiver Sizing

Sizing of the receiver on the satellite resulted in basically a function of the space shuttle capability (~4.5m) to carry into orbit without the complications of on-orbit erection or assembly. To add those complications to the mission satellite would unduly penalize satellite design and packaging. The weight of the receiver due to its size is not a significant driver as has been found in other studies. The weight driver for satellite receivers, whether optical or otherwise, are the heat rejection and storage requirements. The most efficient (~ 50%) power conversion has to reject an equal amount of energy which must be reradiated. This requires enormous radiators for real-time rejection or some technique to store the energy and reject it over the period between encounters. With the rejected energy storage and radiators dominating the satellite receiver weight, the size of the receiver made little weight difference.

System Effects

To understand the system effects of satellite laser power conversion systems, basic differences in the operations from current satellite electrical power systems should be reviewed.

Current solar array electrical power systems operate in a 1-sun (~1.4 kW/m^2) environment producing electrical power continuously except when in the earth's shadow (from 0 to ~30% of the time depending upon the orbit parameters). Energy storage on the satellite is limited to the amount needed during shadow periods and to meet peak power

requirements. If a satellite laser power conversion system operated similarly, then the ratio of laser transmitters to satellites would be near unity which obviously is not cost effective. For the cost of a current satellite electrical power subsystem, a new electrical power subsystem to convert laser energy plus a complete satellite to provide energy cannot be accomplished. This represents the upper extreme in the number of laser transmitters required.

The lower extreme is one laser transmitter; however, the basic operating mode must be changed so that the one transmitter is providing power to all satellites which means that much more than 1-sun's intensity is required for a short period and sufficient energy stored until the next line-of-sight encounter. (A major portion of the satellite's life will be operating from onboard stored energy.) In addition, because the energy is being input at high flux densities, the excess energy cannot be reasonably rejected in real time and must be stored for rejection between energy inputs. Another aspect of this situation is that the required laser power has to increase to provide the higher flux densities. Weights for the energy storage subsystem both for satellite use and rejection far exceed the weight of a current satellite solar array electrical power subsystem and makes their use on satellites impractical, particularly when compared to the lightweight solar array systems being used and developed to higher power levels today.

From one extreme to the other in the number of lasers required, substantially more laser energy is required to be generated than the electrical power requirements of all the satellites combined because of the losses due to conversion and transmission efficiencies. Table II illustrates than an electrical power subsystem for a Laser Power Satellite must be more than 12 times as large (3,870 kW versus 300 kW) as one satellite electrical power subsystem it is replacing — not eliminating. The same [illegible] the entire mission model is considered whether the satellites are to be serviced by one or multiple laser power satellites.

As a result of the parametric analysis, laser power conversion systems were determined to be noncost-effective relative to current satellite electrical power subsystems. This determination could be altered by a break-through in energy storage, energy conversion technologies, or by the synergistic effect of lasers being used in other applications. Section 3, TECHNICAL DISCUSSION, documents the analysis used as the criteria for evaluation of laser power conversion systems.

TABLE II. SYSTEM EFFICIENCIES AND POWER REQUIREMENTS

	Efficiency %	Power (kW)	
		In	Out
Solar Collector	85	11,549	9,816
Solar Cavity	83	9,816	8,148
Thermal Conversion	50	8,140	4,074
Power Generator & Conditioning	95	4,074	3,870
Laser	25	3,870	968
Transmitter Optics	99.7	968	965
Space Transmission	95	965	916
Relay	99	916	907
Space Transmission	95	907	862
Satellite Receiver	99.7	862	859
Thermal Cavity	98	859	842
Thermal Conversion	50	842	421
Power Generator & Conditioning	95	421	400
Energy Storage	75	400	300
Power To Satellite		300	

Section 3
TECHNICAL DISCUSSION

3.1 TASK I: MISSION MODEL DEFINITION

3.1.1 Background

The need for quantities of reliable electrical power has been recognized as an essential element in space operations since the early 1950's. Although the specific system characteristics and actual and projected missions have changed since that time, the basic energy sources have remained the same, as have the basic power conversion technologies. However, much effort and many millions of dollars have been expended in developing the science and technologies involved in space electric power systems.

Since the beginning of the space era, a large number of experts have considered the questions surrounding electric power in space. Although the scale and timing of the research and development efforts in space power in the United States have varied with the course of the space program, the accomplishment of providing satisfactory power as required for over 600 civilian and military space missions has been substantial. There has occurred in satellite power levels a 10-fold increase in each 5 year period over the last 15 years. Whether this trend will continue for space missions is of concern. In general, besides the increase in power requirements, lifetimes have increased markedly and the current period of applications in space undertakings, with its reduced budgets, has generated a definite emphasis on low costs.

3.1.2 Objectives

The objective of the mission model for this study is to present a set of missions with their respective electrical power needs and orbits. These two parameters are primary criteria for the design of a space laser power transmitter. The location of each spacecraft and the quantity of electric power needed can be determined from these two parameters.

The other factors about each spacecraft in the mission model which are useful are the spacecraft weight and the pointing accuracy. These two parameters relate to the stationkeeping energy needs of the spacecraft. Additionally, weight saving tradeoffs can be performed utilizing the baseline weights.

With these parameters, alternative laser power transmitter designs can be evaluated to determine if these designs can meet the power demands of the spacecraft in the mission model and make adequate contact with the spacecraft when the two are in view of each other, and within the appropriate distances from each other. Thus the goal of the mission model is to capture the probable power and orbit characteristics of a typical set of spacecraft for the 1995 to 2005 time period.

3.1.3 Assumptions

Numerous assumptions were made in the derivation of this mission model. These assumptions are:

(1) The trend toward larger and more powerful satellites in space with smaller and less expensive ground equipment will continue. Thus, spacecraft will generally be larger and demand larger power supplies.
(2) The majority of spacecraft in orbit in the 1995 to 2005 time frame will be improved versions of current technology. These mature versions of today's satellites will be communications satellites, earth observation satellites, weather satellites, etc.
(3) The minority of spacecraft in orbit in the 1995 to 2005 time frame will be new or innovations in relation to today's inventory. The missions selected are assumed to be representative examples of future possibilities. Mission function, weight, and power needs were used as criteria for selection.
(4) The military missions would be similar in orbit to those of today. Orbits available were utilized as representative of future missions. Weights were assumed to be similar to civilian spacecraft. Military missions were combined with civilian for this study as there was no reason to examine the military power needs separately at this time.
(5) The space shuttle, or an updated version of the space shuttle, will exist for low-cost transportation to low-earth orbit.
(6) The orbits will be very similar to current practices.

3.1.4 Mission Model Development

The time frame of 1995 to 2005 was selected as the reasonable period for introduction of space laser power conversion technology. This time frame is compatible with NASA and DOD future planning time frame enabling utilization of several sources for inputs. However, because of the emergence of the "shuttle era", there is an element of "wait and see" pervading future planning which prevents a specific mission model from emerging from NASA. To adequately handle the uncertainties of the future, a baseline mission model was developed with built-in flexibility provided by activity level multipliers which have the effect of decreasing or increasing various missions. With this capability, numerous scenarios can be evaluated which capture upper and lower bounds of future mission scenarios.

The mission model derived (Table I) provides the orbit, spacecraft weight, and average power demand in kilowatts. The number of spacecraft per mission type is indicated as well as some indication of activity based on the activity level multiplier concept.

Several key NASA and DoD (Aerospace) sources were utilized to derive the Baseline Mission Model for this study. For the purpose of surveying current projections, contact was made with numerous top NASA and Aerospace Corporation officials familiar with power needs of future spacecraft. As a result of these contacts, several key

studies emerged as valuable sources. These studies then served as the backbone of the Mission Model derived. The studies were:

- Advanced Space Systems Concepts and Their Orbital Support Needs (1980–2000) Final Report December 1976, The Aerospace Corporation.
- Summarized NASA Payload Descriptions, George C. Marshall Space Flight Center, July 1974.
- Selected section of early Space Station work submitted to NASA Headquarters by Jerry Craig/Johnson and Bill Huber/Marshall.
- Review of Spacecraft Launches of past 15 years.
- B. I. Edelson and W. L. Morgan, "Orbital Antenna Farms" Astronautics and Aeronautics, September 1977.
- Jerry Grey, "The Outlook for Space Power," Astronautics and Aeronautics October 1976.
- DOD/AEC Space Power Study, March 1974.

3.1.5 Mission Model Spacecraft

Spacecraft weights were derived in two manners. For those missions which are updated versions of current technology, a multiplier was employed to expand the weight. For new missions not present in the current inventory, the documents which put forth the concepts usually listed the expected weight.

Orbits

The spacecraft orbits were derived by studying the orbits utilized over the past 15 years and by technical description of new satellite mission concepts.

Power Demands

Electric power demands were carefully derived by studying historical trends and surveying future projections. In cases where there was a discrepancy, a range was utilized with an expected value following.

Pointing Accuracies

The pointing accuracies play a role in determining onboard energy demands for station-keeping. Since pointing accuracies are typically a funtion of the payload task, present pointing accuracies were considered sufficiently sensitive for this mission model. Numerous documents were examined to obtain the pointing accuracies for the geosynchronous and low earth orbits. These documents are listed below:

- John H. Disher, "Next Steps in Space Transportation and Operations," Astronautics and Aeronautics, January 1978.
- The Aerospace Corporation, A Review of Communications Satellites and Related Spacecraft for Factors Influencing Mission Success, Contract F04701-75-C-0076, prepared for Military Satellite Communications Office of the Defense Comm. Agency, 17 November 1975.

- Rockwell International, Geosynchronous Platform Definition Study, Volume II, prepared for NASA, June 1973.
- Rockwell International, Tracking and Data Relay Satellite System Configuration and Tradeoff Study, Volume I, prepared for Goddard Space Flight Center, NASA, April 1973.
- The Aerospace Corporation, Standardization and Program Effect Analysis, Final Report, Volume II, prepared for Low Cost Systems Office, NASA, 31 July 1975.
- TRW Systems Group, Earth Observatory Satellite System Definition Study, Volume III Design/Cost Tradeoff Studies, prepared for Goddard Space Flight Center, NASA, 1 October 1974.
- The Aerospace Corporation, Description of the Attitude Control Guidance and Navigation Space Replaceable Units for Automated Space Servicing of Selected Missions, prepared for Office of Manned Space Flight, NASA, 5 April 1974.

Activity Level Multipliers

Activity level multipliers permit development of numerous scenarios for systems analysis and design sensitivity studies. Discussed below is the first "cut" at three scenarios. Others will emerge as the study progresses.

Nominal Case

This is the baseline case which includes missions extrapolated from the present, new missions which have a high likelihood of taking place as indicated by intensive studies, and a few concepts which have not yet gone beyond the preliminary stage.

Discussion of Mission Model

Missions are divided into categories by orbit groupings. Those missions falling under geosynchronous orbits are included in the first group. For security reasons, military spacecraft are included with nonmilitary spacecraft missions. This study is concerned primarily with the location of the spacecraft and the power demands so that this format was deemed acceptable. Location of spacecraft is important in this study as the laser power transmitter must be able to locate and track spacecraft for a duration of time when power can be transmitted via laser beam. It is crucial to determine when various spacecraft will be in view of the transmitter, etc.

Geosynchronous Orbit Missions. Communications satellites compose the bulk of the missions in the geosynchronous category. It was assumed that present generation communications satellites would be replaced with newer and more powerful satellites. Many of the communications satellites would make use of the concept of orbital antenna farms which several payloads utilize a common frame and power supply. The power demand was assumed to be more than the sum of eight current satellites to allow for increased capability of each satellite.

The next largest category of geosynchronous missions, the earth observation and weather satellites, are considered to be updated versions of present spacecraft. The

only deviations from communications or observation satellites included in the mission model are the radar and energy monitoring satellites concepts adapted from the Aerospace Advanced Systems report. The Coastal Anti-Collision Passive Radar will have a need for an average of 300 kilowatts of power.

Low Earth Orbit Missions. The Low Earth Orbit category includes a larger percentage of missions which are still in the development stage. The most demanding in terms of power need is the weather modification spacecraft. Continuation of LANDSAT-type satellites is indicated as well as new ventures such as space processing.

Case 2: High Activity Level. By multiplying the most likely candidates by an integer greater than 1, a higher activity level can be obtained. This scenario thus creates a more demanding environment in terms of total energy needs and number of spacecraft requiring power from the laser source. Based on the sources utilized, this scenario projects a larger than anticipated mission model.

Case 3: Low Activity Level. This scenario indicates the low end of the activity scale where many of the less certain missions have been zeroed out. This scenario indicates a small number of spacecraft which might be in orbit during the time frame. This scenario will test the cost-effectiveness of the laser power system at the low-activity end of the spectrum.

3.2 PARAMETRIC ANALYSIS

The purpose of the parametric analysis with space- and ground-based laser transmitter(s) is to synthesize total laser power conversion systems and evaluate the sensitivities to determine acceptable systems. To properly evaluate the feasibility and cost effectiveness of space-to-space laser power conversion systems, it is necessary to investigate the interfaces and interactions of the primary system elements (satellites in the mission model, laser transmitter(s), and laser energy relay units). Each of the primary system elements is a satellite in itself for which the interaction and sensitivity of the major subsystems must be evaluated. In the case of the satellites in the mission model, the primary concern is the spacecraft electrical power subsystem with minor concern for the attitude control subsystem as it may be affected by the change to the laser power conversion subsystem. For comparison in later tasks, it is necessary that the new laser power conversion subsystem be compatible with the spacecraft with respect to weight and volume as well as electrically. Otherwise, a complete new spacecraft design would be necessary and substantial changes in weight and volume could affect launch vehicles and operations far beyond the scope of this study.

The terms "satellite" and "spacecraft" are many times used interchangeably; however, in this report a "satellite" is defined as a complete space vehicle containing a payload to perform mission requirements and a "spacecraft" to support the payload for functions such as guidance and navigation; command, communication, and control; attitude determination and control; and to provide electrical power for both payload and spacecraft functions.

3.2.1 Space Laser Basing and Energy Transfer Opportunities

The purpose of analysing the energy transfer opportunities is to establish the frequency of opportunities, the time period that energy can be transferred (within line-of-sight) and the range over which the energy must be transferred. The frequency of opportunity affects the satellite energy storage subsystems which provide power to the satellites during the periods between transfers and the energy storage and radiators to reject the excess energy that cannot be converted for satellite use. The time period to transfer energy sizes the laser power required and must be within the time available. The range over which energy must be transferred is needed for selection of laser wavelength and for sizing the laser transmitter aperture and the satellite receiver as well as to establish pointing and tracking requirements.

Opportunity to transfer energy is a function of the laser transmitter orbital parameters and the orbital parameters of the satellites in the mission model (Task I). Figure 1 illustrates the mission model orbits that must be considered when establishing the orbital parameters for the laser. Each orbit illustrated must be considered individually and collectively as well as the satellites positions within their orbit and the position of the sun. The sun supplies energy to the laser transmitter; therefore, the laser transmitter must be in the sun as much as possible. The time the laser is in the shadow of the earth is dependent upon the orbital parameters which can range from 0% in the shade (sun synchronous) to about 30% (low altitude in same plane as the sun). A sun-synchronous inclination was selected for the laser transmitter so that laser energy could be provided at any time. A circular orbit of 6396-km (3460-nmi) altitude (4-hr orbit period) was selected to provide the best combination of frequencies of encounter, time in view, and range of energy transmission. This selection was based on the interaction and phasing with all orbits in the baseline mission model.

The laser orbit altitude had little or no effect on the geosynchronous category of missions in the model; however, because of the ranges involved between LEO and GEO orbits, laser energy relay units are deployed so that the receiver on the satellites can be of an acceptable size. Figure 2 depicts the locations and number of satellites in GEO. The solid circles show the selected locations for relay deployment. The view time per orbit for each satellite varies between 88 and 100% depending upon the time of day. The worst viewing conditions are when the GEO satellite is in the plane of the laser orbit, as would be the cases for the satellites located at 0 and 180° in Figure 2. In these cases, the earth will block the view for about 77° of the orbit or about 21% of the time, as depicted in View AA of the figure. Every satellite will encounter the minimum viewing times twice every 24 hr. Other deployments for the relays were investigated but proved to be nonoptimum. For example, a relay in a 18-hr equatorial orbit would have a view time of about 4 hr within a 10,000-km (5405-nmi) range each time it passed a satellite in GEO. However, the contacts would be 72 hr apart and full-time contact between relays and satellites would require 18 relays. Relays in GEO with the same range limitation can reach about 10° on either side so that 6 relays placed in the areas where they are needed can maintain the same full-time contact with all satellites. To avoid the problem of one satellite blocking the view to another satellite, the relays would be placed in a synchronous orbit with about 1 or 2° inclination so that the relay would oscillate north and south of the equatorial plane. With this deployment scheme, a wide latitude of frequencies of encounters can be permitted.

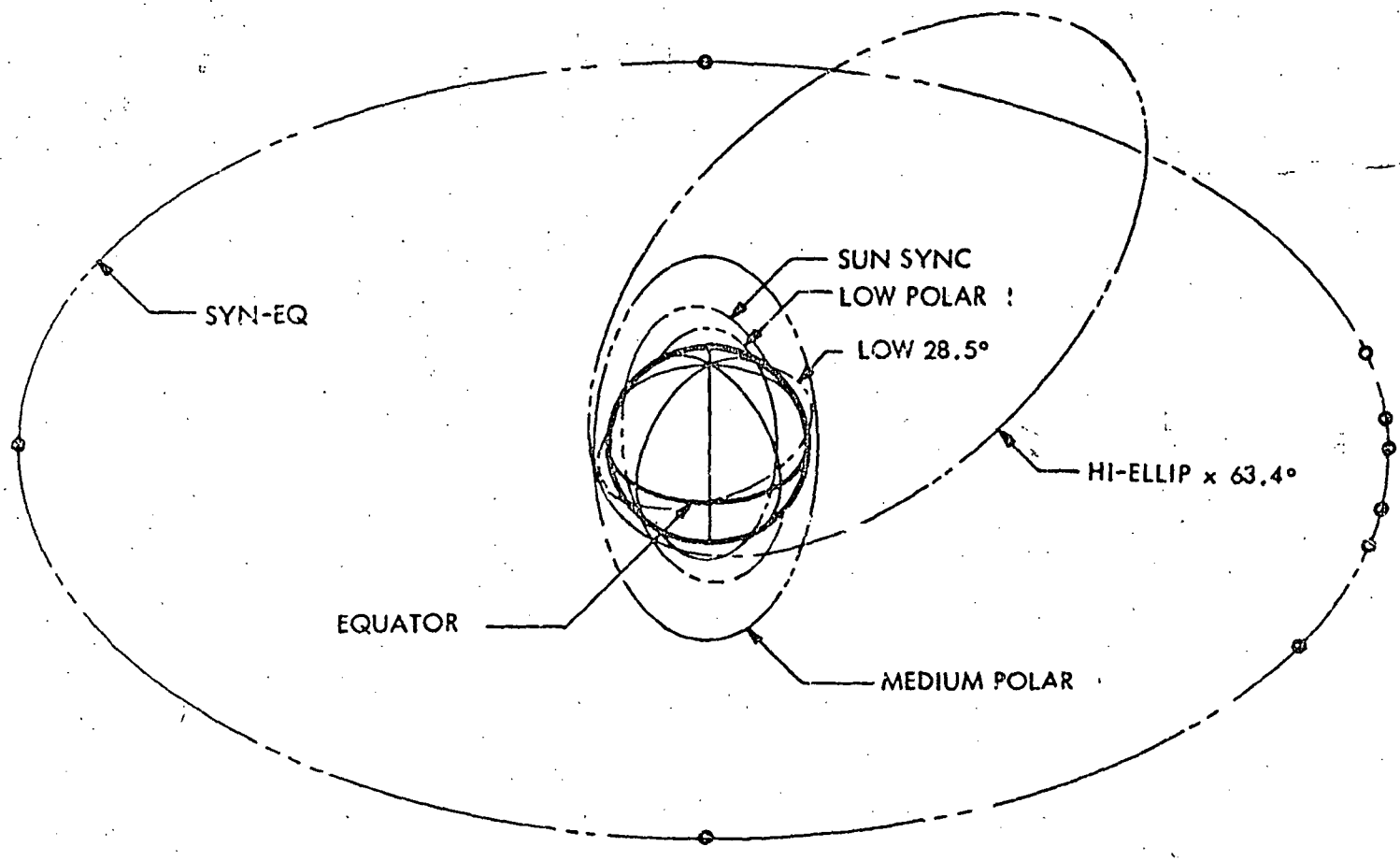

Figure 1. Mission Model Orbits

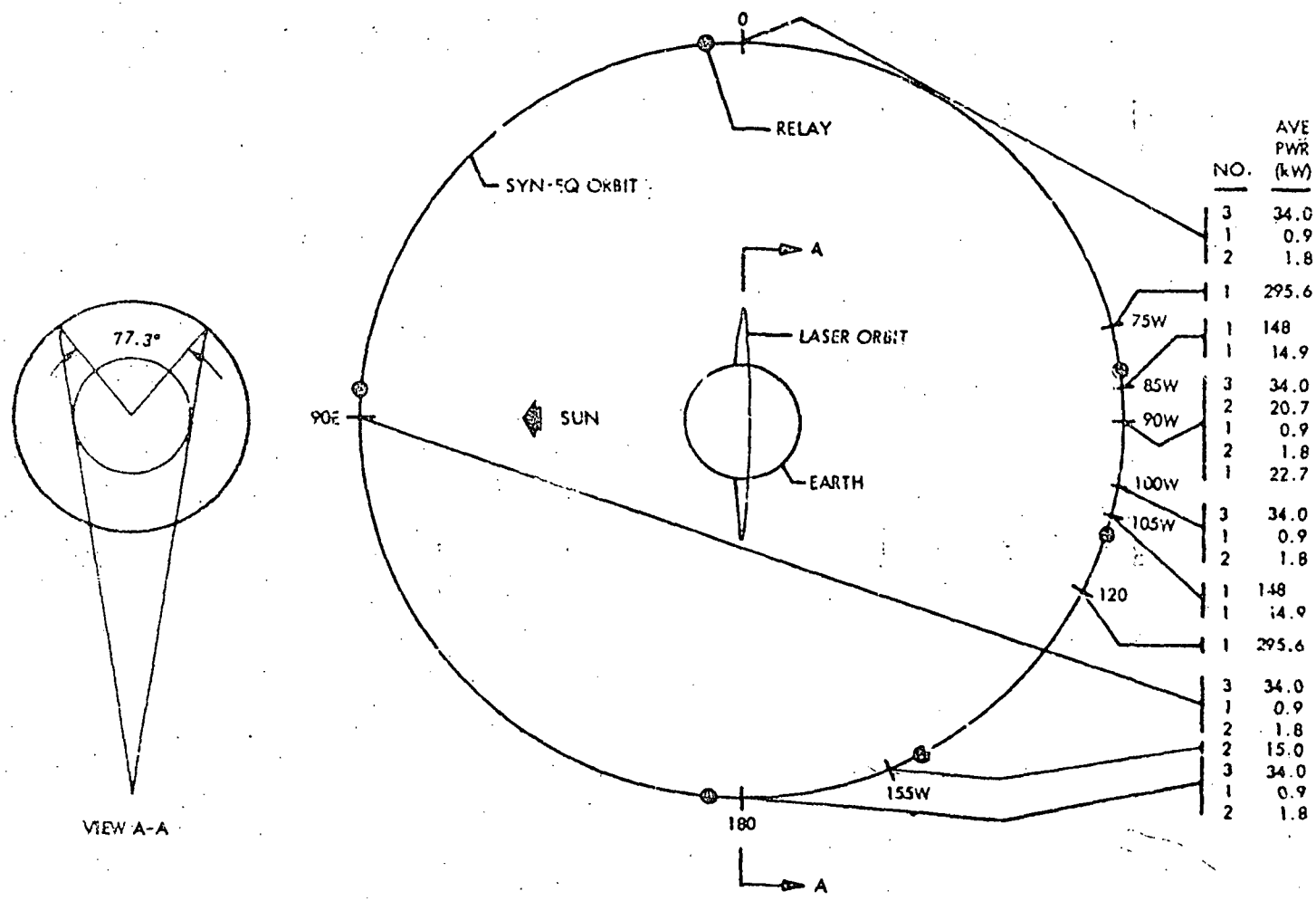

Figure 2. GEO satellite deployment

The satellites of the mission model in low earth orbit present a very different problem in that their orbital periods, altitudes, inclinations, and ellipticity vary from one another. The individual orbital parameters for each mission was examined with respect to the laser in sun-synchronous orbits with periods ranging from 2 to 6 hr. From these data, the 4-hr period for the laser was selected as having the best combination of frequency, time in view, and range. Periods greater than 4 hr produced erratic phasing and frequency of encounter within acceptable ranges for satellites at low altitudes as well as the elliptical orbits. Below 4 hr the same occurred with satellites at the higher altitudes. Generally, if the frequency and range were in acceptable limits, the time in view was also acceptable. The driving mission is the space processing in a 28.5° inclined circular orbit at 555-km (300-nmi) altitude. Figure 3 shows the encounter and ranges over a 10-day period. Examination of the pattern shows that the phasing repeats itself about every 15 days and some of the encounters have ranges that do not get within 10,000 km (5400 nmi). Figure 4 is the same except over a 5-day period and with the phasing changed to begin with the longest range encounter. Figure 5 shows the details of the first encounter of figure 4; however, the encounter time shown is not the minimum encounter time. The minimum encounter time is shown in Figure 6 to be 0.63 hr and occurs as the phasing changes later as may be seen in Figure 3. Similar data were run on the encounter computer program for each mission satellite orbital parameters with variation of the laser power transmitter orbital parameters.

3.2.2 Ground Laser Basing and Energy Transfer Opportunities

This section involves the parametric analysis of the ground-based laser concepts requiring the evaluation of ground site locations, relay orbital parameters and the requirements on the laser transmitters, relays, and power conversion units on mission satellites. The results discussed in this section do not represent a complete analysis in that redirection of the contract eliminated the necessity to complete the analysis.

Ground Transmitter Site Selection

Transmitting a laser beam up through the atmosphere requires that the line-of-sight between laser and relay be free of clouds for transmitting the beam to a satellite at any time. Hence, several ground sites are required such that the probability that all ground stations are simultaneously clouded is extremely remote.

Weather statistics for several locations in the Western United States and Hawaii were used to determine joint probabilities of cloud overcase for the several sites. A minimum of five sites was found to be required to produce a cloud-free line-of-sight probability of 99% from at least one of the five sites at all times. The selected sites are shown in Figure 7 and are located in the Southwest at Edwards AFB, Blythe, Tucson, and El Paso, with an additional site located on the island of Hawaii.

All the candidate sites possess accessible mountains in the near vicinity with elevations of 1,830 m (6000 ft) or more. Hence, they are acceptable for locating a laser transmitter to reduce the detrimental effects of the atmosphere on the propagation of laser beams.

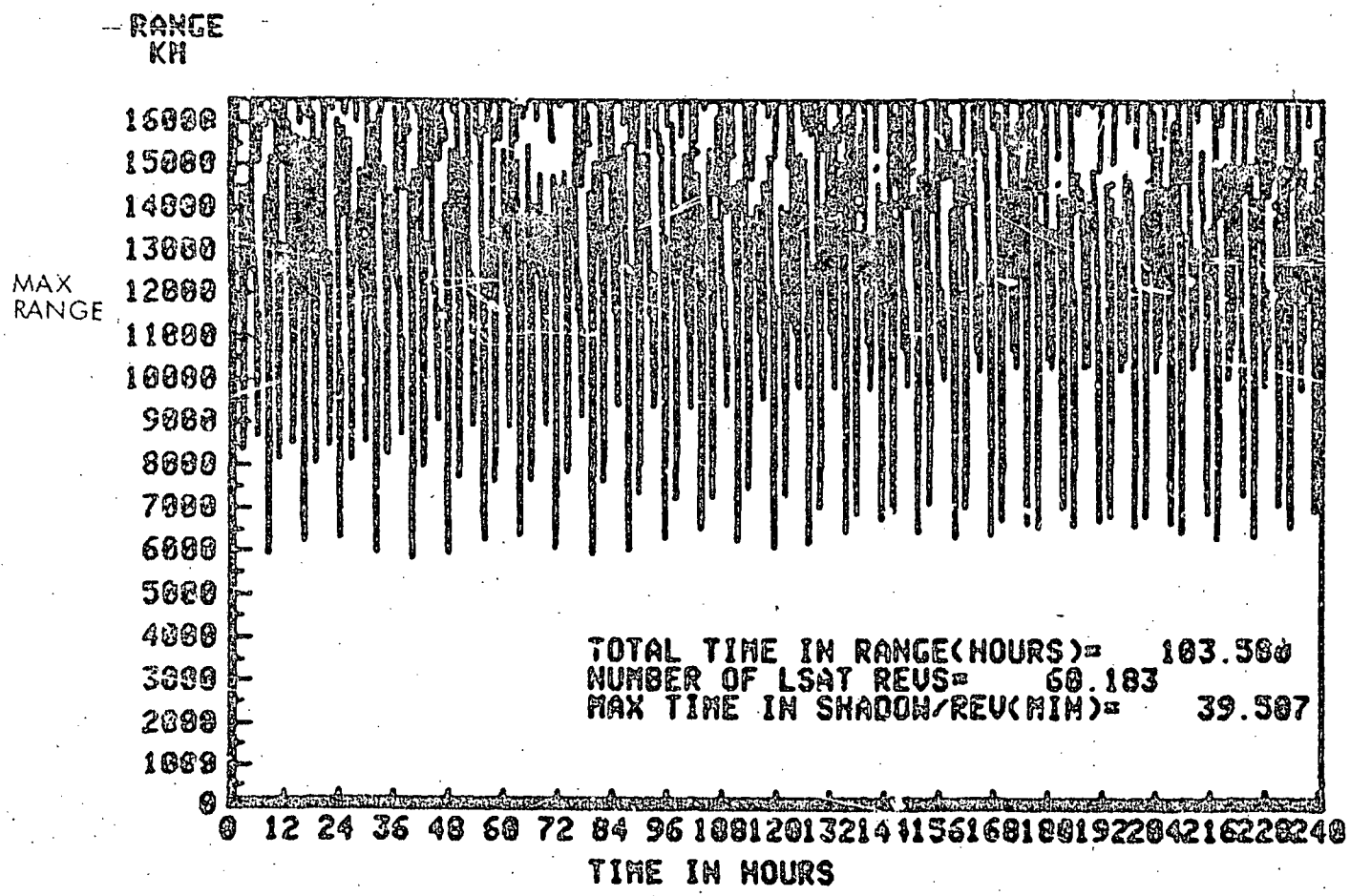

Figure 3. Space processing encounters and ranges (10 days)

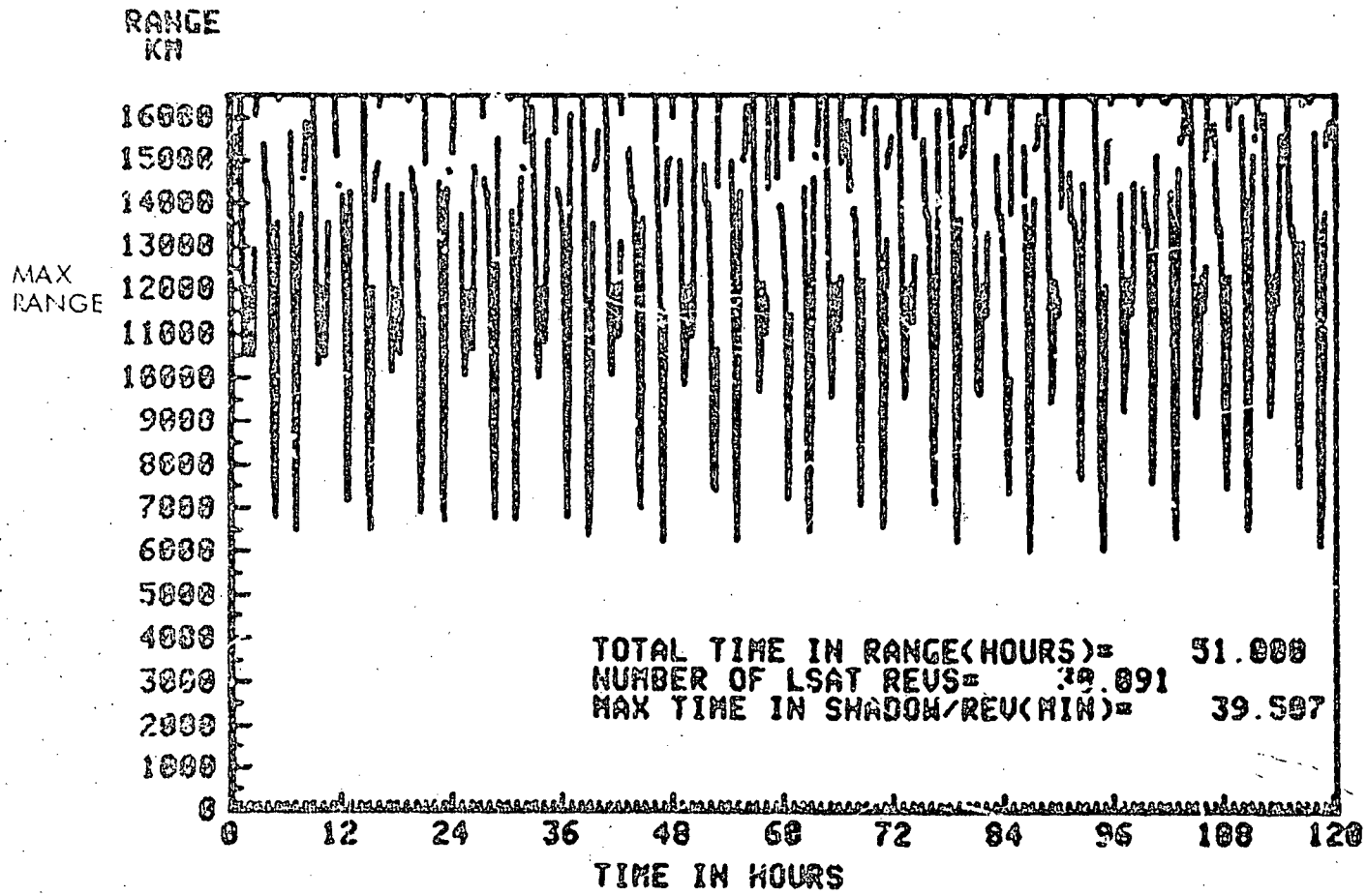

Figure 4. Space processing encounters and range (5 days)

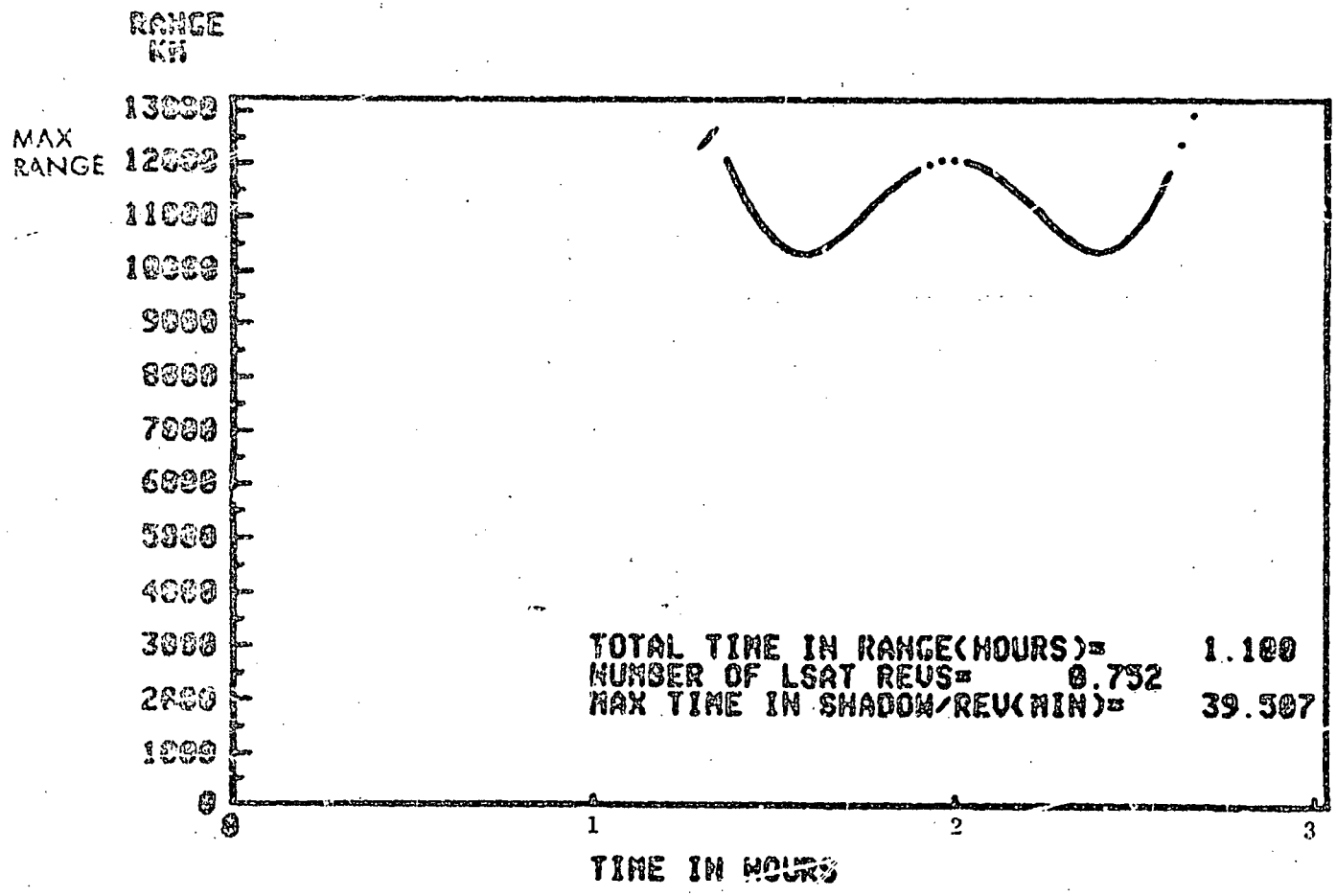

Figure 5. Space processing encounters and ranges (3 hr)

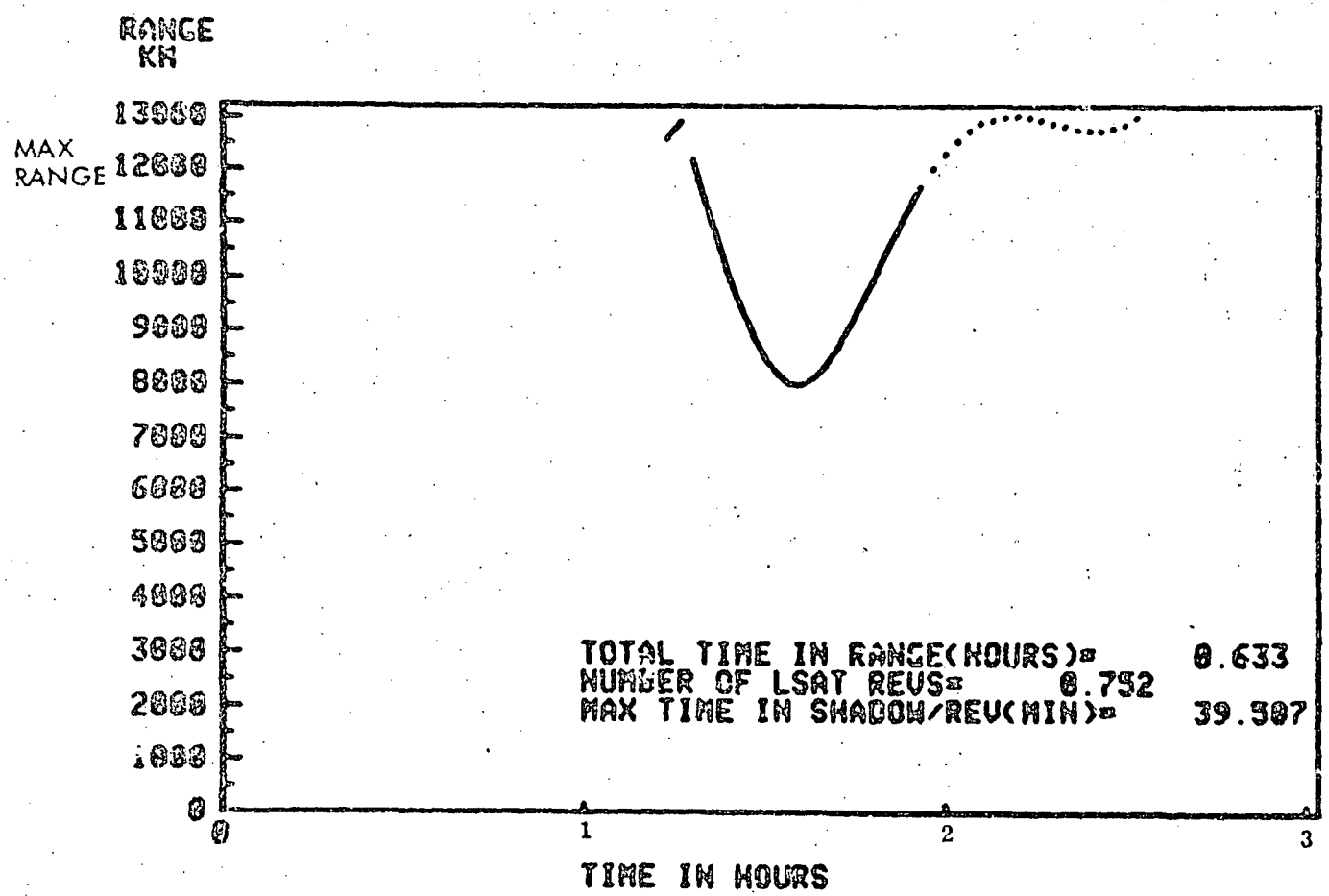

Figure 6. Minimum space processing encounter

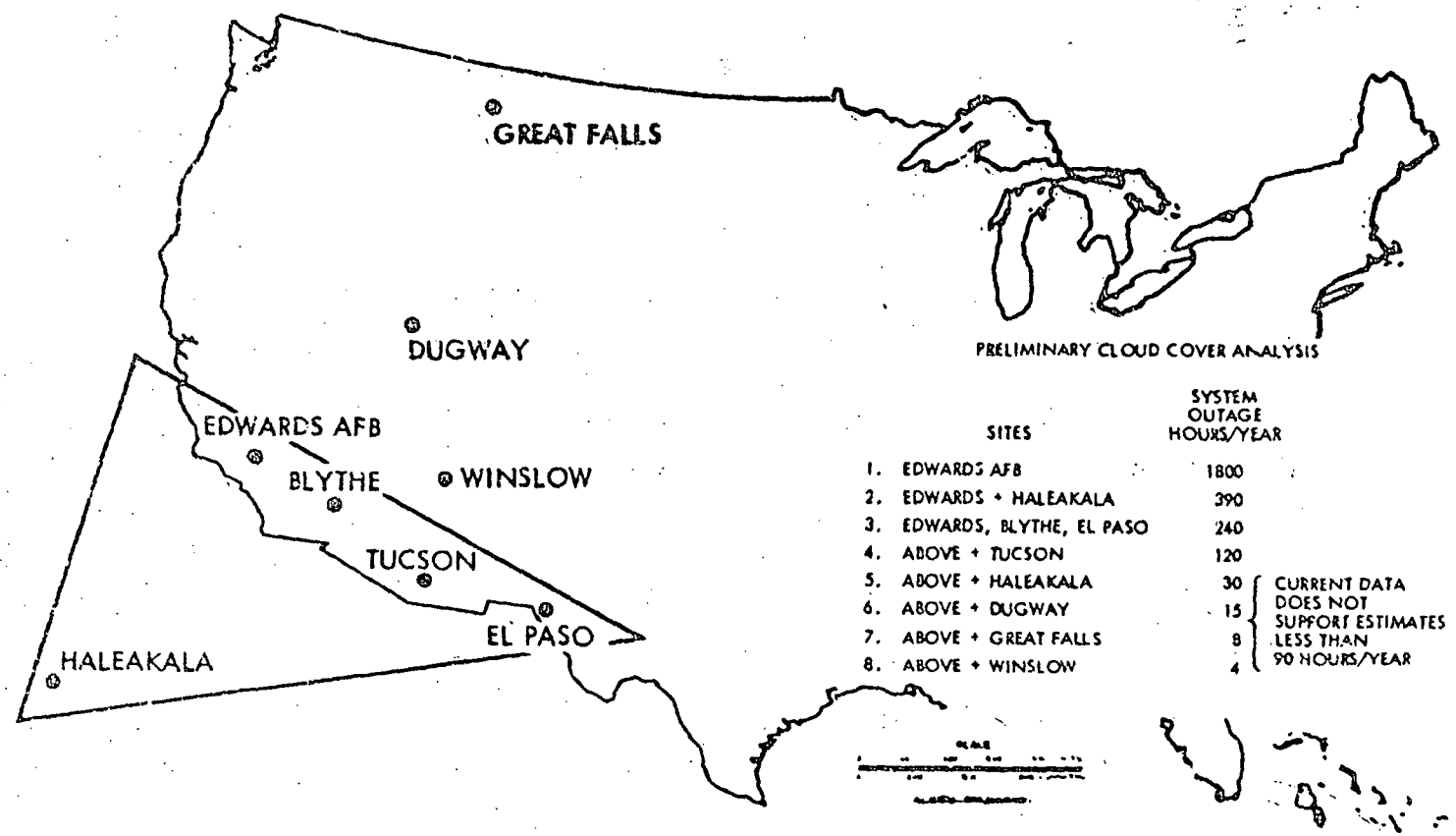

Figure 7. Ground sites for laser transmitters

It appears desirable that transmitter selection should also be made with due consideration of the viewing opportunities that the ensemble has with the relay satellites. The selection would be based on obtaining the greatest viewing time and thus reducing the requirement on the number of relays needed. However, the site selection would be based on the type of relay orbit assumed. For the study, the relay satellite requirement was not used for the ground transmitter selection.

Relay Satellite Deployment

This analysis was undertaken to determine the number of relays required for continuous viewing from ground transmitters located in the Southwestern United States and Hawaii and the ranges and elevation angles from transmitter to relay. For a deployment to be acceptable, it must allow continuous viewing to a relay from both transmitters located in Hawaii and Tucson. The latter site is representative of those sites located in the Southwest United States. Because of the transmission losses from the atmosphere, elevation angles during viewing were constrained to be greater than 30° above the horizon. In addition to viewing time and range for a relay associated with a deployment, the average elevation during viewing was considered an important parameter which was used in addition to viewing time to obtain the best deployment.

The first deployment scheme considered represented locating all relays in circular, equatorial orbit. This arrangement permits the easiest method of analysis since the ground track remains on the equator. However, for ground sites removed from the equator, ranges become large and elevation angles small for fixed orbits. In particular, transmitter sites in Southwest Continental United States result in the greatest ranges while elevation angles are near the 30° constraint. The variation in range and elevation angle with number of relays is shown in Figure 8 in which the transmitter is assumed to be near Tucson.

To improve the viewing characteristics, inclined orbits were analyzed because of nearer proximity they have to sites in the Continental United States. In addition, to improve the time that a relay spends in the northern hemisphere, elliptical orbits were used. Because of this and to avoid stationkeeping to maintain apogee in the north, an inclination of 63.4° was selected. Orbital periods of fractions of a day were used to establish repeating ground tracks every day and hence repeating viewing characteristics.

Figure 8 shows the variation in the range and elevation angle with the number of relays in the configuration for the elliptical inclined orbits. Values shown represent the minimum value between the Tucson and Hawaii sites. For a given number of relays, ranges do not vary appreciably between the inclined and equatorial deployments for the number of relays investigated. Maximum ranges were always less for inclined orbits except for 4-hr relays (requiring 8 relays) when equatorial orbits had slightly less range. In addition, elevation angles for the inclined orbits were much higher than for equatorial orbits and in particular mean elevations are 10° or more higher. Hence, inclined orbits were selected over equatorial orbits for relay deployment.

GROUND SITES ARE TUCSON AND HAWAII
30° MINIMUM ELEVATION ANGLE

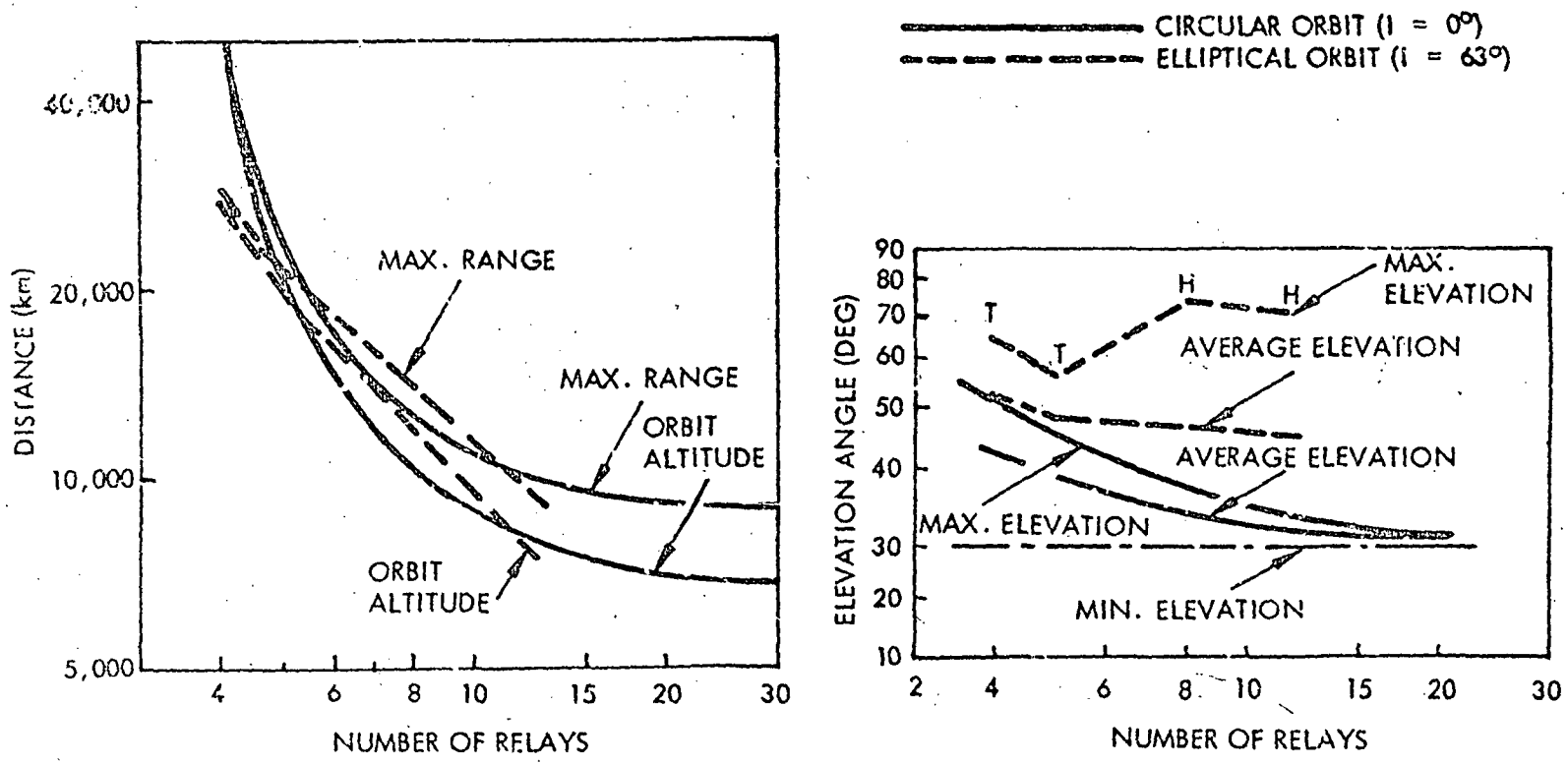

Figure 8. Comparison of relays in equatorial and elliptical orbits

Selection of Inclined Relay Orbits

The approach used to find the optimum inclined relay orbits was to select the longitude of ascending node for given location of apogee to achieve near-maximum viewing time to the worst ground site while maintaining an average elevation angle greater than 40° and at the same time giving good times and elevation angles for the other ground site. Generally, Hawaii possessed the minimum viewing time of the sites considered and hence determined the number of relays required. It was usually found that by locating the apogee at a lower latitude then the maximum 63.4°N, both viewing time and elevation angle were improved for the Hawaii site and degraded for Tucson resulting in a more equitable distribution in viewing time between the two sites.

Contact times were generated between ground sites at Tucson and Hawaii and relay satellites deployed in 3-, 4-, 6-, and 8-hr orbits all having a perigee at 500-km altitude. Both latitude at apogee and longitude at node were varied to give the best total time in view and average transmitter elevation angle. Generally, deployments which were suitable to one site were unsuitable for the other. To improve viewing from Hawaii, it was found that locating the apogee at more southern latitudes improved coverage at Tucson's expense.

For 8-hr orbits, a latitude of 45°N, and node at 15°E resulted in 6.12 hr of viewing from Tucson and 6.42 hr from Hawaii with an average elevation of 52° at both sites. From Hawaii, contact is over one continuous time period per day; however, from Tucson two contacts occur, one of short duration of 37 min. Using a realistic deployment, Figure 9 shows the times per day that a four-relay network would be in view of Hawaii and Tucson. For the arrangement shown, Hawaii is almost continuously in view (can be continuously in view with slight orbit adjustment) but about 1.8 hr of outage occurs for Tucson. By readjusting the orbits, possibly reducing average elevation, continuous coverage at Tucson should be possible with four relays.

With 6-hr orbits, the best latitude of apogee and node was 63.4°N and 8°E. These values resulted in a viewing time from Hawaii of 4.75 hr and an average elevation angle of 48.0°. From Tucson the corresponding values were 5.83 hr and 44.7°. Using five relays, time over a site must exceed 4.8 hr. Because viewing from Tucson amounted to 5.7 hr, it was felt that times at the beginning and end of a viewing opportunity totaling 1.0 hr would not be needed. Hence, low values of elevation angle which are included in the 44.7° average elevation angle for Tucson could be omitted, increasing the average to the corresponding with Hawaii.

For this deployment, two viewing opportunities exist per day from both Tucson and Hawaii. For Hawaii the first is 142 min and the second is 143 min while for Tucson it is 80 and 271 min. Figure 10 shows the viewing opportunities for the squadron for a representative arrangement of the relays in the squad. Outages of 1.75 and 1.5 hr exist for Tucson and Hawaii, respectively. By slightly varying orbital parameters, continuous coverage exist from both sites with five relay satellites.

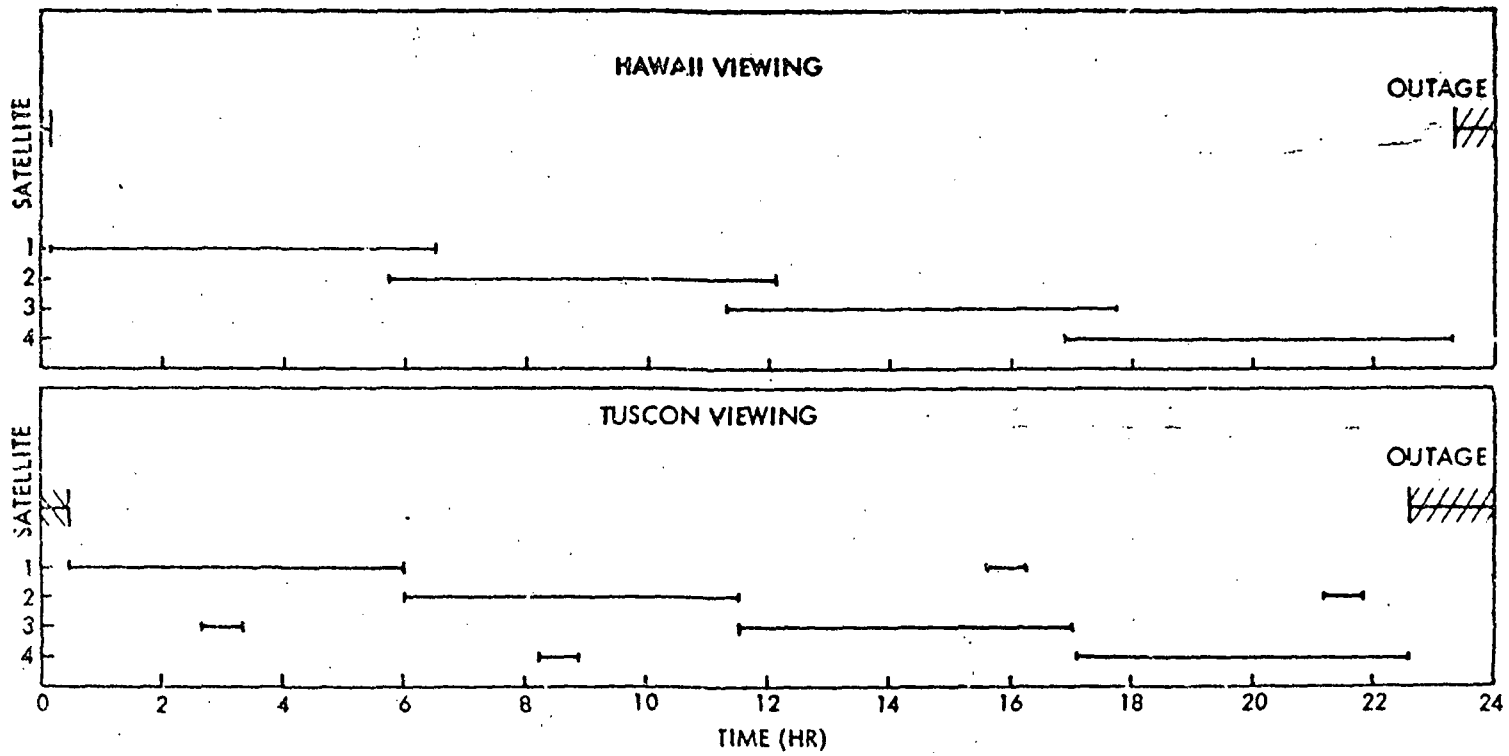

Figure 9. Viewing opportunities for 8-hr orbits (4 relays)

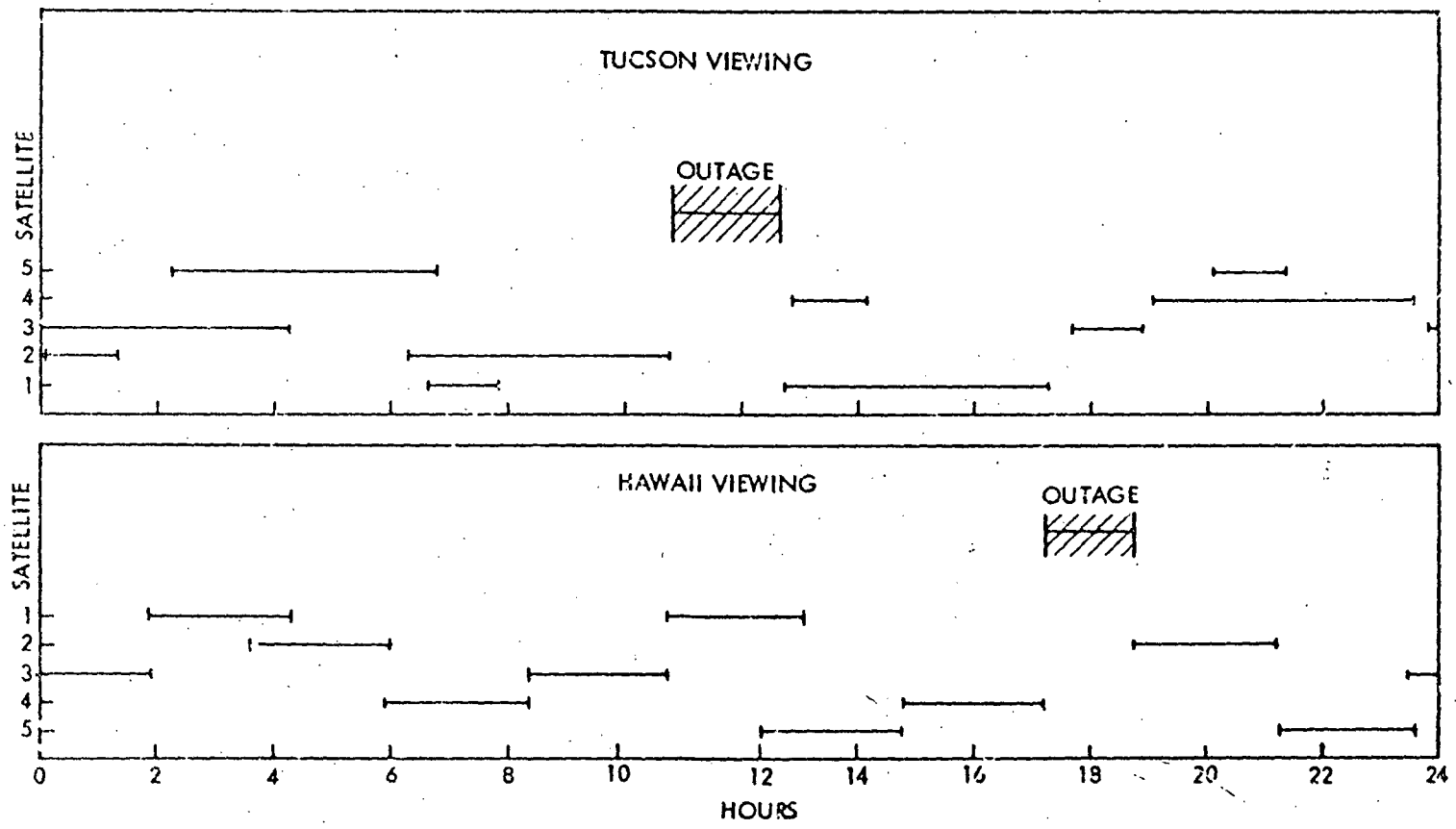

Figure 10. Viewing opportunities for 6-hr orbits (5 relays)

With 4-hr orbit relays, the best latitude of apogee and node were 40°N and 0°. For Hawaii, 3.0 hr was the viewing time and 47.0° the average elevation angle. These orbits resulted in a view time from Tucson of 2.46 hr and 52.3° average elevation. Both sites have three viewing opportunities per day. A typical contact history using eight relays is shown in Figure 11 for the Tucson and Hawaii ground sites. The locations of the relays were chosen to provide continuous viewing from Hawaii. However, an outage of about 2 hr resulted for Tucson. Small orbit adjustments should result in continuous coverage of both sites with an eight relay squadron.

Finally, for 3-hr orbits the latitude of apogee and node locations that were best were 45°N and 5°E. These values produced contact times of 2.14 hr and 3.02 hr at Hawaii and Tucson with average elevation angles of 45.3° and 45.5°, respectively. Three viewing opportunities exist per day to Hawaii and four to Tucson.

A real deployment of twelve relays is shown in Figure 12 which presents the viewing times to Hawaii and Tucson. For the deployment used, Tucson is continuously in view and only about 1-hr outage exists for Hawaii. Thus twelve satellites should provide continuous coverage of both sites with an average elevation angle of 45°.

Uplink Mirror Requirements

The previous section dealt with the deployment of relays in orbit to achieve minimum range and maximum elevation angle for a given number of relays. For each network size and corresponding period, maximum range and mean elevation angle were found. This section concerns using those results to determine the optical requirements of the ground transmitter and relay receiver. Adaptive optics are considered to be necessary and one criterion for describing their complexity is the number of actuators required.

Using elliptical orbits, it was shown that the mean elevation angle exceeded 45° for the deployments considered. Figure 13 shows the variation of the total 1σ beam divergence radius versus number of actuators for three transmitter diameters. This radius includes diffraction effects and the turbulence effect due to the atmosphere which is the most significant part for a number of actuators less than 10^4. Figure 13 is for an elevation angle of 45° and possesses slightly smaller divergence values than those for 30° (30° results in a 20% increase in turbulence).

Figure 14 shows the contribution that only turbulence plays in beam divergence for two values of number of actuators. Generally, as mirror diameter increases for fixed number of actuators, the wave front correction resolution decreases and consequently the turbulence spread increases. For 10^3 actuators, the turbulence spread worsens with increasing mirror diameter until 20 m is reached. The reason for this is that the effectiveness of the mirror diameter exceeds the effectiveness for a given number of actuators.

The 1σ beam spread is found from the formula:

$$\sigma = \left[Q^2 \sigma_o^2 + \sigma_j^2 + \left(.05 \frac{\lambda}{D}\right)^2 + \theta_T^2\right]^{\frac{1}{2}}$$

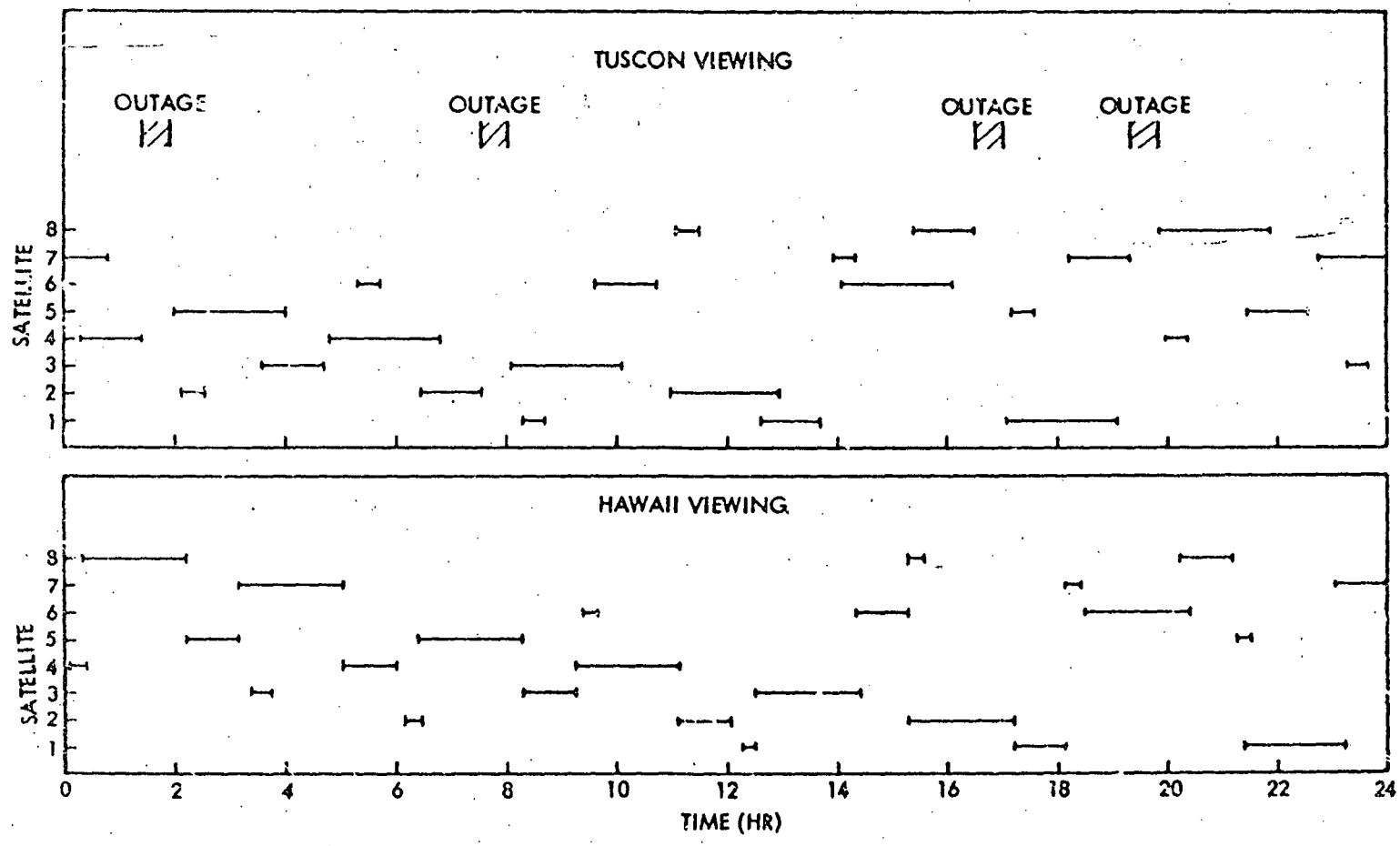

Figure 11. Viewing opportunities for 4-hr orbits (8 relays)

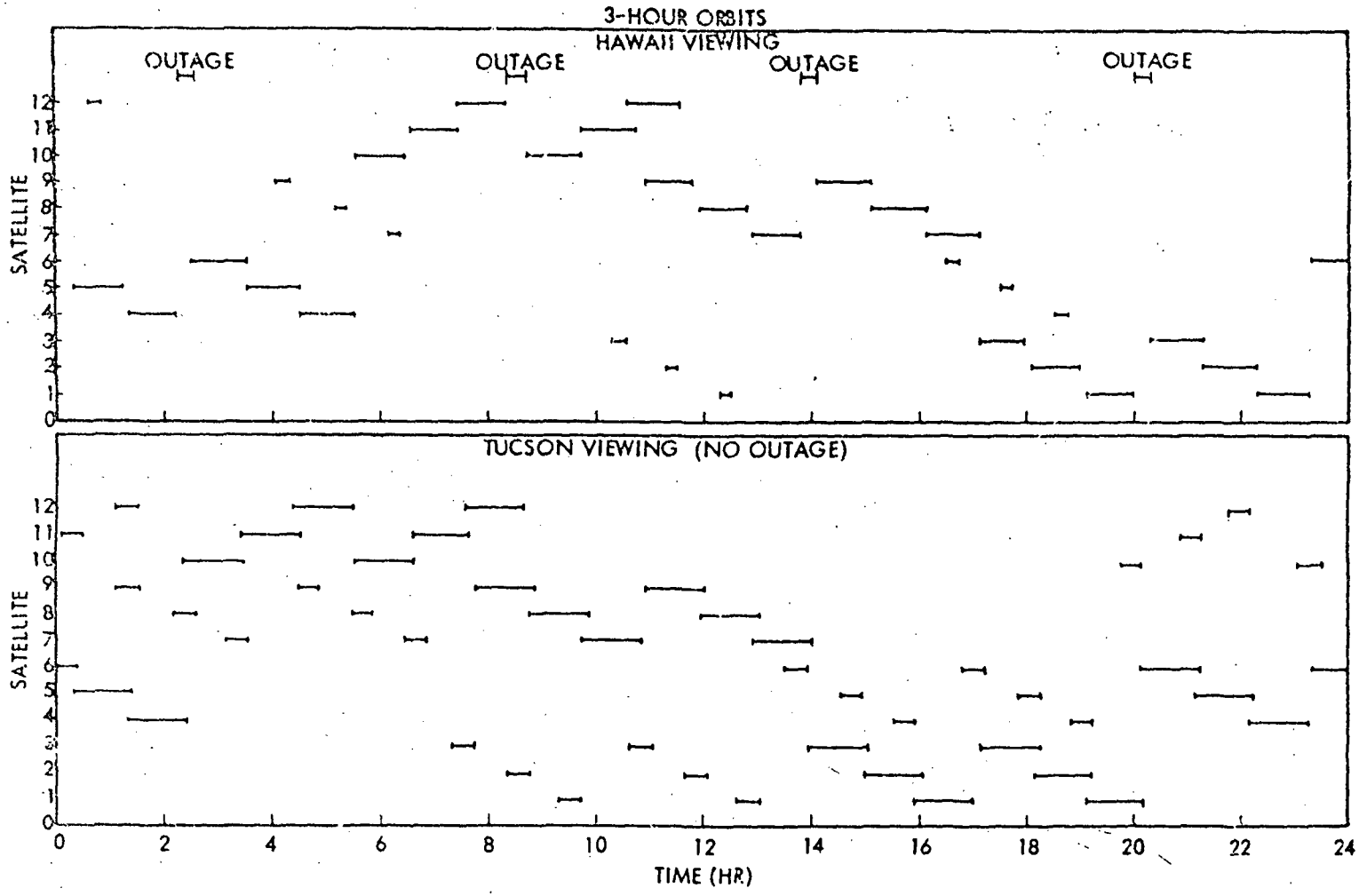

Figure 12. Viewing opportunities for 3-hr orbits (12 relays)

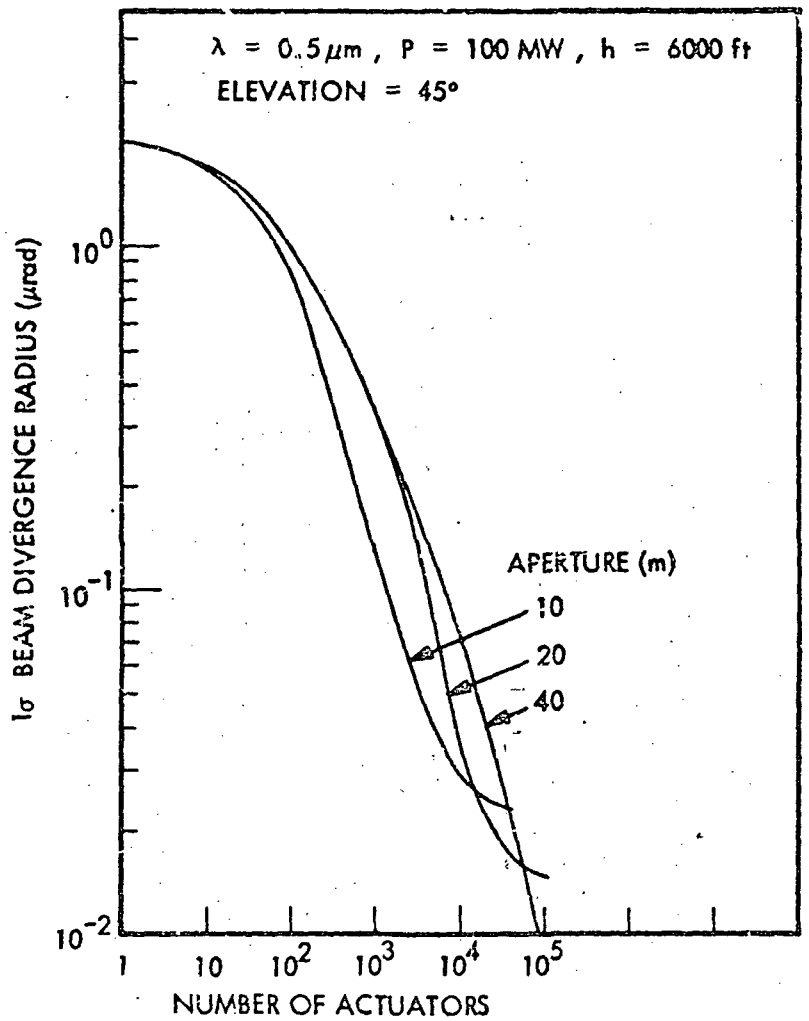

Figure 13. Variation of 1-σ beam radius with number of actuators

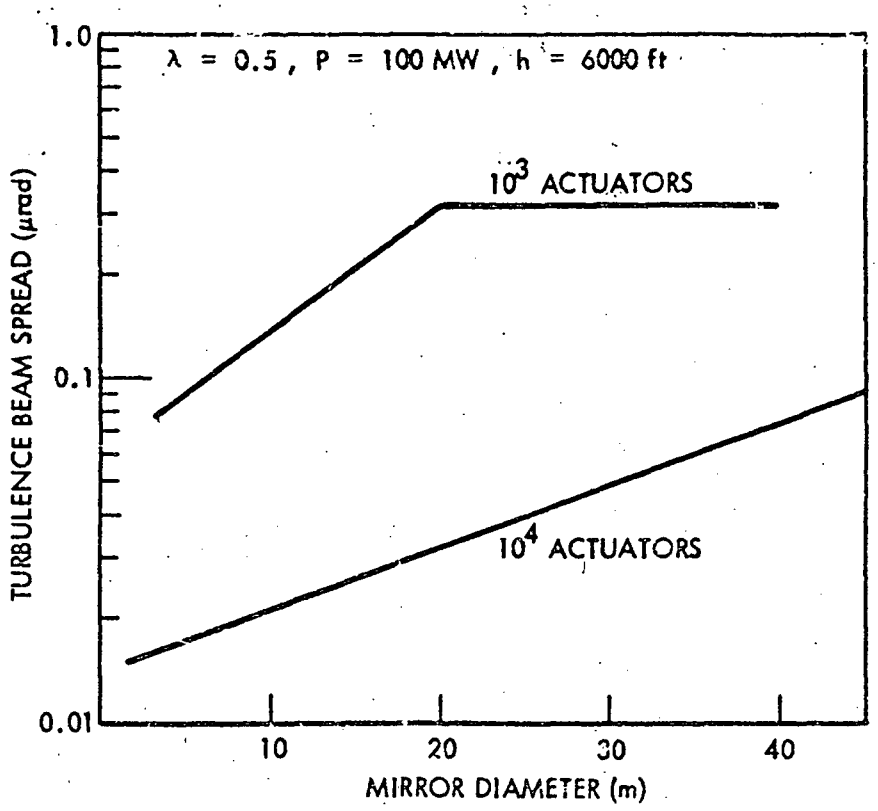

Figure 14. Turbulent beam spread variation

where

$$\sigma_o = 1.3/\pi\ (\lambda/D)$$

$$\sigma_j = 0.05\ \mu\text{rad}$$

and θ_T is found from Figure 14. The beam spread is plotted in Figure 15 as a function of the transmitter aperture (D). From Figure 15 it can be seen that a 4-m aperture is optimum for 10^3 actuators. This requires packing actuators on to the transmitter face plate at about one per 13 cm^2 and requires a computer and software to support this many actuators. For 10^4 actuators, the optimum mirror diameter is about 8 m. For this case, the placement of actuators occurs every 50 cm^2. If the packing density is too great from a manufacturing standpoint, the mirror can be increased to 16 m and still allow the same relay receiver optics.

Table III shows the relay receiver aperture size requirements for the two optimum transmitter apertures for four relay deployments. These apertures correspond to capturing a 2-σ beam at the maximum ranges indicated.

It should be mentioned that thermal blooming was omitted from this analysis. However, if laser power is large (approximately greater than 100 MW), thermal blooming may exist for the small aperture sizes. However, laser power requirements are expected to be significantly less than 100 MW.

TABLE III. RELAY RECEIVER APERTURE REQUIREMENTS

		10^3 Actuators		10^4 Actuators	
No. Satellites in Network	Maximum Range (km)	Transmit (m)	Receive (m)	Transmit (m)	Receive (m)
12	9,700	4	4.6	8	2.5
8	14,300	4	6.8	8	3.6
5	22,000	4	10.5	8	5.6
4	28,700	4	13.6	8	7.3

Relay to Satellite Link

To determine relay transmitter and satellite receiver optical requirements, the operational range between relay and satellite must be analyzed. This analysis was first done assuming the radius vector to relay perpendicular to the satellite orbit plane. For this approximately average situation, the range between relay and satellite was determined as a function of the number of relays. Figure 16 presents the range variation for the case in which the satellite is at a low altitude of 500 km. Ranges are indicated to vary between 15,000 and 35,000 km for relays in 3- to 8-hr elliptic orbits.

OPTIMUM TRANSMITTER APERTURE

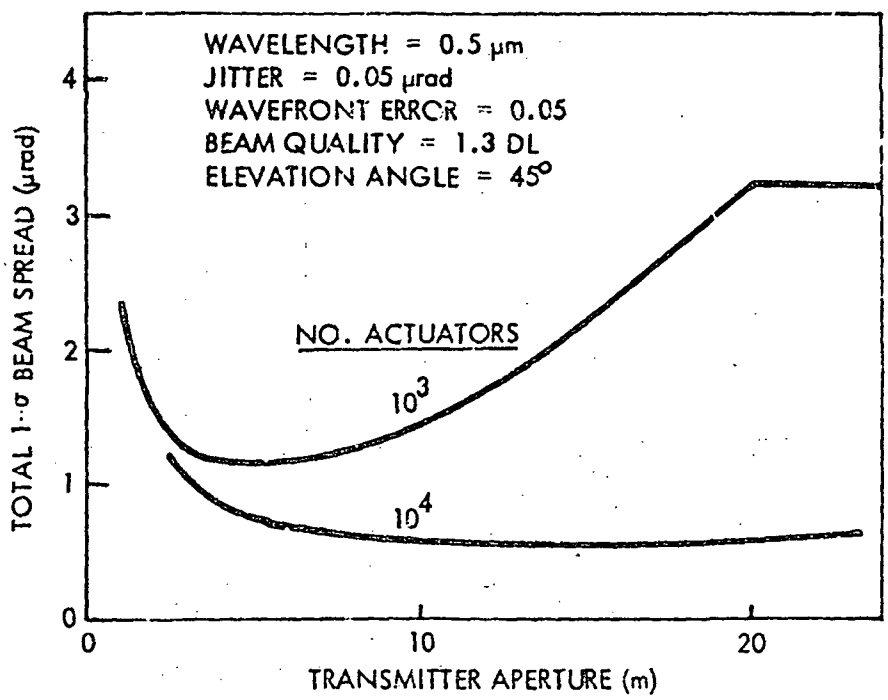

Figure 15. Total beam spread variation

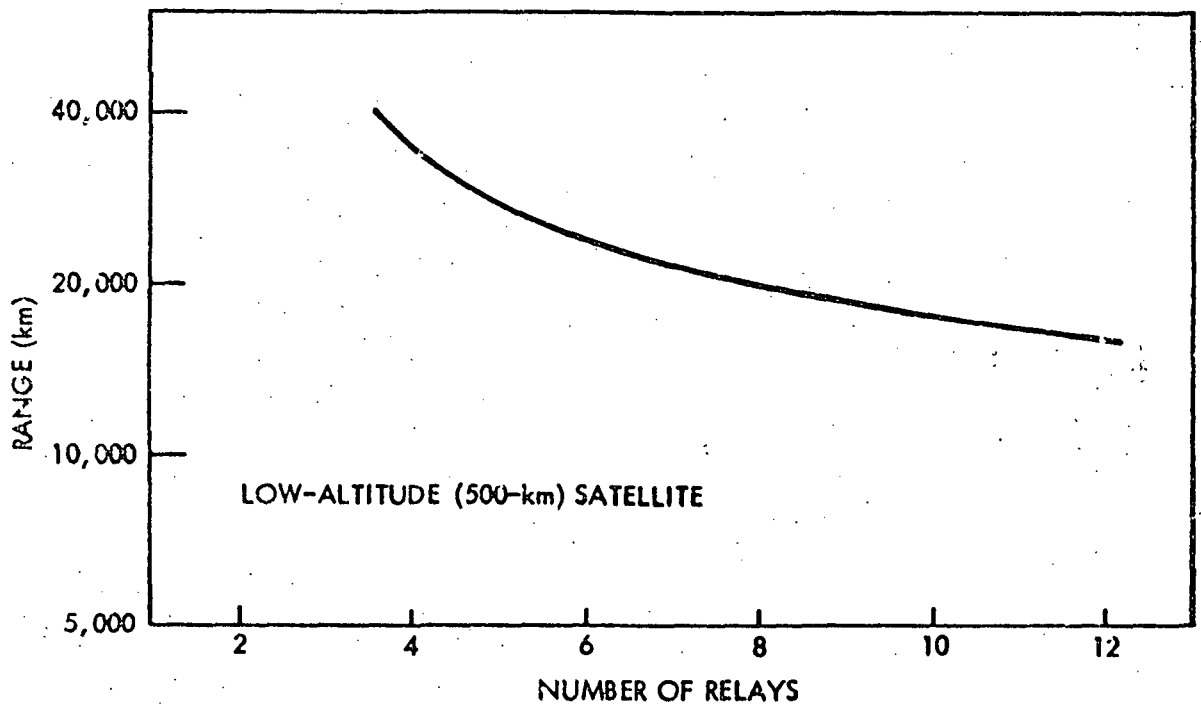

Figure 16. Range from relay to satellite

For this range of values in the range, requirements on the receiver aperture were determined as a function of the relay aperture. Because of the long ranges involved, all of which are in space, reducing jitter is advantageous in reducing beam spread since turbulence is no longer the primary contributor to beam spread as it was for the uplink. Hence, it was assumed that values for jitter could be achieved equal to half the diffraction limit corresponding to a particular relay transmitter diameter. The variation in satellite receiver aperture with relay aperture is shown in Figure 17 for a fixed wavefront error of $\lambda/20$ and represents sizing the receiver for a 2-σ beam. Without going to excessively large transmitters, receiver sizes vary between 1 to 8 m for ranges investigated. Figure 18 shows the variation of receiver with transmitter for the particular cases investigated corresponding to orbits of 3, 4, 6, and 8 hr.

In the event that energy must be relayed to satellites frequently such as once an hour, and over relatively long periods of time such as 15 to 30 minutes, the average range may not be suitable for sizing the transmitter/receiver optics. For this reason, actual time variations in the range to satellites in the mission model from the candidate relay deployments required computation. Time did not permit the computation of the range variation for all relays and satellites. The variation was computed for a four-relay squadron each in an 8-hr orbit during the times the deployment was within view of the Hawaii transmitter. Two satellites in the laser power conversion mission model were included, one being the Space Processing Satellite (300 nmi, 28.5° inclination) representing low earth orbits of less than 600 nmi and the other the Transportation Services/Navigation Satellite (8000 nmi, polar) representing orbits greater than 600 nmi.

Figures 19 through 21 show the variation in range between relay and low-altitude satellites over a 24-hr period for three different orientations of the satellite orbit. During approximately every 6 hr in the day one relay in the deployment is simultaneously in view of the satellite and the Hawaii ground transmitter. The dashed portions of the curves represent times when the satellite is behind the earth and out of view of the relay. As can be seen, very little overlap exists during which times two relays are within range of the satellite provided the satellite is not behind the earth.

The total time that the satellite is in view of a relay appears to be nearly constant for the various orientations included. This variation would be similar to those associated with varying the location of the satellite in its orbit. For this case 15 hr are available per day during which power can be beamed from the Hawaii ground transmitter to LEO satellites.

If energy transfer must take place frequently such that the best times cannot be selected per day, then the range variation is between 10,000 and 36,000 km as opposed to the 34,500-km range found earlier for this case. Thus the earlier results represent the upper bound for the case when transmission must occur at unfavorable times.

It can be seen that periods exist of up to 45 min when the satellite is behind the earth and lost from view of the relay. Energy transfer from the Hawaii transmitter is not possible during those times which would demand multiple coverage relay deployments if continuous time is required. Some reduction in the outage time exists for single coverage if all transmitters are free of cloud cover.

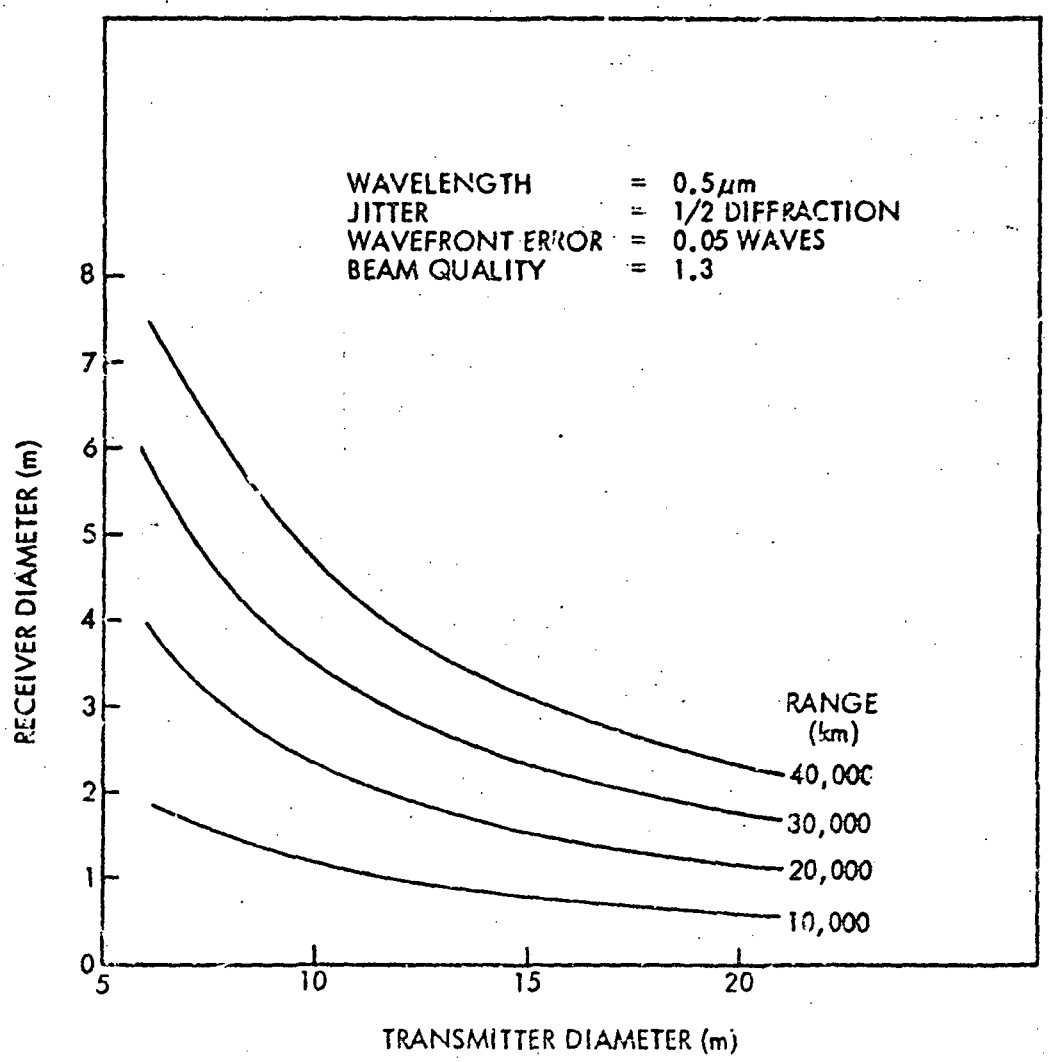

Figure 17. Variation of receiver optics with transmitter

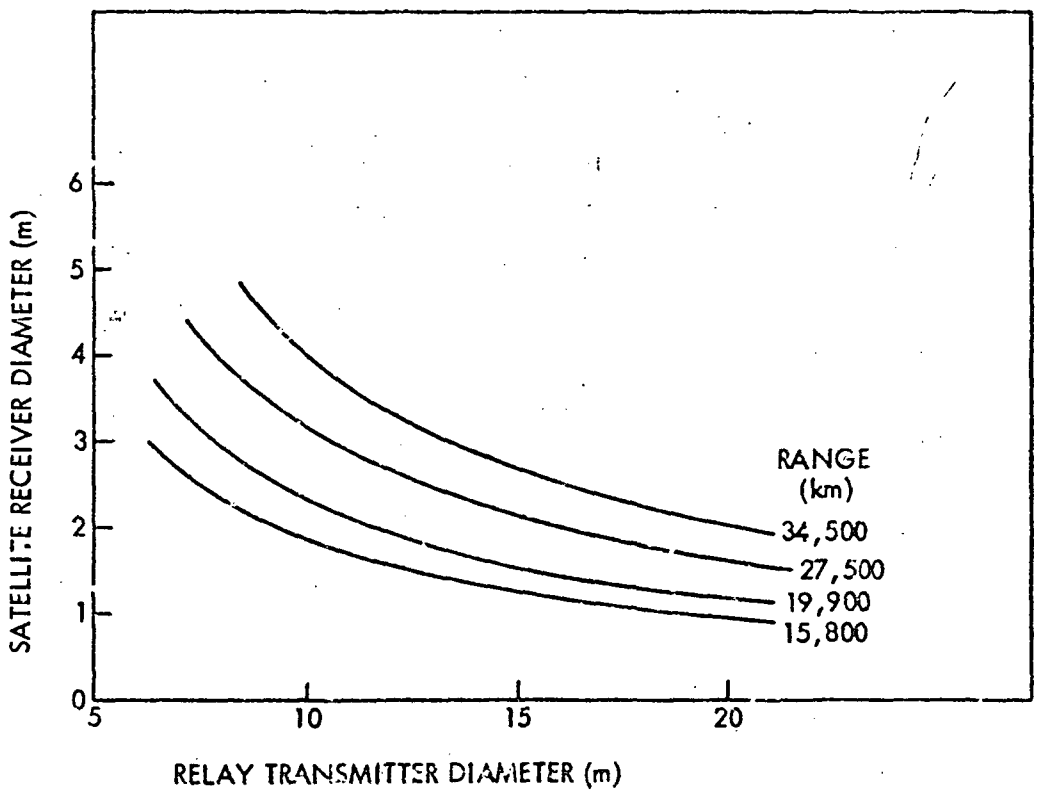

Figure 18. Receiver/transmitter variation for candidate relay deployments

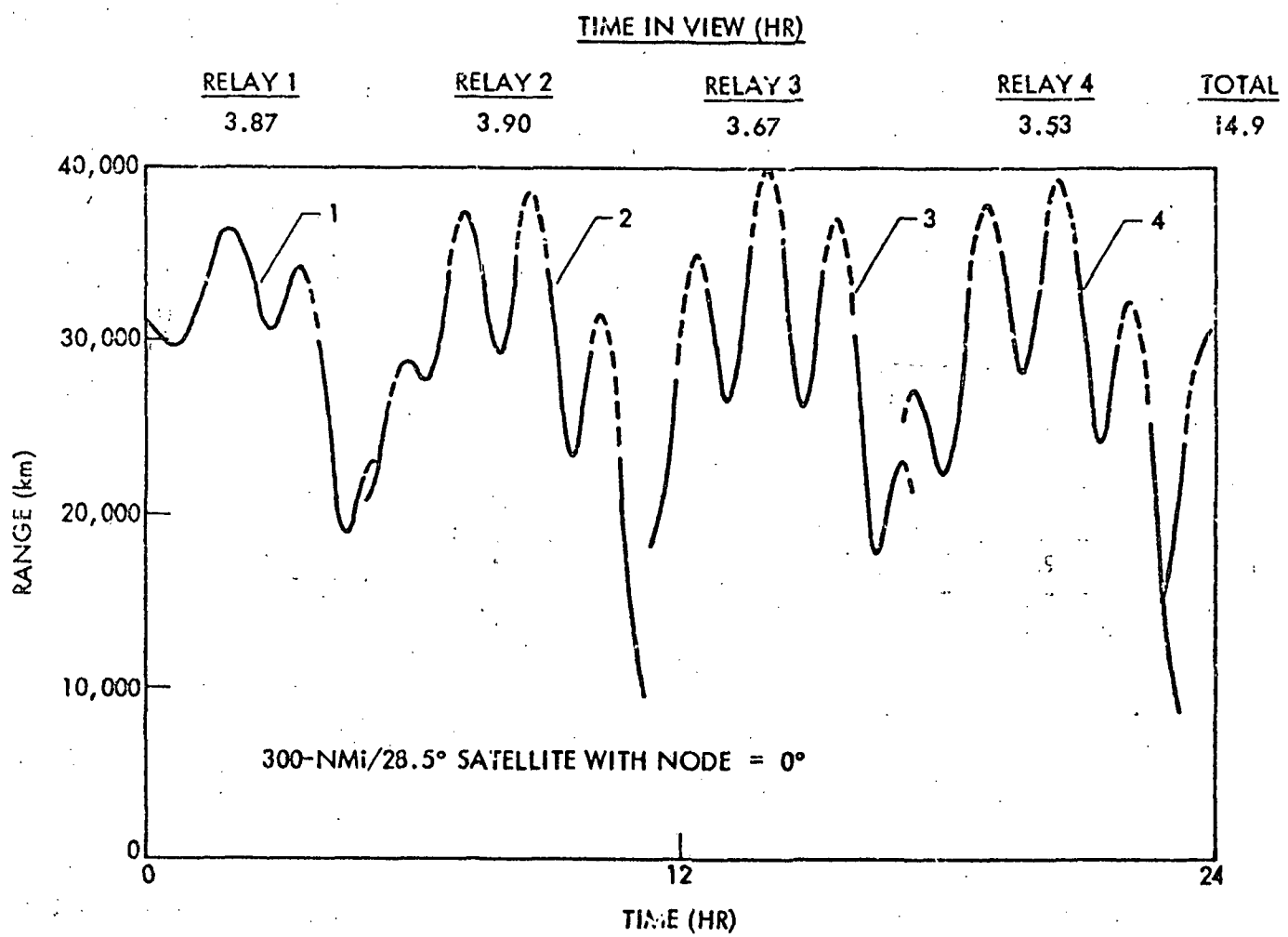

Figure 19. Four-relay network with Hawaii viewing (300 mni, 0°)

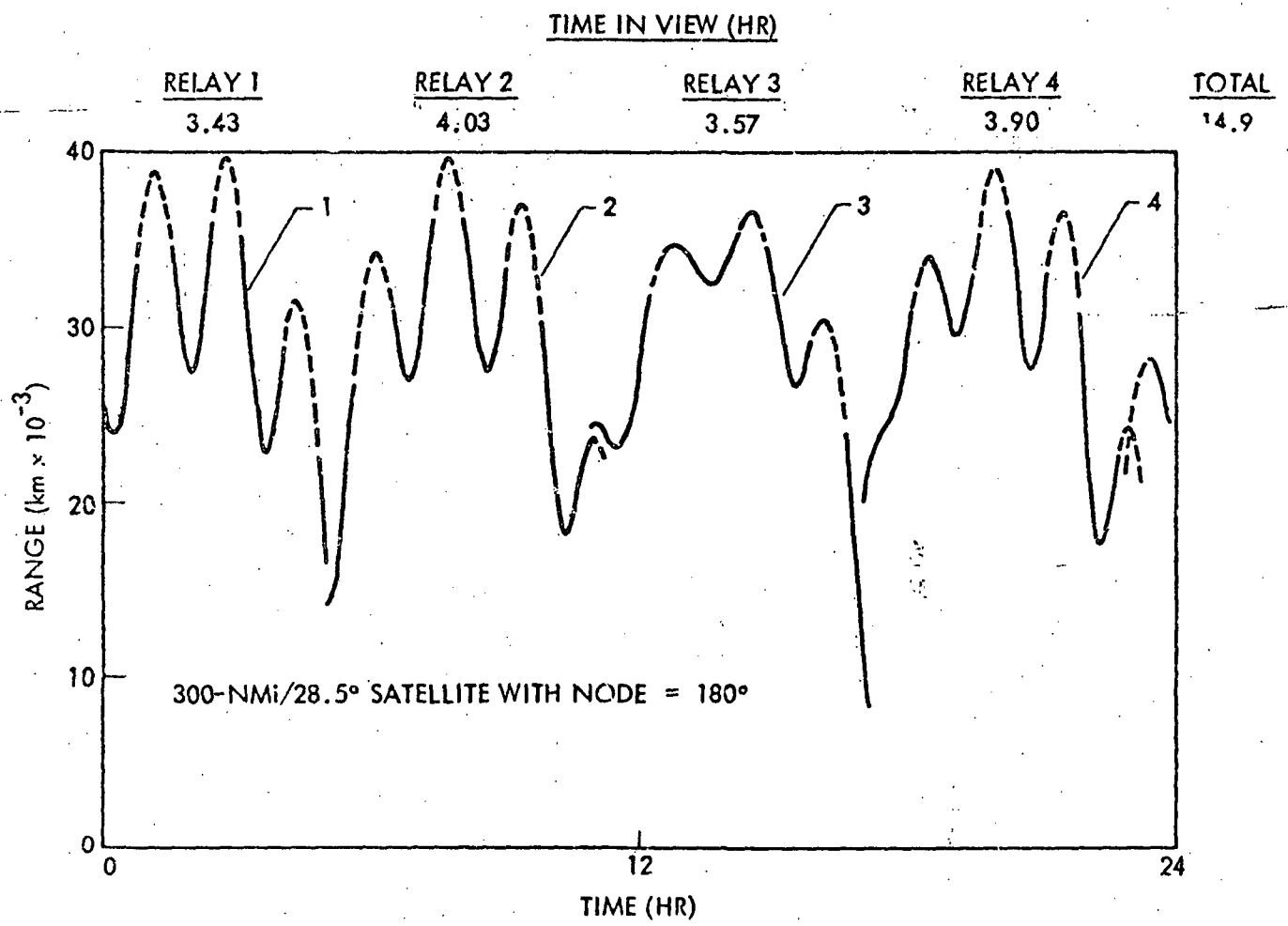

Figure 20. Four-relay network with Hawaii viewing (300 nmi, 180°)

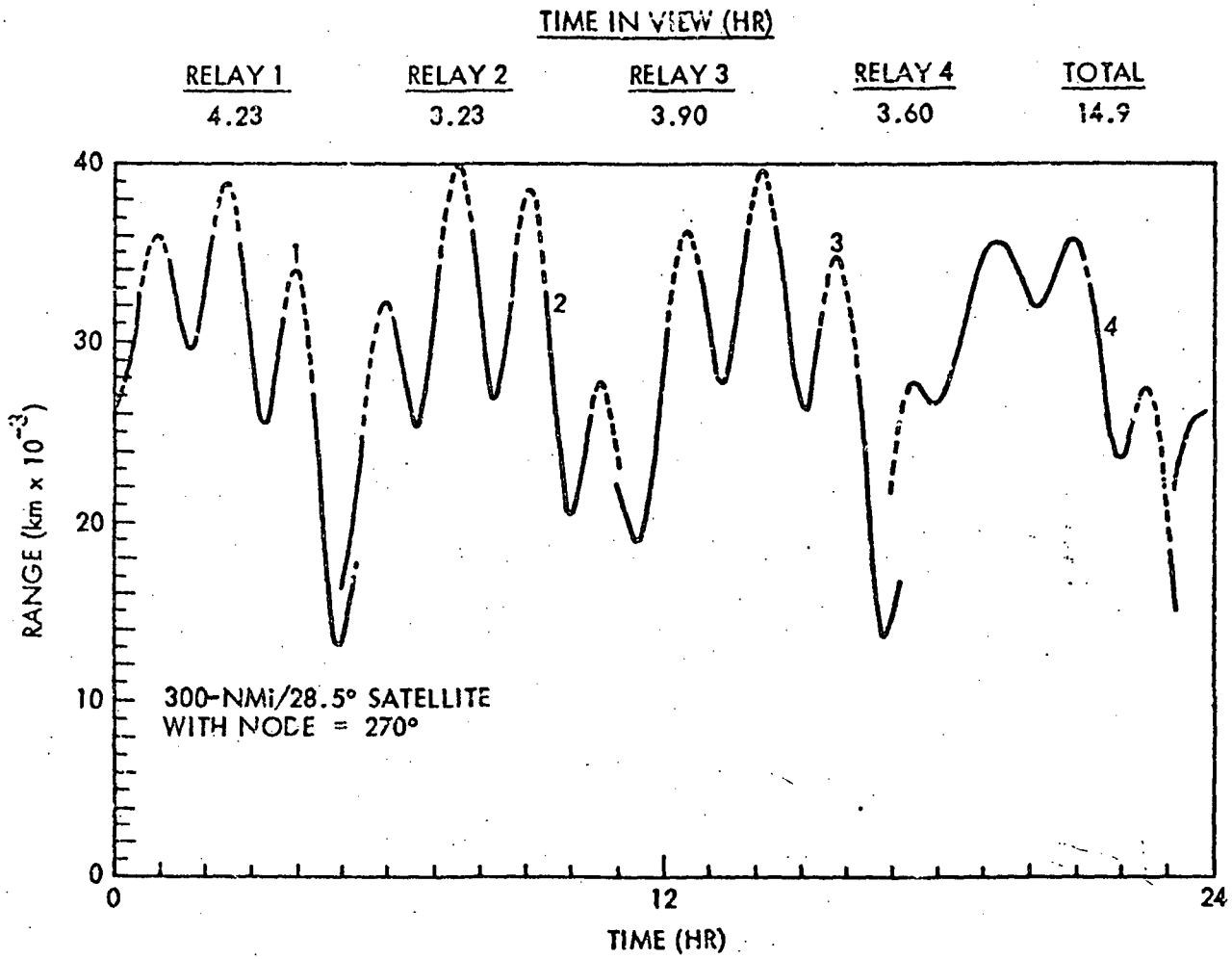

Figure 21. Four-relay network with Hawaii viewing (300 nmi, 270°)

Figures 22 through 24 show the range variation for the 8000-nmi satellite from the four-relay network. Ranges are seen to vary between 54,000 km and 1000 km. In this case, ranges found by the first method would not result in the greatest operational ranges as for example a range of 40,000 km would be predicted for this case as compared to the 54,000-km maximum range found here.

Because of the higher altitude of the satellite, greater contact time is possible when the earth is not obstructing view. Only 2 to 3 hr per day are lost because of earth occultation which may allow single coverage if near continuous coverage is required. Use of the other ground sites would reduce the outage given for this case.

3.2.3 Satellite Receiver Sizing

The satellite receiver size, whether optical or other type, is dependent upon the laser beam spot size and the flux level that will miss the receiver and impinge on the mission satellite. Figure 25 shows the effect of range on spot diameters for 0.5-, 5.0-, and 10.6-μm wavelengths (λ) with a 30-m-diameter transmitting aperture, 0.05-μrad jitter, $\lambda/50$ wavefront error, and a beam quality 1.3 times diffraction. The deployment analysis showed that ranges up to 10,000 km would be required which will require laser wavelengths of less than 5.0 μm to attain a receiver diameter of 5 m or less. Figure 26 shows the laser beam profile flux intensities for a 10,000-km range and a laser power of 10 MW. As may be noted, a 5.0-μm wavelength would have a flux density in the order of 10 W/cm^2 at the edge of a 5-m-diameter receiver. This flux density could be damaging to the mission satellite. Therefore, an even shorter wavelength will be required. To reduce the flux level to approximately that of the sun, a wavelength of about 0.5 μm will be required. With a 5-m receiver and a wavelength of 0.5 μm, the receiver will intercept more than 95% of the laser energy as shown in Figure 27. This preliminary sizing of the receiver illustrates the worst case and depending on the specific parameters of each mission satellite and the ranges during energy transfer opportunities, receivers will be sized equal to 5-m diameter or less.

3.2.4 Power Conversion System Concepts

A wide spectrum of potential subsystems has been examined for the conversion of laser energy to electrical energy on the spacecraft. The important considerations associated with the power conversion subsystems are:

- Applicable wavelengths
- Conversion efficiency
- Conversion time factors
- Weight
- Energy storage requirements

As presented previously, the orbital dynamics and laser utilization constraints restrict the delivery of laser energy to relatively short time spans, requiring that energy be stored to supply the spacecraft until the next energy delivery opportunity. This operational consideration had a significant impact on the power conversion subsystem results.

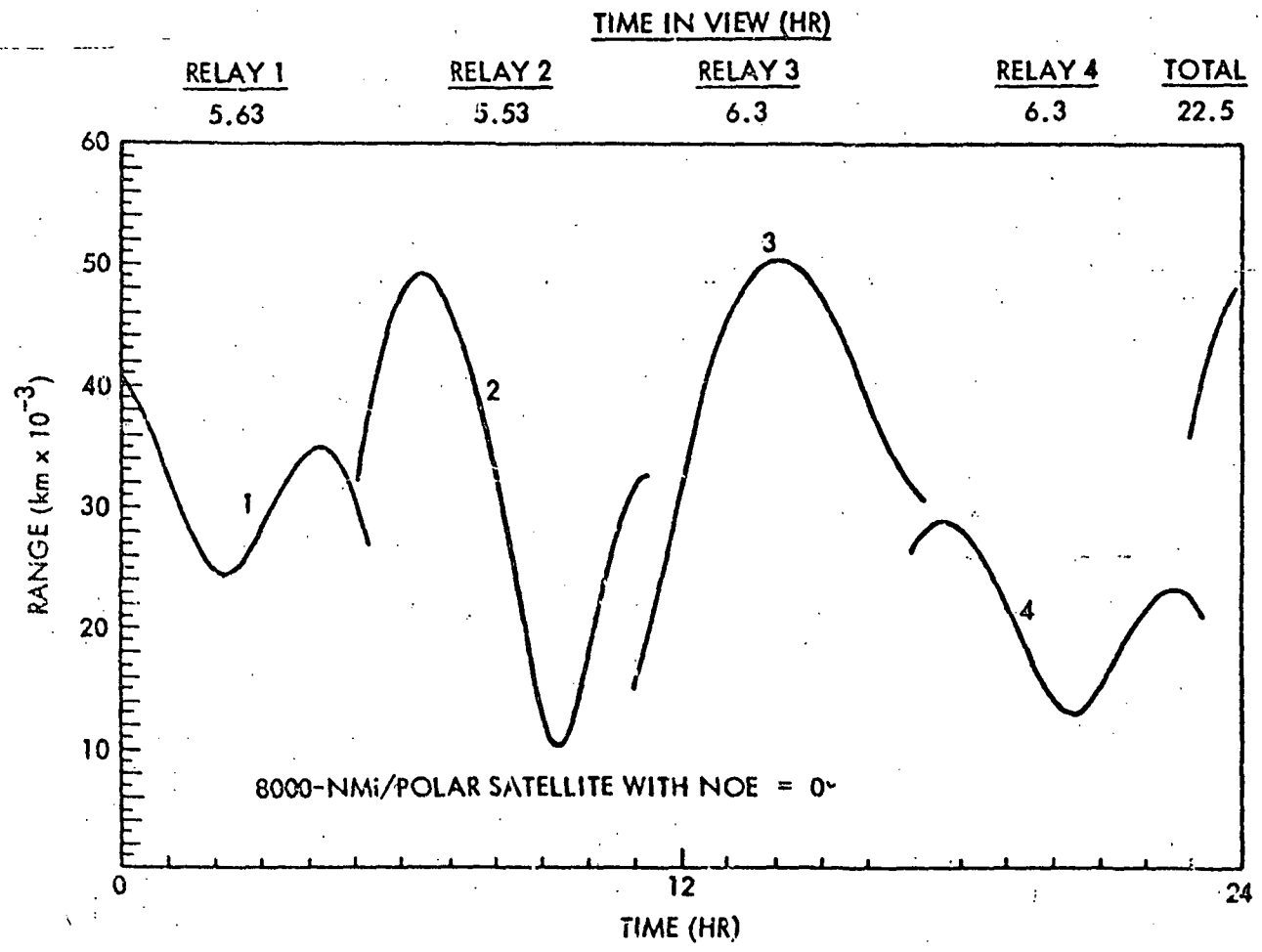

Figure 22. Four-relay network with Hawaii viewing (8000 nmi, 0°)

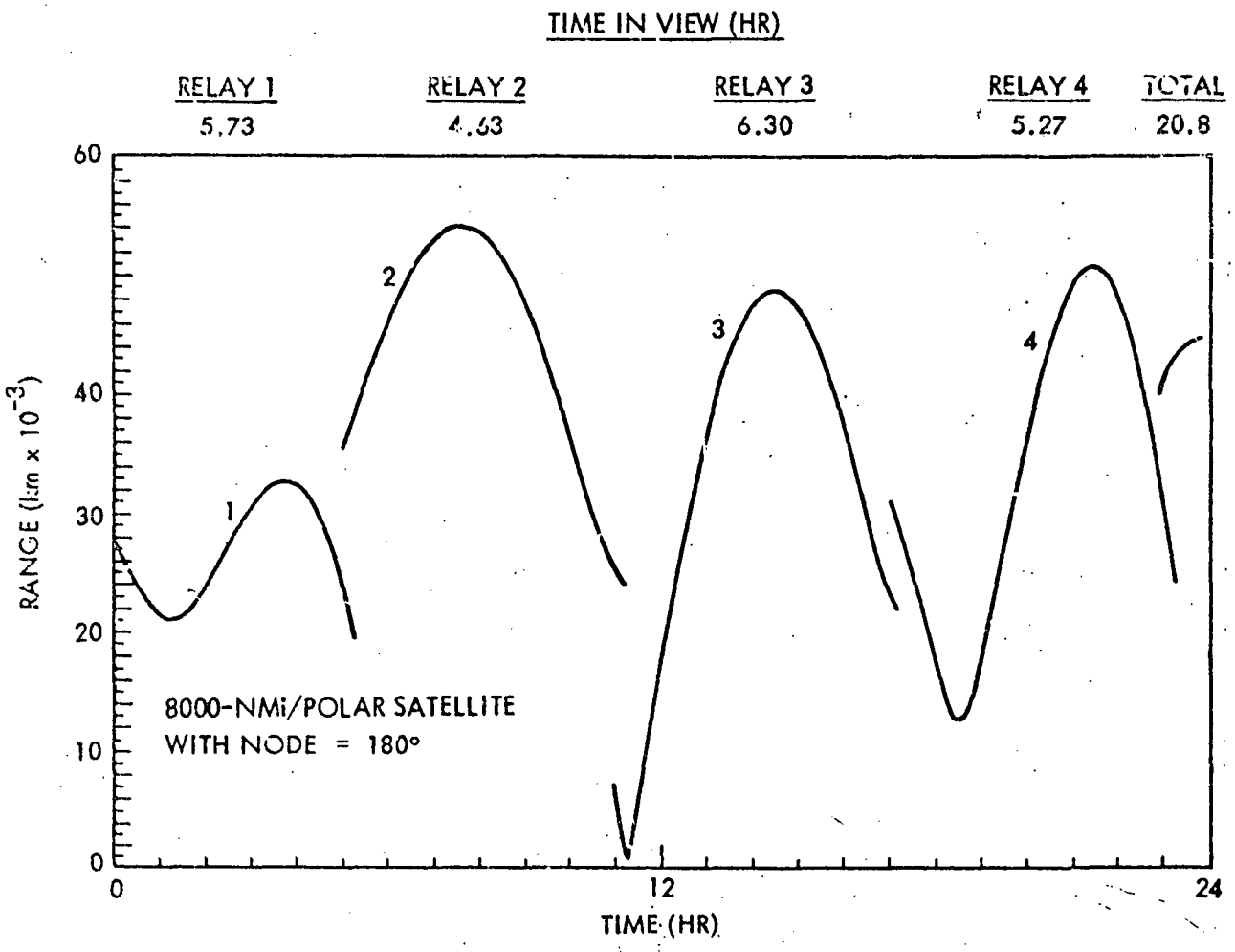

Figure 23. Four-relay network with Hawaii viewing (8000 nmi, 180°)

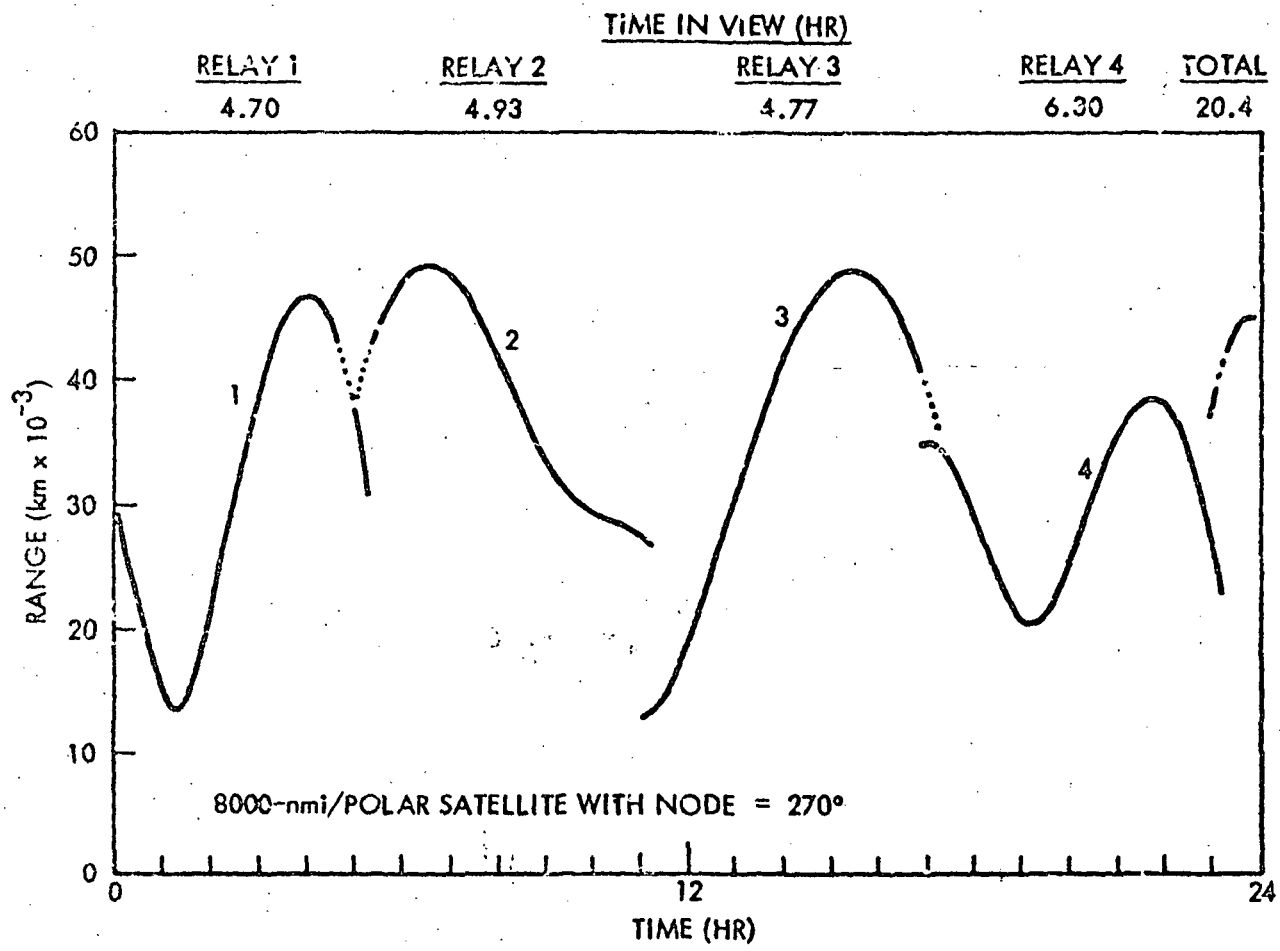

Figure 24. Four-relay network with Hawaii viewing (800 nmi, 270°)

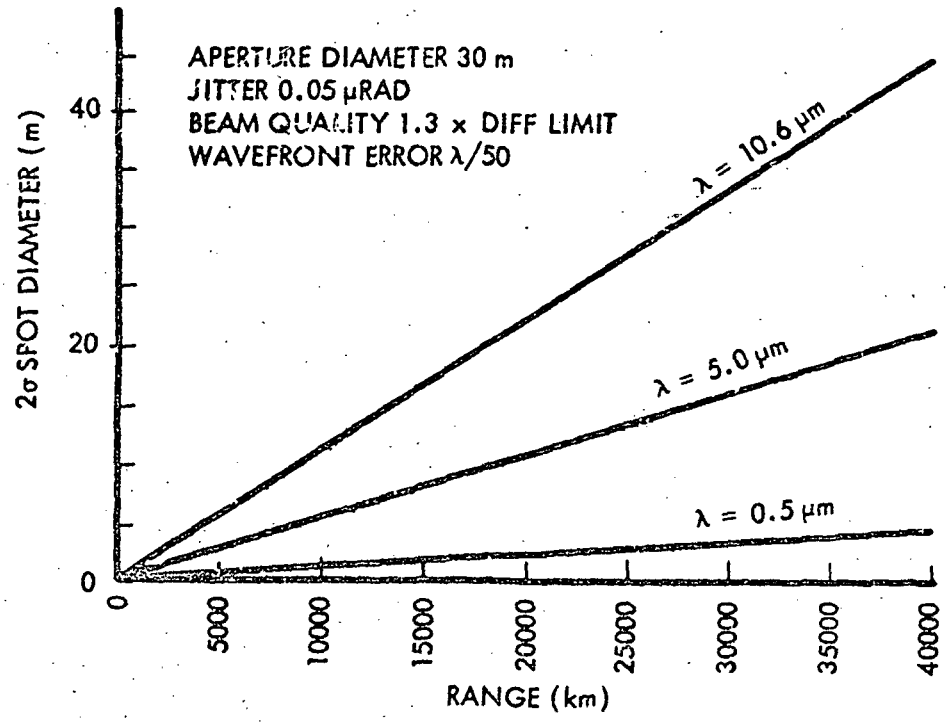

Fig. 25 Effect of Wavelength on Spot Diameter

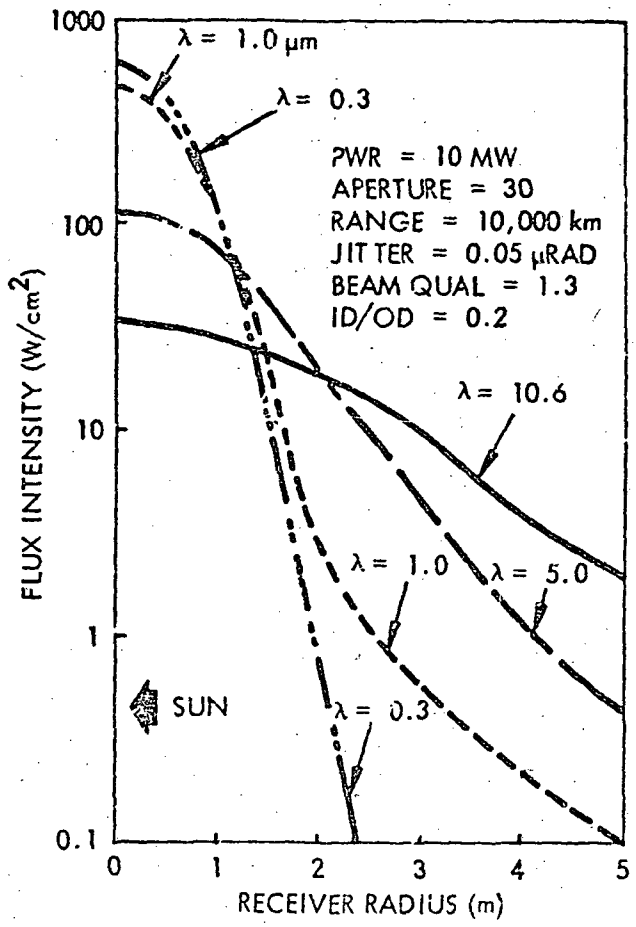

Fig. 26 Beam Profiles at Receiver

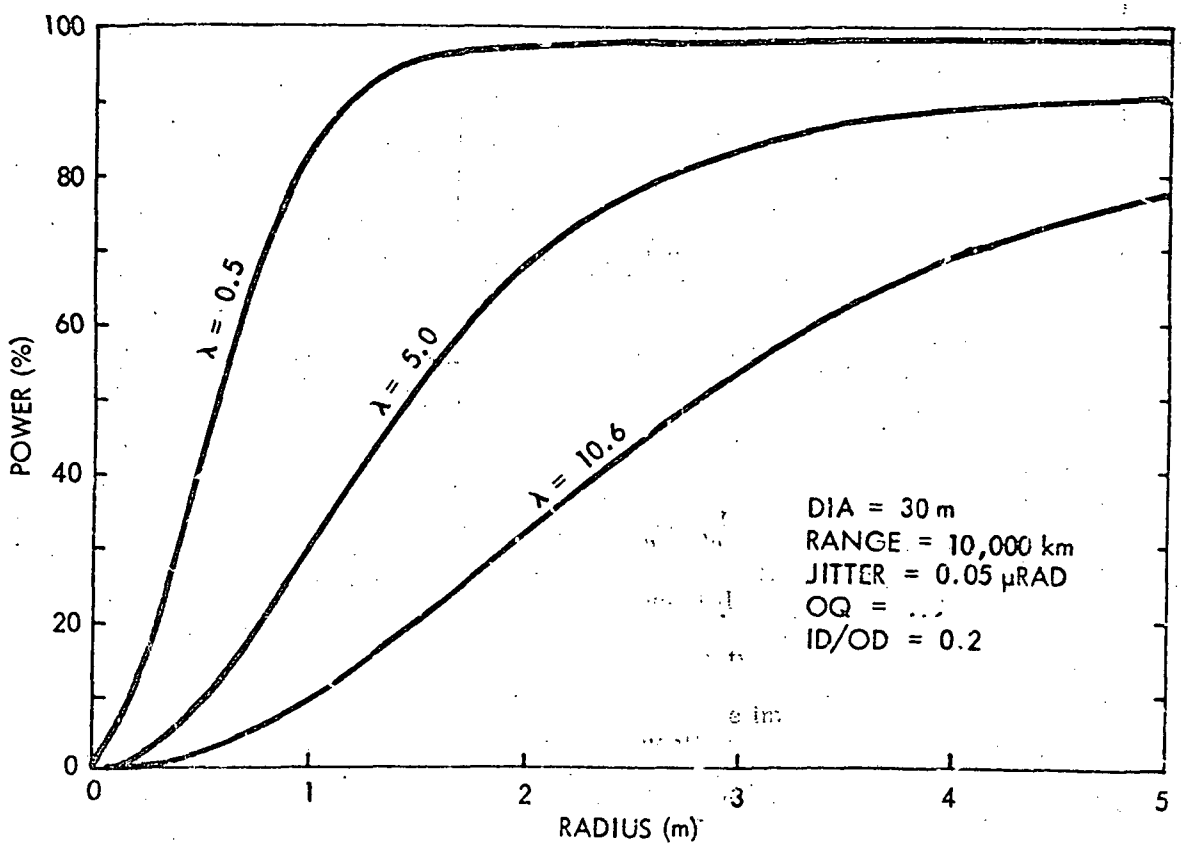

Fig. 27 Receiver Efficiencies

The power conversion subsystems initially considered are summarized in Table IV. Conversion efficiencies are not shown since these are a function of a number of variables.

3.2.4.1 Establishment of the Candidate Subsystems

The potential power conversion systems presented in Table IV were examined to select those for inclusion in the subsystems and to eliminate those which are not well suited for the missions or offer no particular advantages.

It was concluded that the optical diodes and antireflection coated metal oxide semiconductor offered no particular advantages over the photovoltaic cells, and it was not necessary to evaluate these separately. The technologies for the optical diode and the antireflection coated metal oxide semiconductors are at a very early state of development, but the indications are that the efficiencies would likely not exceed those of the photovoltaic specifically tailored for lasers, and the weights would not be less.

The photo-assistance cells are not considered applicable to the space missions defined for this study because of the high-energy laser energy input rates and the collection and storage of the output gases.

The remaining power conversion concepts were employed to establish candidate subsystems as presented in Table V. The matrix considers the method of receiving, storing (as applicable), and conversion to electrical power, including more than one cycle in order to utilize as much of the energy as possible. Heat rejection approaches are important considerations in the thermodynamic cycles, and alternate possibilities were included in the matrix.

As the evaluations of the power conversion subsystems progressed, it was found that it was not necessary to consider all the possibilities presented in Table V, since some produced little impact upon the conclusions. The power conversion subsystems were subsequently grouped into three categories:

(1) Real-time conversion to electrical or mechanical energy
(2) Real-time conversion to electrical energy, plus bottoming cycle utilizing delayed conversion
(3) Energy storage with delayed conversion

These subsystems categories are evaluated in subsequent sections.

3.2.4.2 Power Conversion Subsystems

Power conversion concept data were principally derived from utilization and expansion of previous studies (Refs. 1 through 32). The assumptions regarding efficiencies and weights are considered to be optimistic in order to allow for future technology improvements.

TABLE IV. POWER CONVERSION DEVICE SUMMARY

Power Conversion Device	Applicable Laser Wavelength (m)	Energy Input	Energy Output
Photovoltaic Cell	0.3 to 1.0	Laser	Electrical power
Optical Diode	> 0.3	Laser	Electrical power
Antireflection Coated Metal Oxide Semiconductor	0.4 to 2.0	Laser	Electrical power
Thermoelectronic	> 0.3	Laser	Electrical power
Thermionic	> 0.3	Laser/Heat	Electrical power
Photo-Assistance Cell	< 0.6	Laser	Hydrogen and oxygen for fuel cells or engines
Brayton, Rankine, or Stirling Cycle (w/wo Energy Exchanger)	> 0.3	Heat	Mechanical (for electrical power generation)
Magneto Hydrodynamics	> 0.3	Heat	Electrical power

ORIGINAL PAGE IS
OF POOR QUALITY

TABLE V. MATRIX OF POTENTIAL POWER CC

FOLDOUT FRAME

	SYSTEM	RECEIVER				STORAGE OR CONVERSION OF ENERGY FROM RECEIVER						FIRST CYCLE ENERGY TRANSFER TO FLUIDS		ENERGY EXCHANGER			FIRST THERMODYNAMIC CYCLE AFTER RECEIVER (TOPPING)						CONVERSION OR STORAGE FROM FIRST CYCLE				
		TELESCOPE	DIRECT HEAT EXCHANGER	THERMIONIC	PHOTOVOLTAIC ARRAY	LIF PHASE CHANGE	LIH PHASE CHANGE	H_2O	MOTOR/FLYWHEEL/ GEN./BATTERY	BATTERY	INDUCTION	PLASMA PRODUCTION	HEAT EXCHANGER	WAVE ENERGY EXCHANGER			THERMIONIC	TELEC	MHD	BRAYTON	RANKINE	STIRLING	OUTPUT/BATTERY	OUTPUT/INDUCTION	GEN./BATTERY	GEN./INDUCTION	MOTOR/FLYWHEEL/ GEN./BATTERY
E ALL INPUT ENERGY AS AND CONVERT TO ELECTRICAL R AS CAN BE USED OR BATTERY ED	1 TO 3	X				X							X							X-1	X-2	X-3	X				
	4 TO 6		X			X							X							X-4	X-5	X-6	X				
E ALMOST ALL INPUT ENERGY AT AND CONVERT SLOWLY ECTRICAL POWER; CHARGE RIES AND SPINUP FLYWHEEL DIRECTLY GENERATED RICAL POWER	7 TO 9			X			X		X	X	(X)		X							X-7	X-8	X-9	X				
	10 TO 11				X			X	X	X	(X)										X-10	X-11	X				
-TEMPERATURE PLASMA UCTION.	12 TO 14	X										X						X					X	(X)			X
IGNIFICANT HEAT STORAGE STEM	15 TO 17	X										X							X				X	(X)			X
	18 TO 19	X										X		X						X-18	X-19						
-TEMPERATURE PLASMA PRODUCTION	20 TO 22	X										X						X					X	(X)			X
STORAGE AFTER SECOND E FOR HEAT REJECTION	23 TO 25	X										X							X				X	(X)			X
-TEMPERATURE PLASMA UCTION.	26 TO 28	X										X						X					X	(X)			X
STORAGE AFTER FIRST CYCLE	29 TO 31	X										X							X				X	(X)			X
	32 TO 33	X										X		X						X-32	X-33						
LE. CYCLE DIRECT VERSION WITH DISCARD ERGY	34	X										X						X					X	(X)			
	35			X						X	(X)												X	(X)			
	36	X															X						X	(X)			
	37				X					X	(X)																
	38				X					X	(X)																

PAGE
QUALI

ENTIAL POWER CONVERSION SUBSYSTEMS

2 FOLDOUT FRAME

	CONVERSION OR STORAGE FROM FIRST CYCLE						FIRST-CYCLE REJECTED HEAT DISPOSITION								SECOND CYCLE ENERGY TRANSFER TO FLUIDS		SECOND THERMODYNAMIC CYCLE (BOTTOMING)						CONVERSION OR STORAGE FROM SECOND CYCLE						SECOND CYCLE HEAT DISPOSITION					
	OUTPUT/BATTERY	OUTPUT/INDUCTION	GEN./BATTERY	GEN./INDUCTION	MOTOR/FLYWHEEL/GEN./BATTERY	FLYWHEEL/GEN./BATTERY	THERMIONIC/BATTERY	RADIATOR	SECONDARY LOOP/RADIATOR	LiF PHASE CHANGE	LiH PHASE CHANGE	H_2O	HYDROCARBON PHASE CHANGE	DIRECT H.E. TO FLUID.	HEAT EXCHANGER		THERMIONIC	MHD	BRAYTON	RANKINE	STIRLING		OUTPUT/BATTERY	OUTPUT/INDUCTION	GEN./BATTERY	GEN./INDUCTION	MOTOR/FLYWHEEL/GEN./BATTERY	FLYWHEEL/GEN./BATTERY	RADIATOR	SECONDARY LOOP/RADIATOR	LiF PHASE CHANGE/RADIATOR	LiH PHASE CHANGE/RADIATOR	H_2O/RADIATOR	HYDROCARBON PHASE CHANGE
	X					(X)		X																										
	X					(X)		X																										
	X					(X)		X																										
	X							X																										
	X	(X)			X									X					X-12	X-13	X-14							X	X					
	X	(X)			X									X					X-15	X-16	X-17							X	X					
						X		X																										
	X	(X)			X									X					X-20	X-21	X-22							X					X	
	X	(X)			X									X					X-23	X-24	X-25							X					X	
	X	(X)			X					X					X				X-26	X-27	X-28		X						X					
	X	(X)			X					X					X				X-29	X-30	X-31		X						X					
						X					X				X				X-32	X-33			X						X					
	X	(X)						X			X																							
	X	(X)						X			X																							
	X	(X)						X			X																							
								X																										
								X				X																						

Photovoltaic Converter.

Photovoltaic converters of the p/n junction type which are fabricated for specific wavelengths can have up to 45% efficiency when converting laser monochromatic light (Ref. 1). Of course, these are only applicable to wavelengths less than 1 μm. An applicable photovoltaic cell may be the Al (Ga) As ternary. To assume the best forseeable performance, an efficiency of 45% at 473 K (200 °C) was utilized for wavelengths of approximately 0.5 μm. It was also assumed that intensities up to about 600 kW/m^2 were acceptable (approximately 500 suns).

The photovoltaic array was assumed to be the laser radiation receiver. Since the waste energy (55% of incident) must be removed, a circulated water heatsink was provided as shown in Figure 28. Between irradiations, the water is cooled by rejecting the heat to space from the back side of the receiver. Since the upper temperature of the water is fixed at about 450 K (for a cell temperature of 473 K), the heat storage for a given weight of water can be increased by lowering the initial temperature of the water. However, since the waste heat must be rejected between laser irradiations, a fixed energy input and heat rejection time will determine the water weight related to an initial temperature. A computer program was utilized to establish minimum water weights based on laser energy input and time available for heat rejection. This computer program also calculated the entire weight of the receiver consisting of the water, heat exchanger, substrate, and photovoltaic cells.

Thermoelectronic Converter

Background information for the thermoelectronic converter (TELEC) was derived from Refs. 2 and 3, and information from Rasor Associates. The TELEC is a plasma device which absorbs the laser beam by inverse bremsstrahlung with the plasma electrons. The principal configuration of the TELEC requires a narrowly focused, collimated beam with a long optical path in the plasma to absorb nearly all of the beam energy (Figure 29). Cesium provides a good media because of its low ionization potential and large atomic mass.

In a sense, the TELEC device is a heat engine which has a peak cycle temperature which is the electron temperature of the plasma. The electrons diffuse out of the plasma, striking two electrodes of different areas. The larger one is designated the "collector," and the smaller the "emitter." An electric current is generated between the electrodes.

The design concept shown in Figure 29 was selected by Rasor Associates since it does not require the emitter to be in the path of the laser beam. LMSC estimated the weight of this type of device, assuming that the emitter was tungsten, the collector and busbar molybdenum, and that the device was cooled by the melting of lithium hydride. (The heat stored in the lithium hydride could subsequently be used in other energy conversion processes.)

The energy conversion in a TELEC device is in real time, requiring storage of the electrical energy. This requires substantial battery capability, which was a major consideration in subsequent tradeoffs.

52

Preceding Page Blank

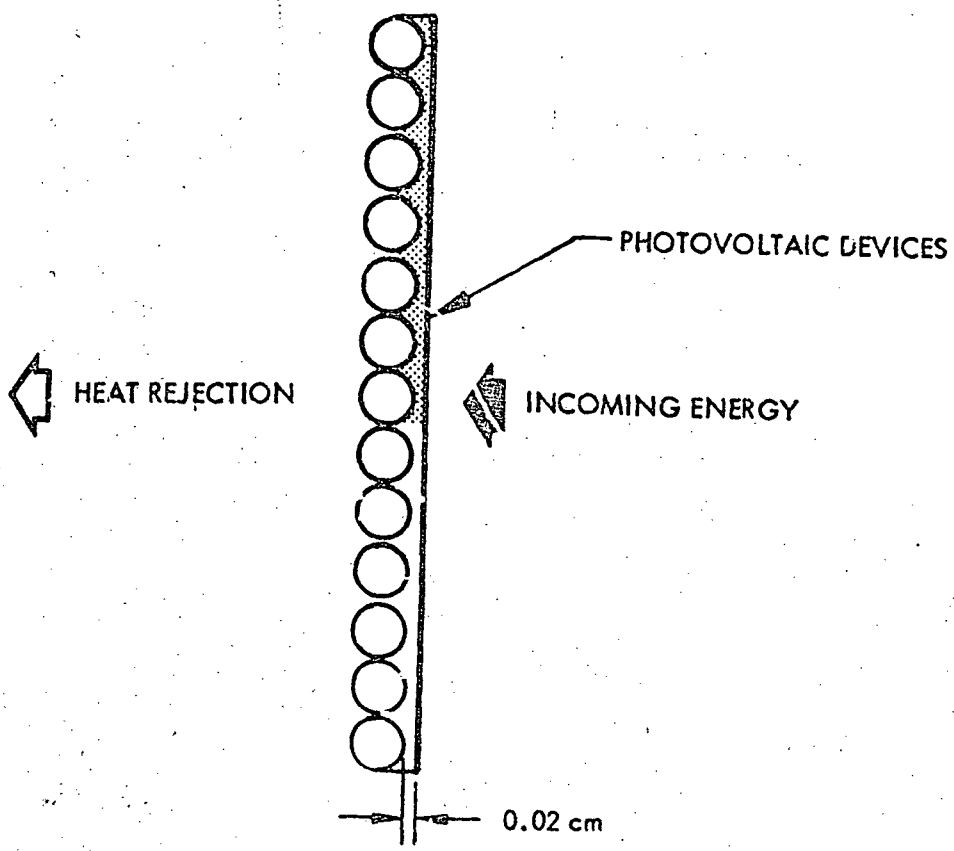

Figure 28. Photovoltaic receiver and thermal control

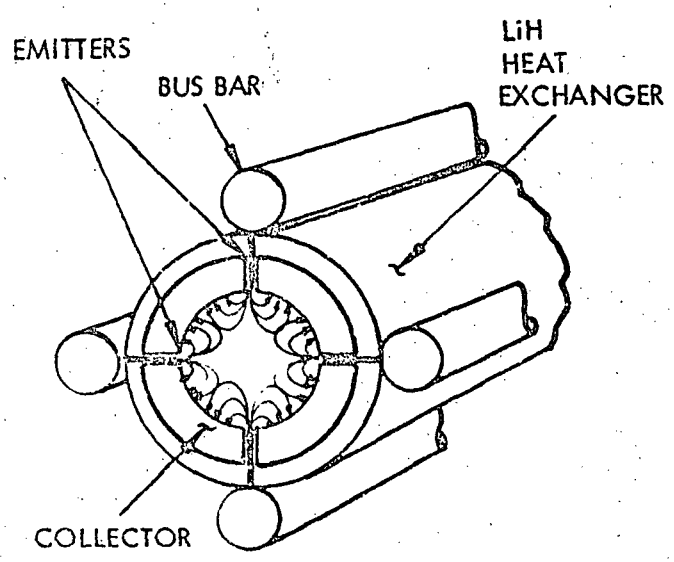

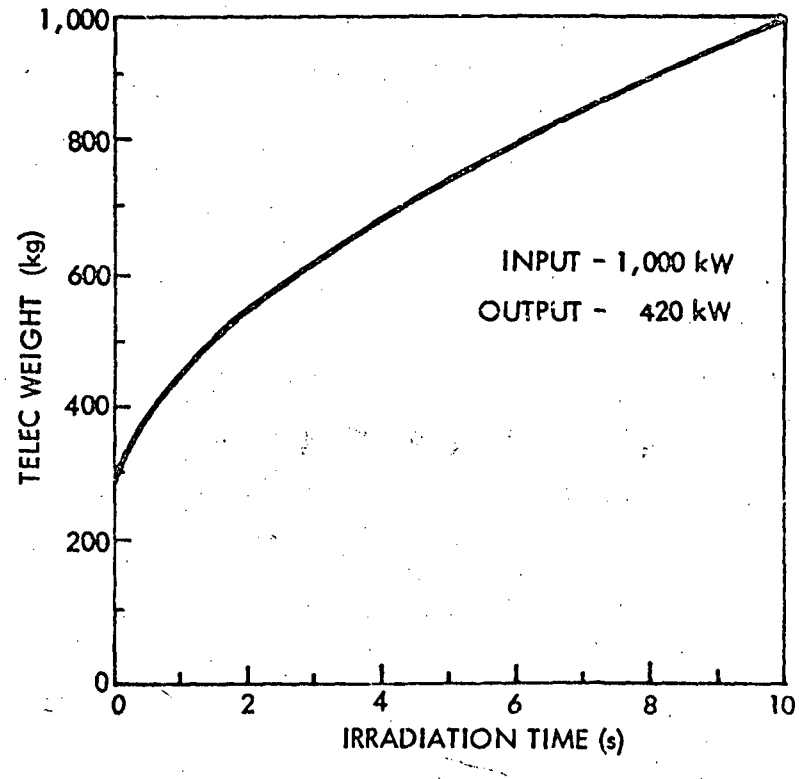

Figure 29. TELEC device concept and typical weights

Thermionic Converter

The thermionic devices convert heat directly to electricity. A metal electrode is heated sufficiently to emit electrons (the emitter). The electrons cross a narrow interelectrode gap and are collected by another metal electrode (the collector). The flow of electrons constitutes an electric current which provides power to the load. Data utilized in the analyses were derived principally from Refs. 1 through 4. Typical data are presented in Figures 30 and 31. The likely upper limit for the converters is 100 A/cm^2, which corresponds to less than 400 W/cm^2 of heat input. Therefore, in the design of the thermionic receiver, the energy distribution of the beam must be such that it does not exceed 400 W/cm at any point in the beam.

Brayton Cycle

The Brayton cycle evaluation was based on actual data compiled from a literature search and from cycle calculations which attempted to normalize the data to fixed parameters such as turbine inlet temperature. The literature search was extensive and evaluated both nuclear- and solar-powered Brayton cycles designed for space application. The data which were the basis for the power subsystem predicted mass and efficiency as a function of electrical power level, are presented in Table VI. The available data ranged from 0.5 kW_e output to multimegawatt output.

Evaluation of the available data led to the conclusion that the helium-xenon mixture would be superior for closed Brayton cycle applications. The effect of increasing working fluid molecular weight is a reduction in the turbomachinery rotational speed and an increase in the cycle pressure level while maintaining wheel diameter and specific speed. If a pure inert gas is used, an increase in molecular weight results in a decrease in heat transfer coefficient which translates to increased heat exchanger size (Figure 32).

However, by mixing highly conductive helium with a heavy gas, such as xenon, both the thermal conductivity and molecular weight can be increased with favorable results to the turbomachinery and the heat exchangers. Based on considerable development efforts with a He-Xe mixture at a molecular weight of 83.8 and the significant (~50%) reduction in heat exchanger size (as compared to an inert gas of equal molecular weight), the mix was selected for all Brayton cycle evaluations.

Cycle analyses and evaluations were conducted to determine the effect of electrical power output on cycle performance. Since a large number of factors, such as turbine inlet temperature, heat rejection temperature, turbomachinery efficiencies, system pressure drops and recuperator effectiveness affect overall power cycle efficiency, detailed cycle analyses were not accomplished in this study. The approach used was to compile Brayton cycle data over a range of power levels from 0.5 kW_e to several MW_e (Refs. 5 through 19).

However, only the 1 to 100 kW_e is presented in detail in Table VI since this appeared to be the range of greatest interest for Brayton cycle applicability in this study. Plotted data, such as cycle efficiency, are presented out to 1000 MW_e. Typical cycle

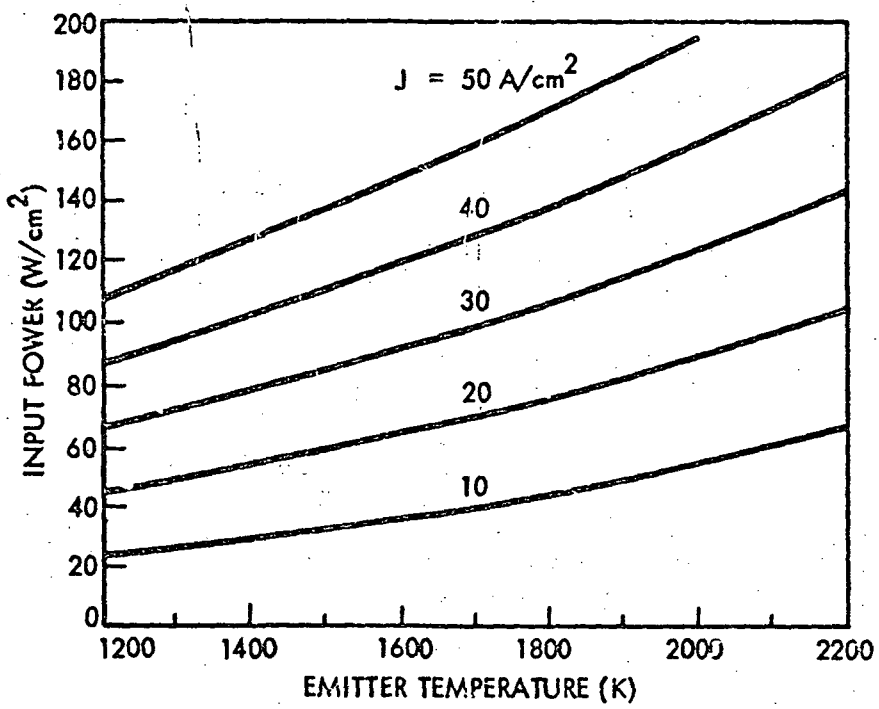

Figure 30. Converter input power requirements (Ref. 4)

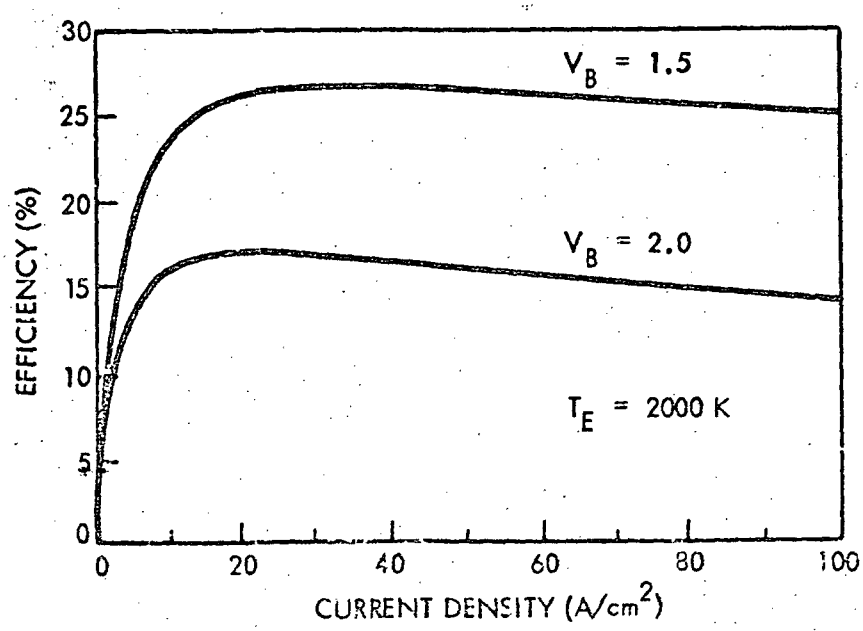

Figure 31. Converter efficiency as a function of current density and barrier index (Ref. 4)

TABLE VI. BRAYTON POWER SYSTEMS

References	5	6	6	6	9	10	6	6
Parameter								
Power Level (kW_e)	1.3	2.6	5	7.25	10.5	20	35	100
$\dot{m}$ (lb/s)	0.203	0.406	0.916	0.657	1.32	1.125	4.55	6.18
TIT (°R)	2,060	2,060	1,660	2,000	2,060	1,960	1,760	1,960
P_{t_1} (psia)	57.6	57.6	33.6	22.4	43.2	82.7	62.7	163.7
η_{cycle}	0.27	0.27	0.137	0.29	0.26	0.36	0.168	0.132
P_1 (psia)	37	37	33.6	12.25	23.7	31.3	62.7	81
T_1 (°R)	485	485	620	525	540	540	650	770
Working Fluid	He-Xe	He-Xe	Ar	He-Xe	Ar	Ar	Ar	He-Xe
Mol Weight	83.8	83.8	40	60	83.8	40	40	40
η_c	0.76	0.76	0.832	0.813	0.79	0.83	0.853	0.845
R_c	1.56	1.56	1.781	–	1.9	2.06	1.956	2.12
η_t	0.82	0.82	0.894	0.878	0.89	0.893	0.911	0.911
R_t	1.52	1.52	–	–	–	–	–	1.666
Rad. Area (ft^2)	31	62	329	600	790	798	1,466	2,800
Sink Temperature (°R)	390	390	–	400	450	–	–	388
BRU (lbm)	35	70	60	70	–	178	110	220
N	52,000	52,000	48,000	–	36,000	64,000	34,000	–
Radiator (lbm)	80	110	275	300	790	225	2,000	3,000
Recuperator (lbm)	106	212	50	+243 120	–	108	145	220
HEX (heat source)	55	110	60	260	–	750(3-5)	95	–
Controls	10	12	140	–	–	–	140	155
Ducting etc.	60	87	75	75	–	–	200	120
Specific Mass (lb/kW_e)	266	227	132	–	–	63	77	37

Notes:

$\dot{m}$ = mass flow
TIT = turbine inlet temperature
P_{t_1} = turbine inlet pressure overall
η_{cycle} = 8-cycle efficiency
T_1 = compressor inlet temperature
T_1 = compressor inlet temperature

η_c = compressor efficiency
R_c = compression action
η_t = turbine efficiency
R_t = expansion ratio
Rad = radiator

BRU = Brayton Rotating Unit (includes alternator)
N = RPM
HEX = heat exchanger

ORIGINAL PAGE IS
OF POOR QUALITY

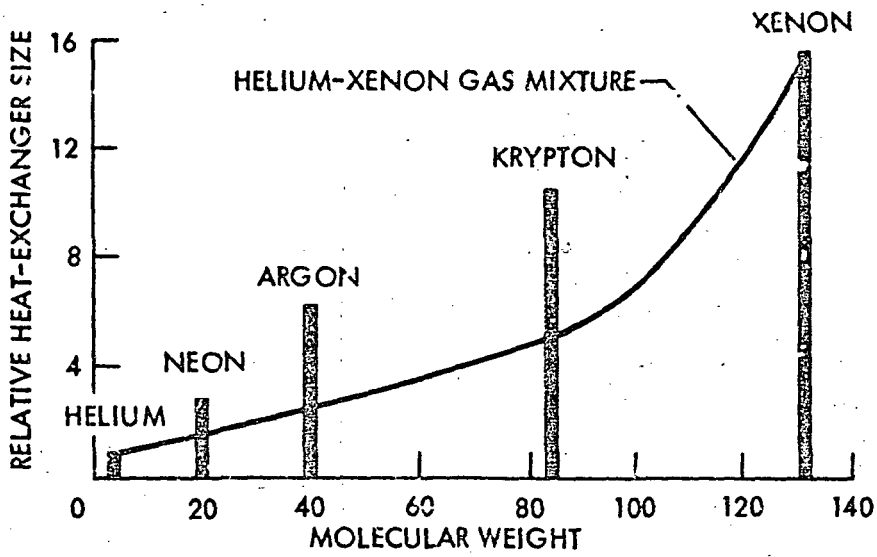

Figure 32. Effect of molecular weight on heat exchanger size (Ref. 5)

data are presented in Figure 33. The data were obtained from a number of brochures supplied by the AiResearch Division of the Garrett Corporation. The data illustrate a typical state-of-the-art Brayton cycle system, i.e., turbine inlet temperature of 1144 K, heat rejection temperature of approximately 220 K, and a helium-xenon working fluid with a molecular weight of 83.8. The system features a single stage radial compressor and a single stage radial turbine. As power levels increase, single stage turbomachinery can be used to at least the 100-kW_e level. As power levels reach the 1-MW range, it was assumed that both the turbine and compressor were multistage, axial-flow machines and appropriate component efficiencies and weights were used in the presented data.

Based on these assumptions and data from Refs. 6 and 7 and Table VI, it was found that compressor and turbine efficiencies formed a band of data. These predicted efficiencies are presented in Figure 34. The lower edges of the bands typify existing state-of-the-art equipments. The upper edges of the bands is a combination of actual equipment plus improvements that can be achieved in the future. These predicted efficiencies assume that single-stage radial flow turbomachinery will be used where possible. If specific speed for a single stage machine does not result in an acceptable efficiency, a multistage machine would be used.

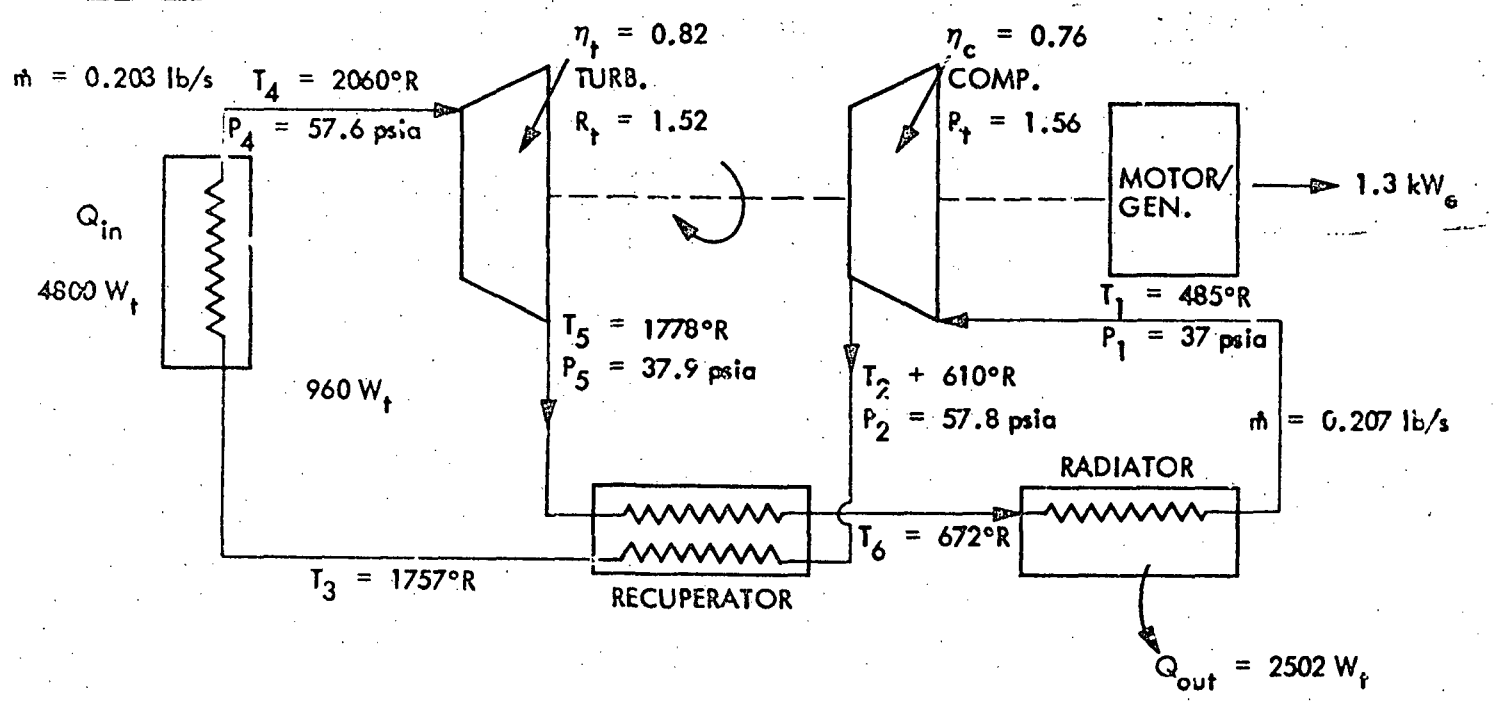

η_{cyc} = 27%
He-Xe = WORKING FLUID
Mol. Wt = 83.8

Figure 33. 1.3 kW_e Brayton cycle schematic

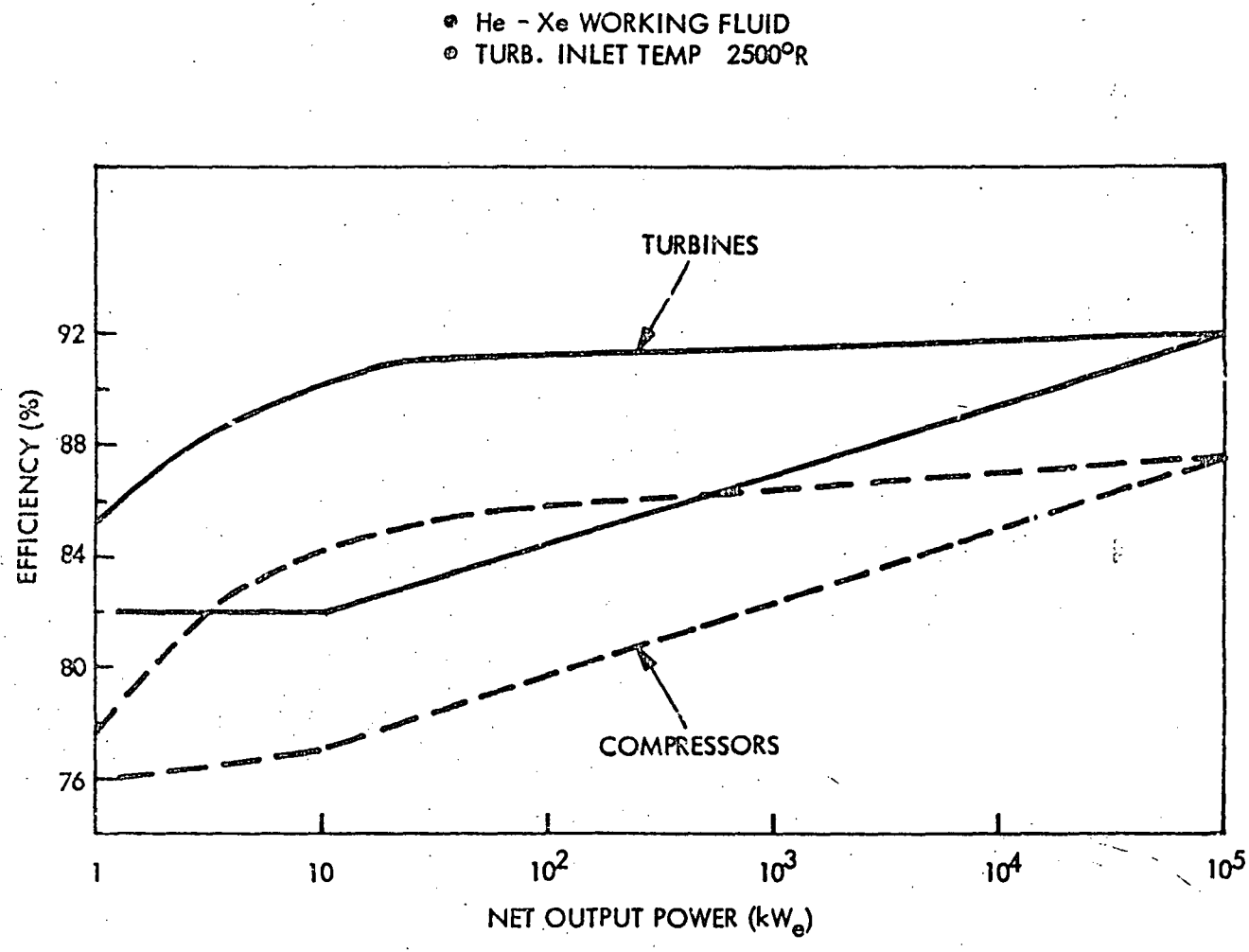

Figure 34. Brayton cycle turbomachinery predicted efficiencies

As power level increases, radiator size will increase. Therefore, the schematic shown in Figure 33 would be modified by changing from the gas radiator to a liquid radiator and a liquid/gas heat exchanger for cooling of the turbomachinery working fluid. The use of a liquid heat rejection loop may require increased radiator area but should result in lower overall system mass. The higher density cooling fluid results in higher heat transfer coefficients, lower system pressure drops, and lighter radiators as less armor thickness is required due to a smaller vulnerable area. Optimization studies were not conducted but review of available data indicates that the crossover between a gas and liquid radiator is in the 40 to 50 kW range.

Based on the data of related references and predicted trends for component efficiency improvements, Brayton cycle power system efficiencies were developed and are presented in Figure 35. The presented efficiencies are based on actual measured or calculated values for cycles reviewed in the literature search. The state-of-the-art approach (see Table VI) was considered to be a turbine inlet temperature (TIT) of 1144 K. This would allow use of conventional superalloys for turbine wheel materials. Advanced technology superalloys are predicted to increase turbine inlet temperature to the 1250 K range and for subsystem mass calculations, the higher temperature was used. The maximum TIT of 1395 K shown on Figure 35 is based on use of refractory materials, such as molybdenum, for the turbine wheel(s). While this would result in higher system efficiencies and lower system mass, for long-life application it is riskier and is not warranted for power levels of interest, i.e., 1 to 50 kW_e. For high-power levels, such as 1 MW_e or greater, the 1395 K TIT or even higher would be recommended due to the decreased mass and increased efficiency.

Brayton system specific mass was calculated and is presented in Figure 36. The calculated mass is for the Brayton cycle system only and does not include satellite structure, power conversion equipment other than the alternator, and the heat source for the Brayton cycle working fluid. The plotted data come basically from the data of Table VI, the cited references, and application of data from the references. Where possible, actual equipments weights were used and extrapolated for the effect of the 1250 K turbine inlet temperature. The 1250 K TIT was selected based on the use of advanced superalloy materials for the turbine wheel(s). Due to the improved overall cycle efficiency, all data presented in Figure 36 are for regenerated cycles. For the higher power levels (> 1 MW_e), multistage machinery is probable. Due to the increased complexity, it was assumed that where multistage turbomachinery is used, that no interstage cooling or reheating is used.

Rankine Cycle

The Rankine cycle data presented herein is a compilation of actual cycle data from the cited references. Where possible, actual cycles were obtained as were actual or predicted component weights from the reference material. Where data could not be conveniently acquired for a specific component, such as mass, it was estimated by using available data from similar equipments. The literature search reviewed proposed actual Rankine cycles for output powers from 1 kW_e to 12 MW_e. Both nuclear and solar heat sources were used and for the data presented herein, data from cycles using solar heat sources were favored as it is considered to be more like a laser source heat input.

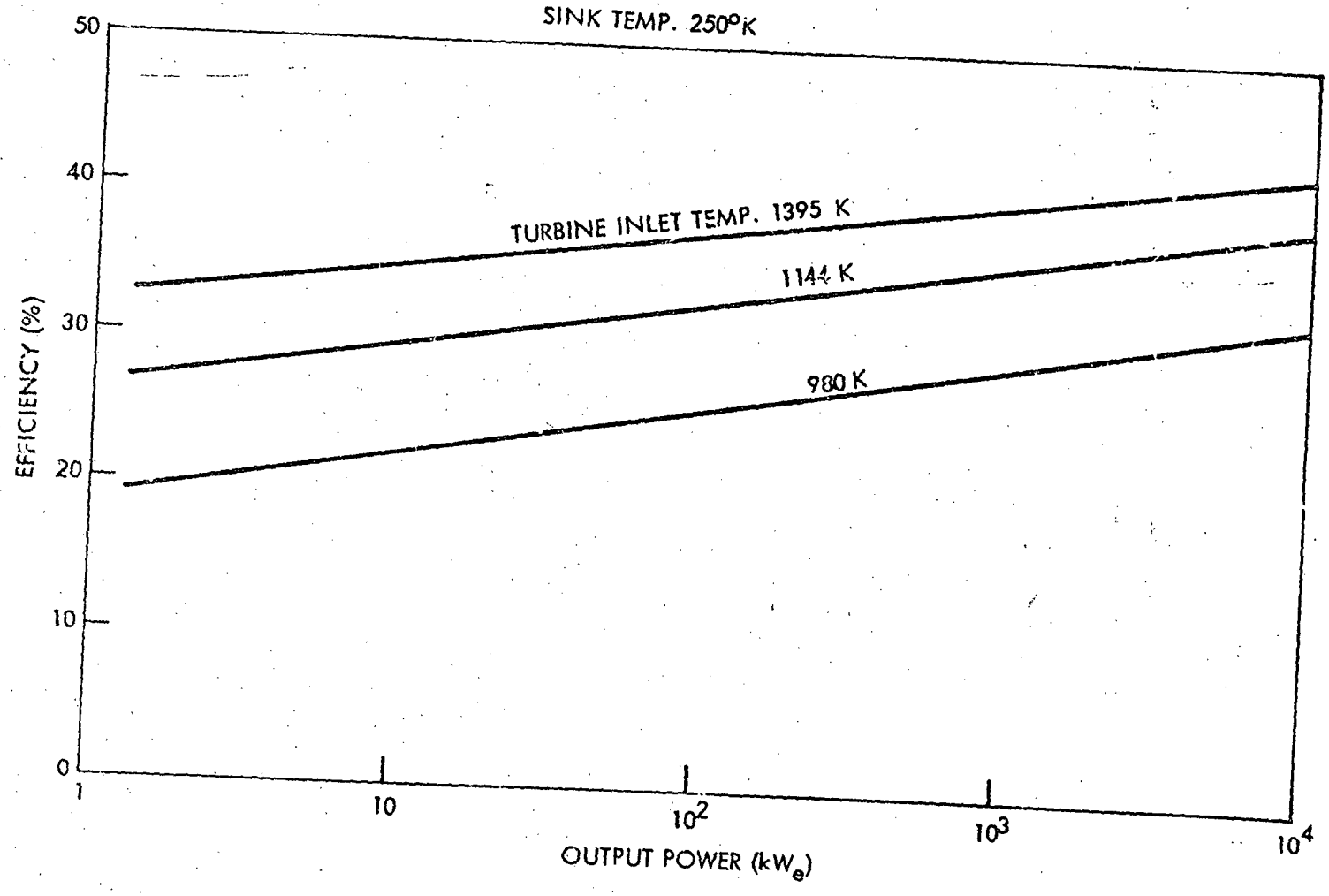

Figure 35. Brayton cycle efficiency

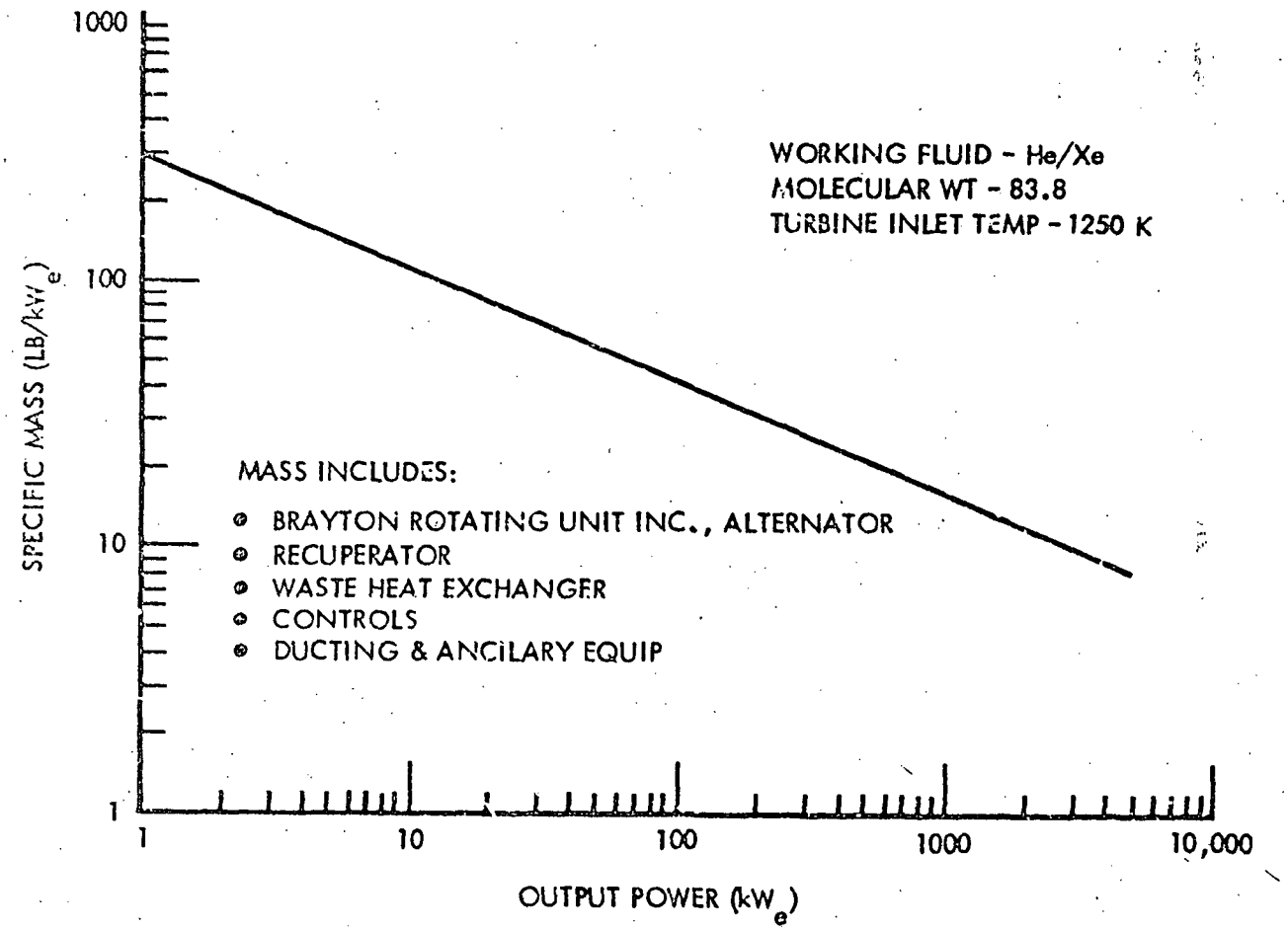

Figure 36. Brayton power system specific mass

The available data are presented in Table VII and as can be seen, ranges from organic fluids at the low power levels to potassium at the higher ends. Table VII does not present all the data obtained but is considered to be a representative sample for the power range evaluated. Specific references which supplied the data or the majority of the data for a given power level are also listed in Table VII. Some component mass data of Table VII were generated as available data did not always list all components. The areas left blank in Table VII were due to the lack of readily available data. As the range of data adequately covered the range of interest, extensive additional search was not deemed prudent.

The data of Table VII formed the basis of the specific mass curve presented in Figure 37. As noted, the specific mass does not include the heat source, or any heat storage media. Also, the data does not include any power conditioning equipment but does include the generator or alternator. Support structure is not included but interconnecting ducting for the Rankine cycle working fluid is included. The data represent the lower bound since the system would be used in the 1980's and available data were from the mid to late 1960's. Advancing technology should continue to improve in the areas of high strength, lightweight materials; thus the approach taken is deemed sound.

A typical Rankine cycle schematic is presented in Figure 38. The data is for an organic fluid and comes from Ref. 24. The schematic shows the basic components of a Rankine cycle power system with one addition for lower power Rankine cycles using organic fluids; that is, the regenerator. At higher power levels the jet condenser is replaced by a conventional condenser. In some cases the condenser is also combined with the radiator. Where data indicated, this approach was used in the component masses presented.

As can be seen from Table VII, Rankine cycle power system efficiencies would range from approximately 13 to 25%. As shown in Figure 39, these data follow a generalized pattern and are a function of cycle temperature ratio. It can be seen that maximum Rankine cycle efficiency will be on the order of 25%. If a binary cycle were used, it is probable that overall cycle efficiency on the order of 35 to 40% could be achieved.

Piston Engine Cycles

Based on the fact that Stirling and diesel cycles have theoretical higher efficiencies than the Brayton, these cycles were evaluated for potential onboard conversion of laser heat energy to electrical energy. An extensive literature search revealed a minimal amount of data on these cycles for the proposed application.

Review of data from Refs. 30 and 31 showed that for Stirling cycles, overall efficiency would be about 19% for the 0.5- to 1-kW_e range and approximately 40% for the 20- to 30-kW_e range.

However, the Stirling cycle has potential areas of concern for long-life application. As pointed out in Ref. 32, the cycle is sensitive to imperfect sealing of the piston rings and the crankcase seal. Both of these areas need major improvements before

TABLE VII. RANKINE CYCLE POWER SYSTEMS

Power Level (kW_e)	1.5	6.4	15	20	35	30	100	375	6,000
$\dot{m}$ (kg/s)	0.02	0.11	0.07	0.15	1.46	0.57	2.1	[illegible].44	130
T_1 (K)	645	645	1,228	645	950	950	[illegible]50	1,422	1,256
P_1 (psia)	109	–	–	106.8	265	240	240	163	79.[illegible]
η_t	0.70	0.75	0.83	0.78	0.60	0.70	0.73	0.813	0.84
N (rpm)	24,000	–	24,000	–	12,000	24,000	24,000	19,200	10,000
T_2 (K)	611	–	630	554	633	592	629	933	975
P_2 (psia)	0.25	–	0.1	0.12	14	7.[illegible]	14.5	5.44	8.5
η_{cycle} (%)	20.4	19.5	25.6	23.9	–	15.6	13.9	18.7	17.5
Working Fluid	Byphenyl	Dowtherm A	Hg	Dowtherm A	Hg	Hg	Hg	K	K
MASS (kg)									
Turbo Alternator	18	31	64	36	264	17	172	590	5,000
Condenser	20	19	36	40	54	160	622	109	1,200
Regenerator	20	23	–	–	66	–	–	–	–
Radiator	–	124	230	305	907	166	639	1,290	13,800
Fluid, Pumps, etc.	32	111	110	109	68	305	1,243	1,410	3,500
Controls	15	18	18	20	21	21	26	545	1,200
Sp. Mass (kg/kW_e)	70.0	50.9	30.5	25.5	39.4	24.1	27.0	10.5	4.1
References	3-20 3-21	3-22	3-23	3-24	1-5	3-20	3-20	3-25	3-26

Notes:

$\dot{m}$ = mass flow
T_1 = turbine inlet temperature
P_1 = turbine inlet pressure
η_t = turbine efficiency
N_2 = turbine speed
T_2 = turbine outlet temperature
P_2 = turbine outlet pressure
η_{cycle} = overall efficiency

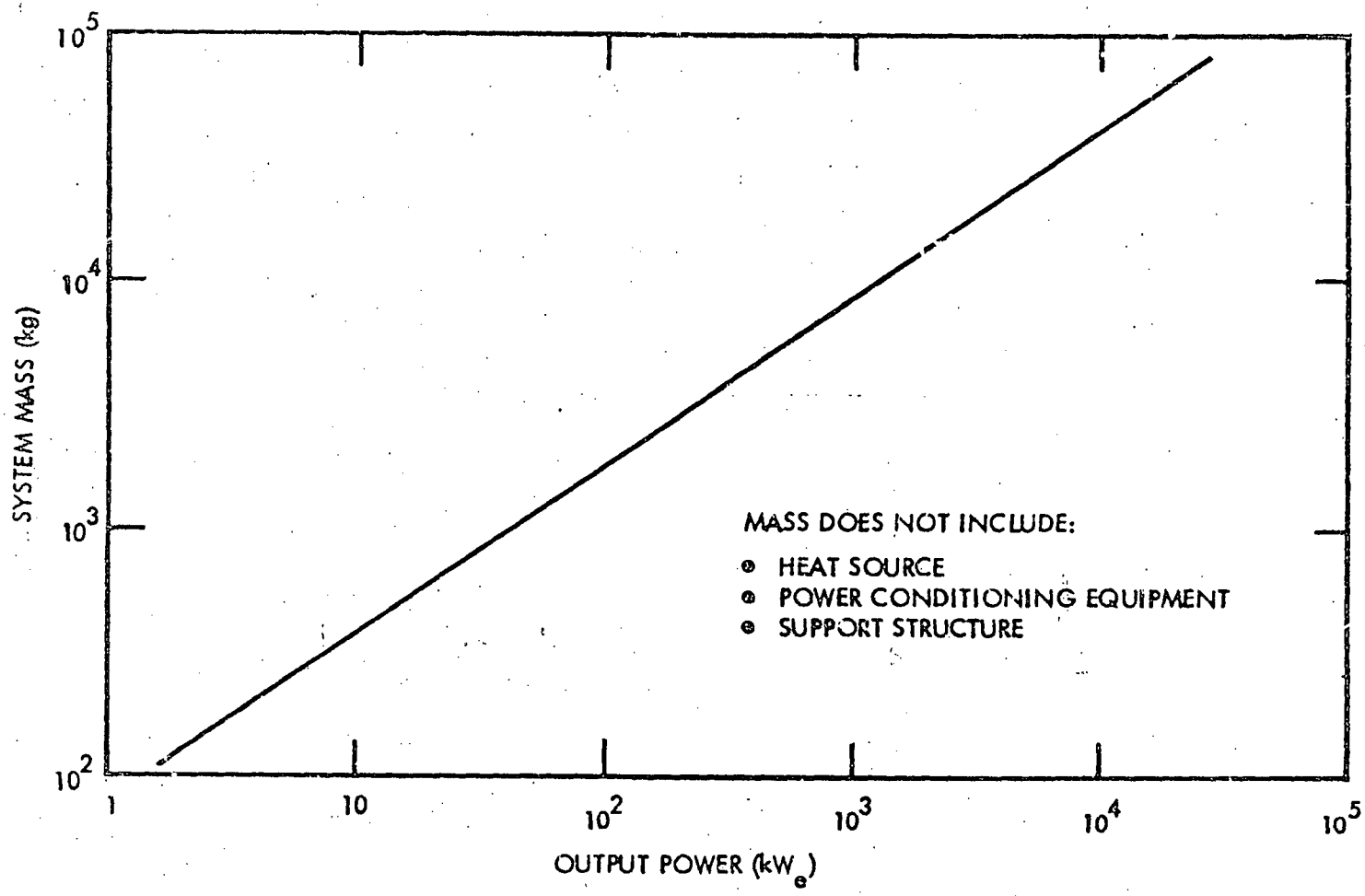

Figure 37. Rankine cycle power systems

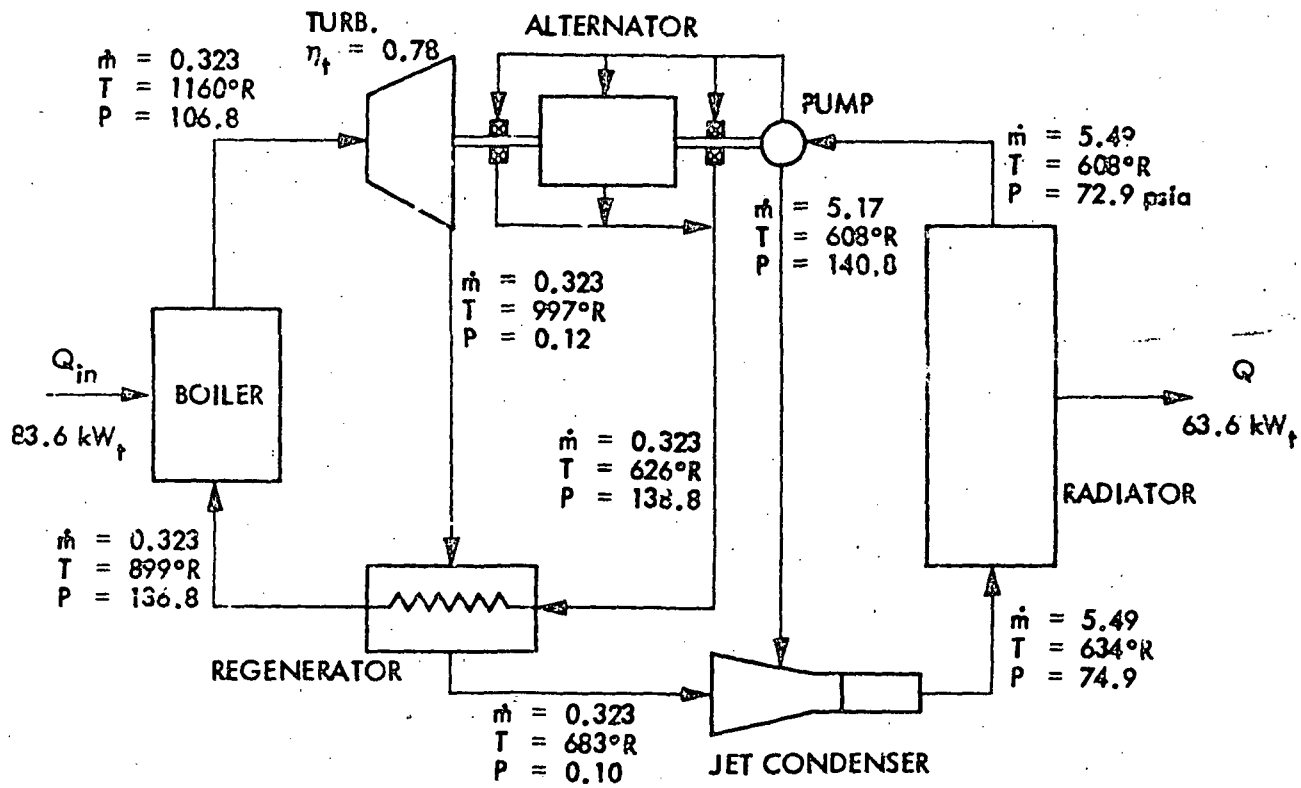

η_{cyc} = 23.9%

Figure 38. 20 kW_e Rankine cycle power system

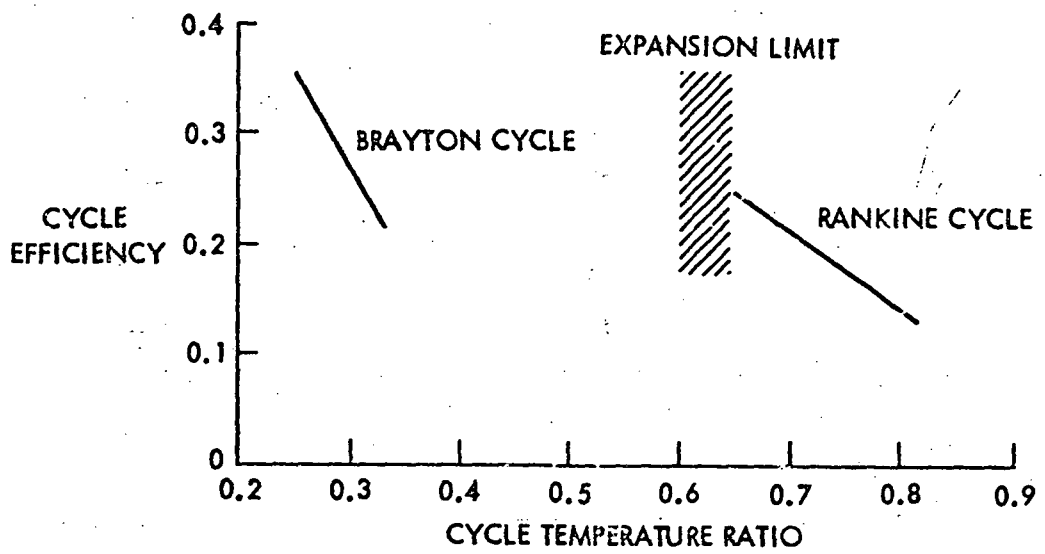

Figure 39 Dynamic Power Cycle Efficiency Comparison (Ref. 1)

multiyear life without maintenance can be considered. In addition, since helium or hydrogen are the most common working fluids, additional problems are presented with diffusion of the gases through the metal of the heater and the diaphragm seal.

In Figures 40 and 41, at low power levels (< 20 kW), the piston engine concepts have potential for the highest cycle efficiencies. As shown in Figure 40, the diesel cycle has a higher potential at lower power levels than even the high-efficiency Brayton/energy exchange cycle. As shown in Figure 41, the Stirling cycle has a higher potential efficiency than any other cycle.

However, since both of the cycles rely on piston rings to seal, they have the same potential seal/life problems. Additionally, they have not been demonstrated to any significant extent in the closed-cycle application. As shown in Figure 40, they also do not have a significant improvement in overall cycle efficiency as compared to the Brayton/energy exchanger cycle.

High-Efficiency Energy Exchanger/Brayton Cycle

As shown in the previous sections, the efficiency of typical Brayton and Rankine power cycles at power levels of interest would be in the order of 35 and 25%, respectively. The working fluid of these systems would be supplied heat by onboard phase-change

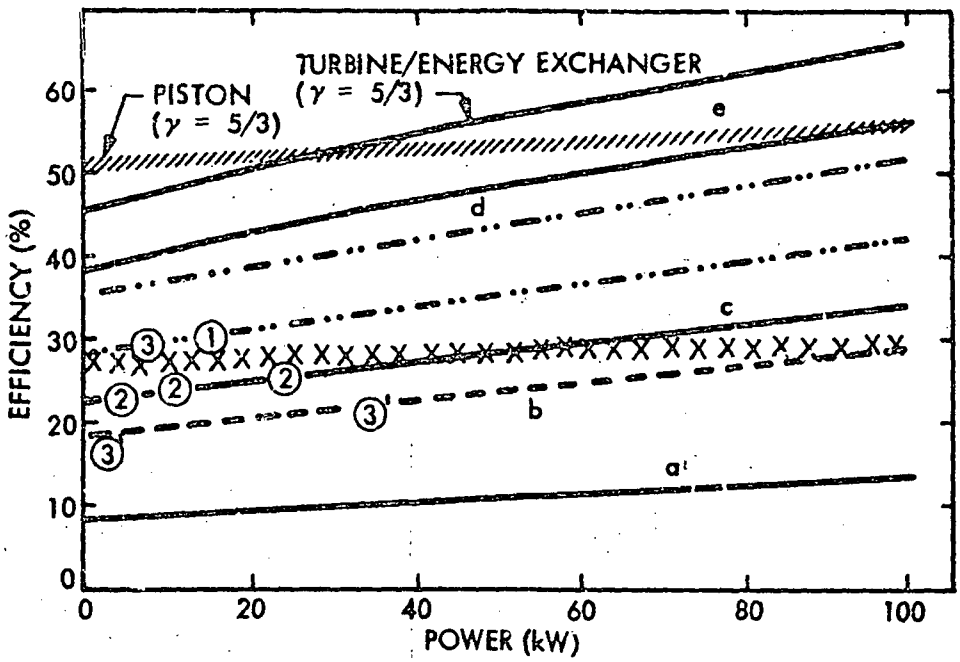

POINTS:

① SOLAR BRAYTON (Ar)

② SOLAR BRAYTON

/// DIESEL ENGINES, γ = 5/3 (Ar)

③ ISOTOPE BRAYTON (Xe/He)

③' SNAP 2 AND 8 BRAYTON (Xe/He)

xxx DIESEL ENGINE, γ = 1.24 (COMBUSTION)

CURVES:

a. COMPUSTION GAS TURBINES (FOR VEHICLES) WITH REGENERATION; T_{max} ~ 950 K, γ = 1.24

b. Ar GAS TURBINES (CLOSED CYCLE) WITH REGENERATION; T_{max} ~ 950 K, T_{min} = 345 K, γ = 5/3

c. He-Xe GAS TURBINES (CLOSED CYCLE) WITH REGENERATION; T_{max} ~ 1080 K, T_{min} = 300 K, γ = 5/3 (RANGE OF PERFORMANCE DUE TO COMPONENT EFFICIENCIES)

d. He-Xe GAS TURBINE/ENERGY EXCHANGER WITH REGENERATION; T_{man} ~ 3000 K, T_{min} = 300 K, γ = 5/3

e. SAME AS d AND WITH INTERCOOLED THREE-STAGE COMPRESSION (RANGE OF PERFORMANCE DUE TO COMPONENT EFFICIENCIES)

Figure 40. Overall efficiency comparison of power cycle concepts (Ref. 29)

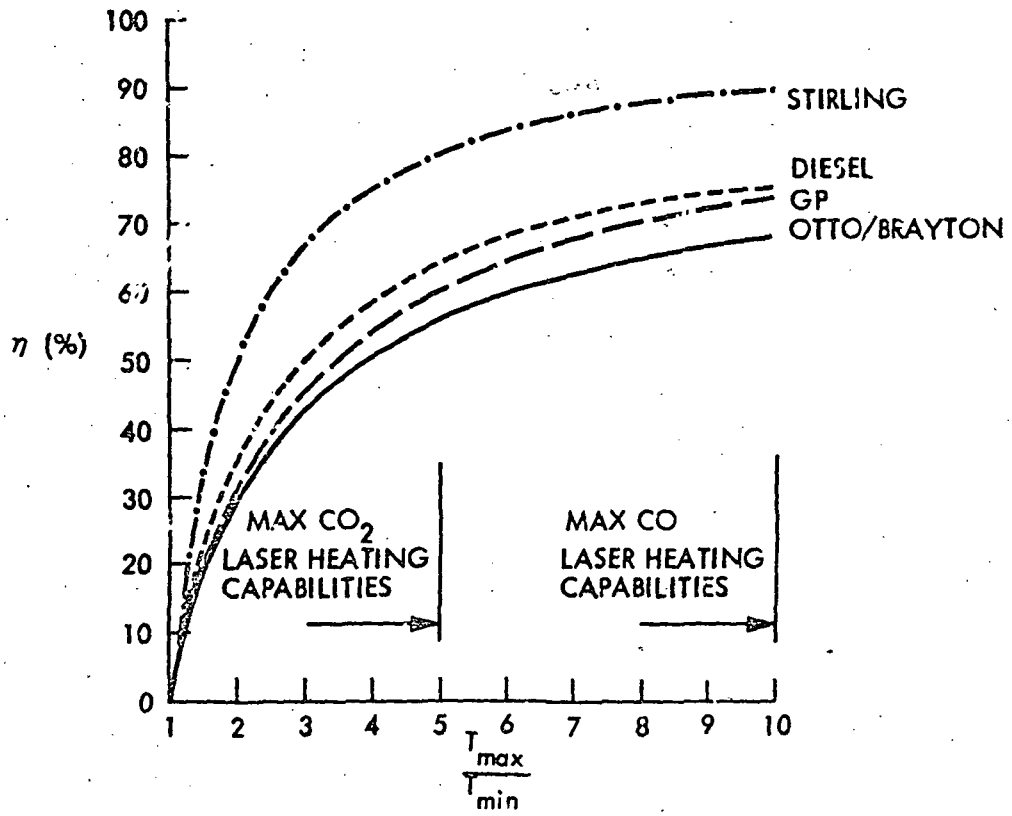

Figure 41. Comparison of maximum work Diesel, Otto, and Brayton cycles with GP and Stirling cycles (minimum and maximum temperatures and minimum pressure held constant)

material. These relatively low efficiencies would thus require a large mass for the heat storage to the detriment of the dynamic power system.

To improve overall cycle efficiency, a study was conducted of approaches that could be used with temperatures associated with laser heating of materials. One of the concepts evaluated was the use of a wave energy exchanger. Based on the work presented in Ref. 28, and others, a Brayton cycle combined with the wave energy exchanger has a predicted overall cycle conversion efficiency of 50% or greater in the 20- to 60-kW_e range.

The wave energy exchanger is a device which transfers work from one gas to another by unsteady gas dynamic compression and expansion within tubes which rotate with respect to stationary supply and exhaust manifolds. The proposed wave energy exchanger approach is described in detail in Ref. 27 where it is shown that the device can be used to circumvent the turbine inlet temperature limitations of gas turbines. That is, 1170 K, for superalloy turbine wheels which would be required to operate continuously for many years.

The approach used to determine the estimated efficiency of a Brayton cycle using an energy exchanger was to apply the techniques of Refs. 28 and 29. As previously stated, turbine inlet temperature was limited to 1170 K and based on use of a phase-change material for storage of the beamed onboard laser energy, the energy exchanger inlet temperature was limited to 2150 K.

Based on the work presented in Refs. 28 and 29, a Brayton-type power cycle was constructed and is presented in Figure 42. As can be seen, the cycle features three compressors in the driver gas loop (Loop D). The cycle also features a 300 K minimum temperature and 1170 K into the regenerator which is deemed to be the maximum allowable for multiyear use. The selection of three intercooled compressors was based on work reported in Ref. 29 which found this arrangement to be the best configuration.

The use of the wave energy exchanger requires that there be impedance matching between the driver and the driven gas (loop D and loop d). The driven gas must be of a lower molecular weight and the ratio of molecular weights must equal the ratio of turbine inlet temperature to cycle maximum temperature. Using Figure 42 as a reference, this becomes:

$$\frac{T_{11}}{T_8} = \frac{M_{11}}{M_8} = \frac{1170}{2150} = 0.544$$

Based on previous Brayton cycle analysis, a helium-xenon mixture at a molecular weight of 83.8 was selected for the driver gas. Using the above ratio, a molecular weight of 45.6 was calculated for the driven gas. Using a regenerator effectiveness of 0.9, an energy exchanger efficiency of 0.85, the compressor (η_{CD}) and turbine (η_{td}) efficiencies shown on Figure 42 and the equations derived in Ref. 28, cycle

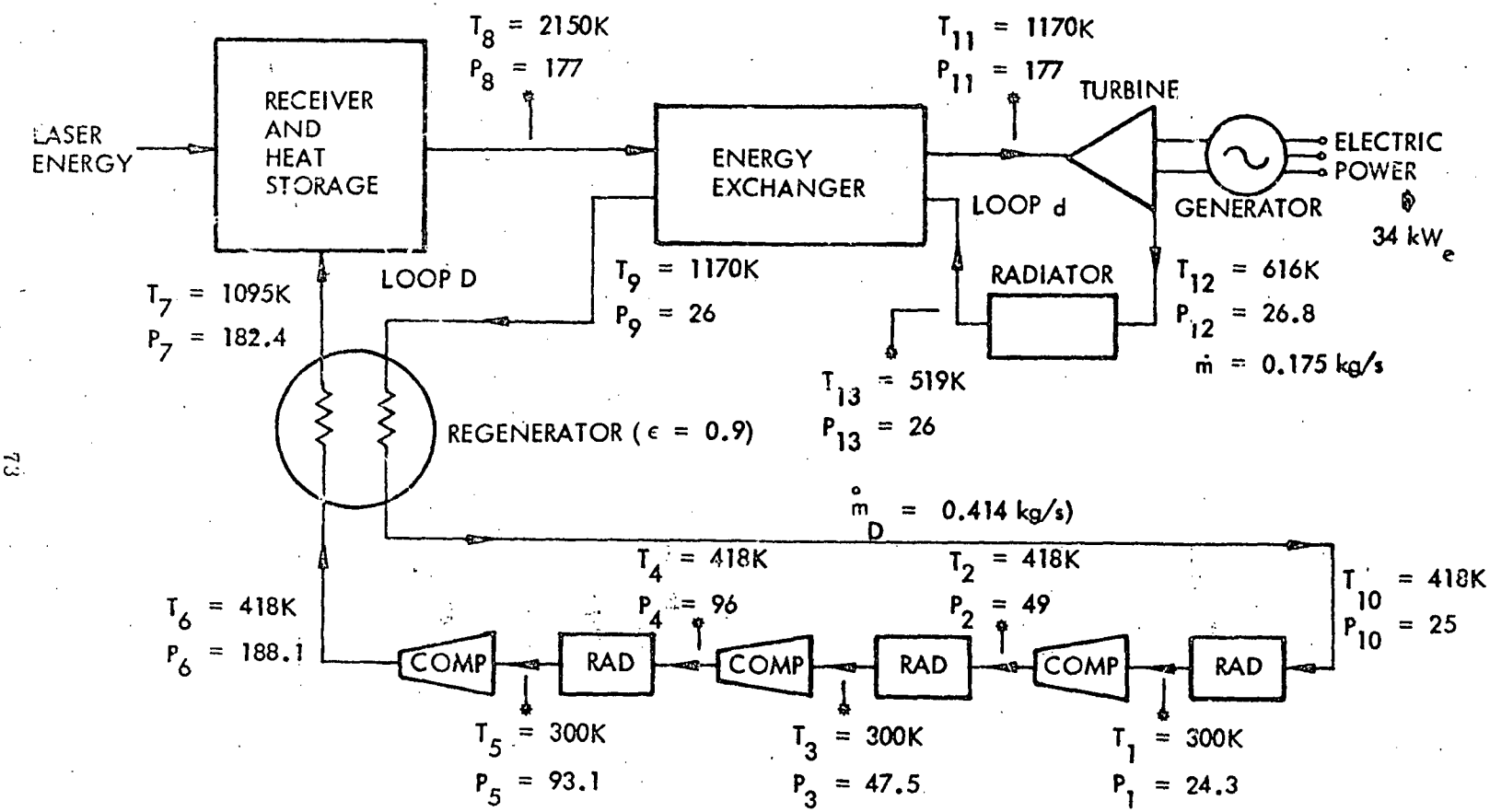

NOTE: (1) ALL PRESSURES ARE IN PSIA
(2) LOOP D FLUID IS He-Xe, Mol. Wt = 83.8
(3) LOOP d FLUID IS He-Xe, Mol. Wt = 45.6
(4) OVERALL CYCLE EFFICIENCY = 49.5%
(5) η_c = 0.823 and η_t = 0.894

Figure 42. Energy exchanger/Brayton cycle power system

calculations were made. The computed pressures and temperatures are shown in Figure 42 and resulted in an overall cycle efficiency of 49.5%. As shown in Figure 42, the output power is 34 kW_e and based on an alternator efficiency of 90% the mass flow weights for the two loops (D and d) are calculated and are shown on the figure.

The three compressors would be radial flow machines and have a pressure ratio of 2.02 each. Based on an assumed speed of 24,000 rpm, the specific speed was calculated using the equation:

$$N_s = \frac{NQ^{1/2}}{H_{id}^{3/4}}$$

and found to be 130. This value is in the range where the assumed compressor efficiency of 82.3% can be achieved (Ref. 3-13).

Using the same techniques and assuming a radial flow turbine for a specific speed of 50, a turbine speed in excess of 200,000 rpm was calculated. Since this is not only an unacceptably high speed but does not match compressor speed, it was concluded that multistages would be required. Since multistage radial flow turbines result in a complicated machinery arrangement and interstage reheat was not required, it was concluded that the turbine should be a multistage axial flow machine. Detailed calculations on the turbine were not done but rudimentary calculations indicate that it would be a 7- to 8-stage machine to get a rotation speed that matched the compressor and could satisfy the temperature and pressure ratios required for the cycle.

Based on available data for the types of components that are used in the cycle, subsystem mass was estimated and is shown in Table VIII.

TABLE VIII. HIGH EFFICIENCY ENERGY EXCHANGER/BRAYTON CYCLE SUBSYSTEM MASS (kg)

	Quantity	Mass
Compressors	3	28
Turbine	1	30
Alternator	1	32
Recuperator	1	66
Driver Loop Heat Rejection S/S	AR	600
Driven Loop Heat Rejection S/S	AR	690
Controls		64
Plumbing, etc.		90
		1,600

The energy exchanger mass was not included as data were not available to do a calculation. Also not included would be the heat storage material, the heat source heat exchanger, any satellite support structure or the power distribution equipment.

3.2.4.3 Energy Storage

As discussed in section 3.2.2, the energy transfer opportunities dictate that the laser energy must be transferred at a high rate, followed by use of this energy by the satellite over a long period of time. This requires some form of efficient energy storage.

Electrical Energy Storage

The high charge rate associated with energy transfer by laser radiation imposes very severe requirements on batteries. Conventional solar cell electrical power systems charge the batteries while the satellite is in sunlight, and the batteries discharge while the satellite is in the earth's shadow. Energy transmission by laser must occur during the transfer opportunities, and enough storage must be provided until the next opportunity. In addition to the high charge rate considerations, battery cycle life is an important consideration, and cycle life is dependent upon the degree of discharge allowed. In turn, the degree of discharge is directly related to the weight of batteries required.

Nickel-cadmium cell weight relative to a dimensionless charge rate is shown in Figure 43. The feasibility of cell construction, as a function of charge-rate and cell capacity, is shown in Figure 44. Cycle life relative to the degree of discharge is presented in Figure 45, also as a function of operating temperature. Scaling factors relating the NiCd data to the nickel-hydrogen (NiH_2) and regenerative fuel cells (RFC) are as follows.

$$\text{Weight}_{NiH_2\ \text{System}} = 0.6\ \text{Weight}_{\text{NiCd System}}$$

$$\text{Weight}_{\text{RFC System}} = 0.3\ \text{Weight}_{\text{NiCd System}}$$

$$\text{Volume}_{NiH_2\ \text{System}} = 2.5\ \text{Volume}_{\text{NiCd System}}$$

$$\text{Volume}_{\text{RFC System}} = \left[1 + 2\left(\frac{10 - P}{10}\right)\right] \text{Volume}_{\text{NiCd System}} \quad \text{if } P < 10\ \text{KW}$$

$$= \text{Volume}_{\text{NiCd System}} \quad (\text{if } P \geq 10\ \text{KW})$$

The battery data were employed in analyses to determine the weights of batteries required for satellite requirements which were representative of those in the mission model. The results are presented in Figure 46. As shown, the optimum degree of discharge appears to be at about 36%. This value was utilized in the analyses.

Mechanical Energy Storage

The conversion of laser energy to mechanical energy for storage requires the production of electrical power (by some means such as TELEC) and the operation of an

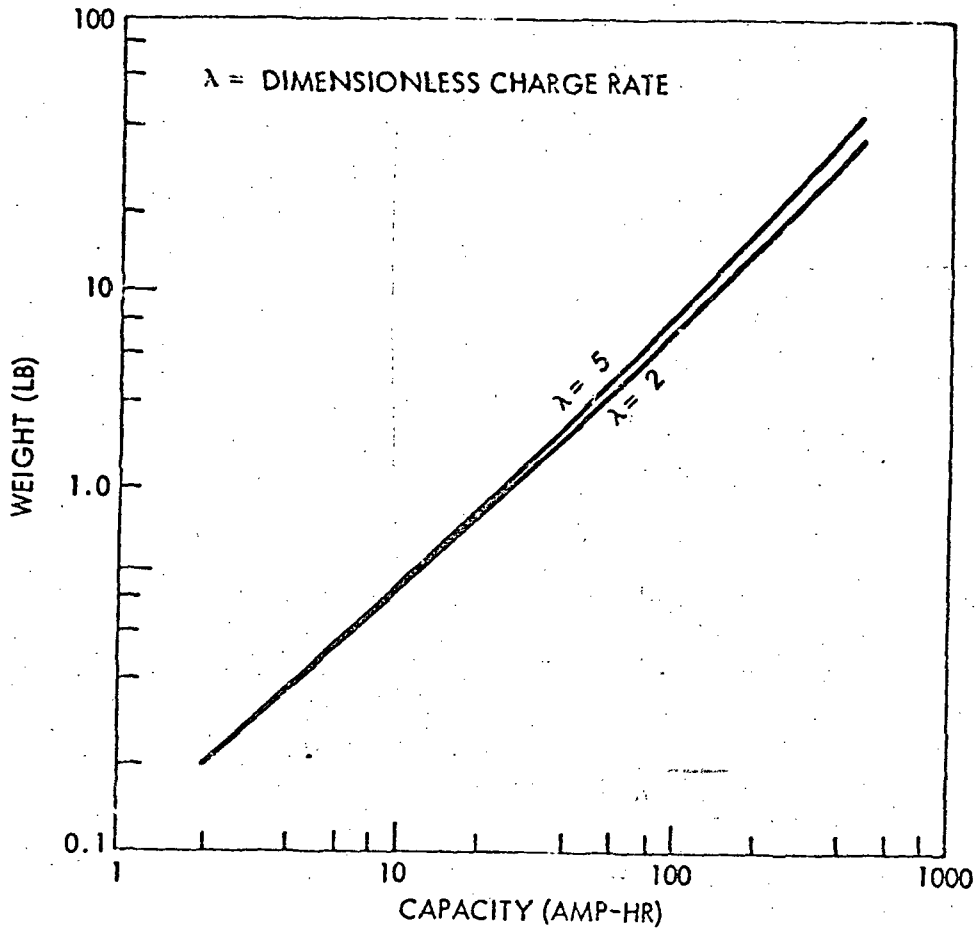

Figure 43. NiCd cell weight

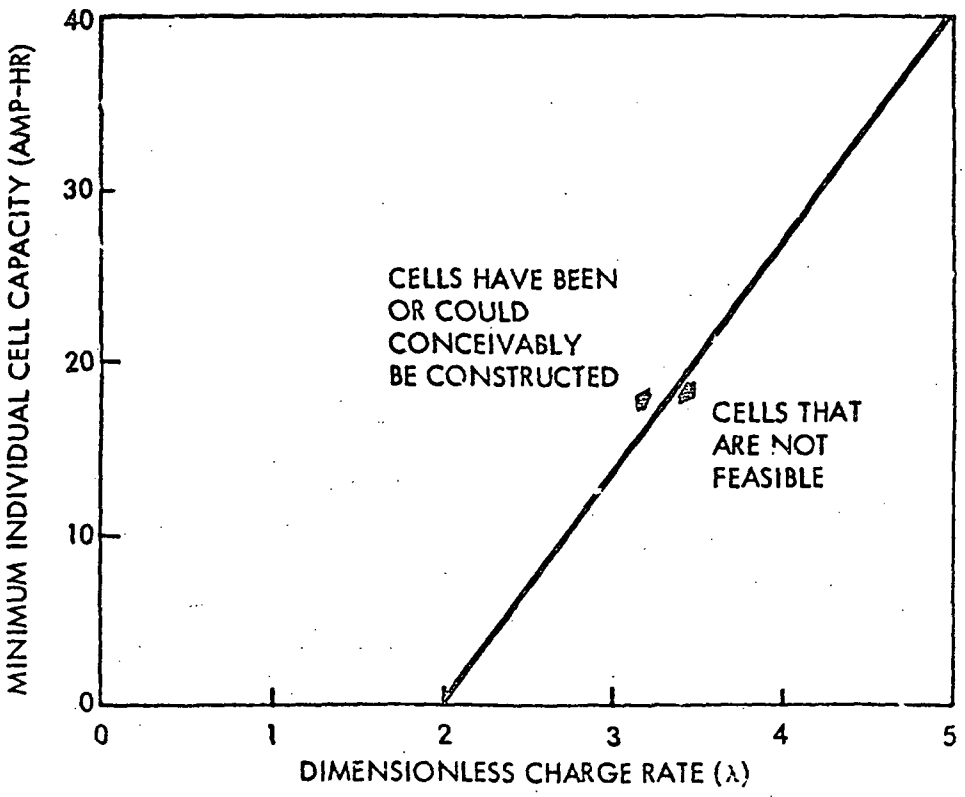

Figure 44. Feasible storage cells

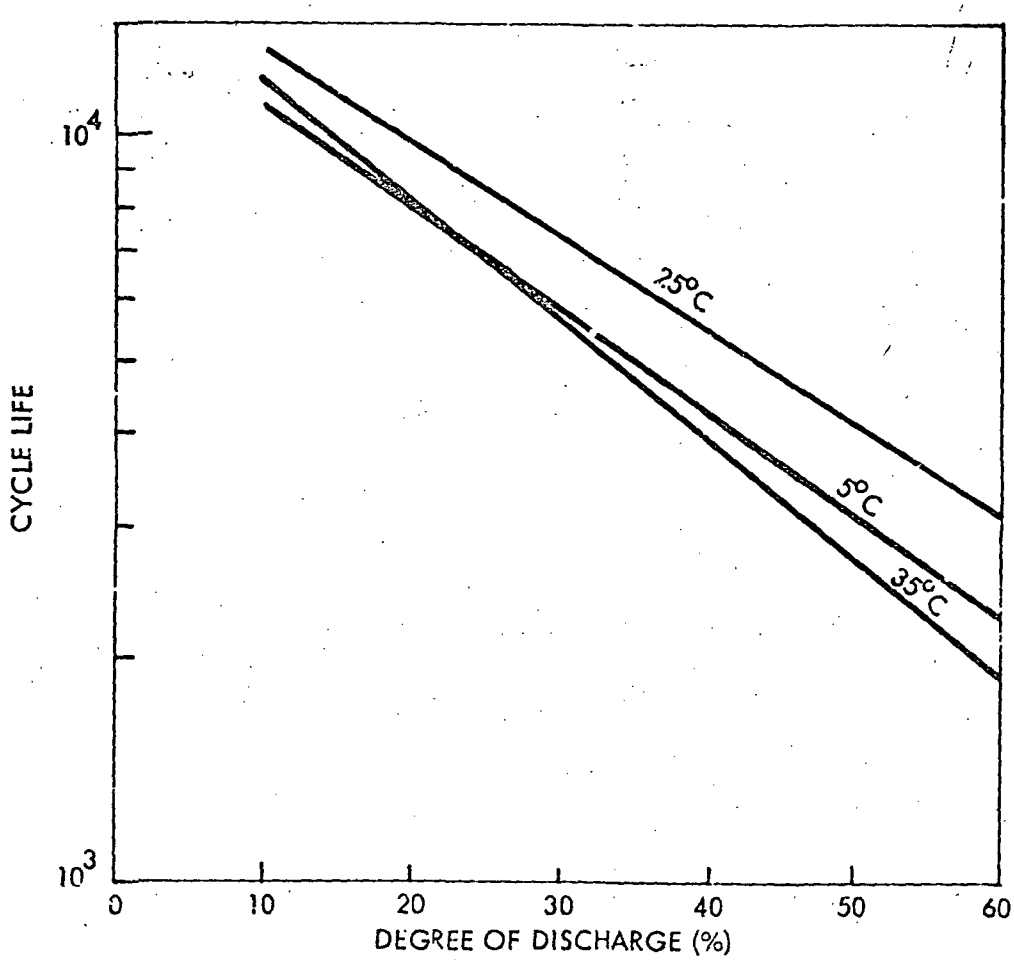

Figure 45. Temperature effect to cycle life

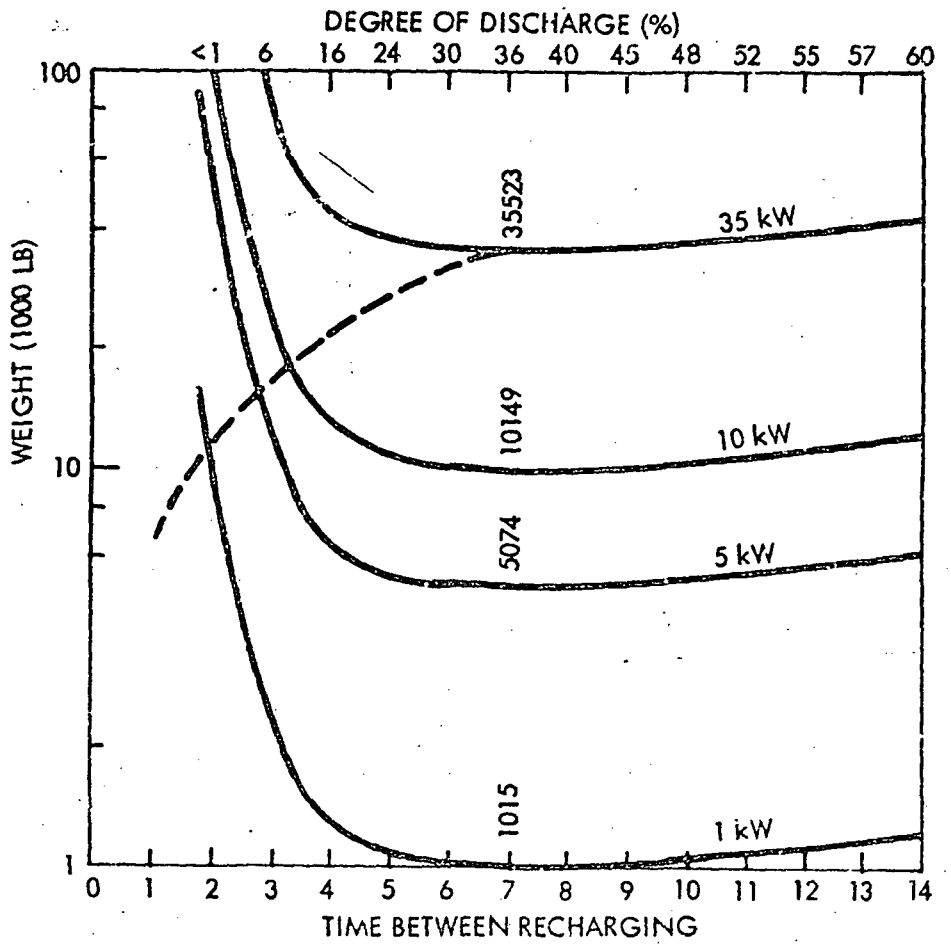

Figure 46. Nickel-cadmium battery optimization

electric motor to store the energy in a flywheel. To remove the stored energy requires that the flywheel transfer its energy to an electric generator. One of the related problems is speed control As energy is taken from the flywheel, its speed drops. However, there cannot be large speed variations in the electrical generator, which leads to substantial energy transmission problems.

The state-of-the-art in flywheel technology is presented in Figure 47. The maximum achievable energy density in future years appears to be less than 100 W-hr/lb.

Heat Storage

The laser energy may be stored as heat and then converted to electrical energy on a demand basis. This can be accomplished by having the heat storage as an integral part of the receiver. Possible approaches which were examined are presented in Figure 48.

Heat Storage in Photovoltaic Concept. The storage of heat in the photovoltaic concepts is for the purpose of heat rejection. The temperature of the water is too low for use in efficient thermodynamic cycles.

Heat Storage for Use in Mechanical Energy Conversion. Heat can be stored in high temperature molten salts, as shown in Figure 48, for use in efficient thermodynamic cycles. The only practical method is to provide for energy storage by having materials with high heats of fusion and sufficiently high melting temperatures.

If heat storage is used in conjunction with thermionic devices, then the temperature of the molten salt must be sufficiently low to allow the device to function efficiently. This is approximately 1000 K if the emitter is operating at 2000 K.

The heat is transferred to the energy conversion subsystem by heating the working gases (or liquids) by means of heat exchangers in contact with the molten salt.

3.2.5 Evaluation of Power Conversion System

3.2.5.1 Evaluation of Real-Time Conversion to Electrical or Mechanical Energy

As discussed in previous sections, the time available for energy transfer by laser is relatively short. Energy that is transferred must be stored rapidly. The principle real-time conversion methods are shown in Table IX. Since the real-time conversion produces electrical energy at a high rate, it must be stored in batteries, induction storage, or transferred to a flywheel.

TYPE	SHAPE	ENERGY DENSITY (W-HR/LB)
CONSTANT STRESS		CURRENT ISOTROPIC MATERIAL: 3-14 COMPOSITE MATERIAL: 10-30
NEAR CONSTANT STRESS		
CONICAL DISK		NEAR TERM (3-5 YRS) ISOTROPIC MATERIAL: 5-15 COMPOSITE MATERIAL: 30-40
FLAT DISK		FAR TERM (7-10 YRS) COMPOSITE MATERIAL: 60-70
THIN RIM	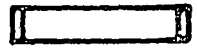	

Figure 47. Flywheel summary

TYPE	STORAGE TEMP. (K)	HEAT STORAGE MATERIAL	CONFIGURATION
PHOTOVOLTAIC	450 (MAX)	H_2O	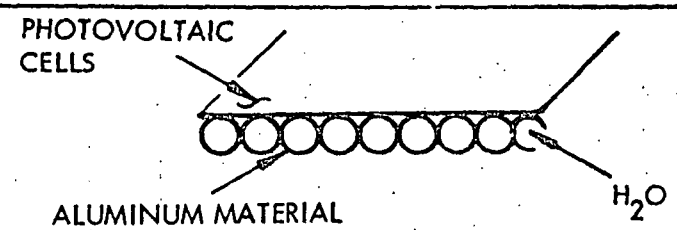
CONVENTIONAL BRAYTON, RANKINE, OR PISTON	1700	SILICON	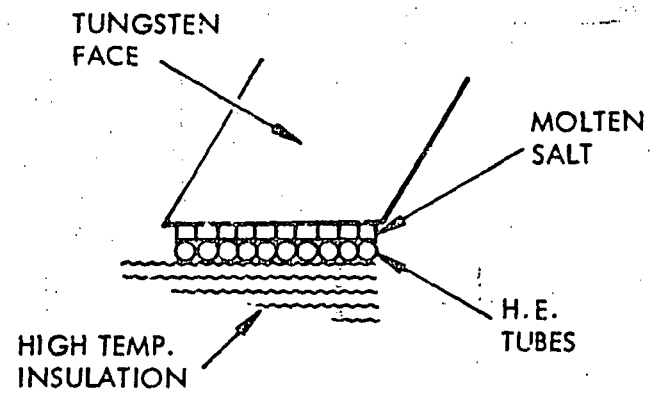
ENERGY EX-CHANGER WITH BRAYTON OR RANKINE	2100	$BeO + M_gO$	
THERMIONIC RESIDUAL HEAT	950	LiH	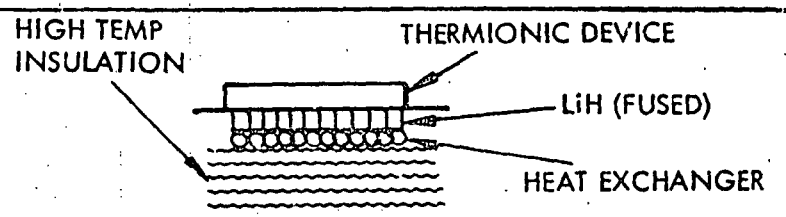

Figure 48. Heat storage receivers

TABLE IX. REAL-TIME CONVERSION TO ELECTRICAL OR MECHANICAL ENERGY

RECEIVER	CONVERTER	ENERGY STORAGE	WASTE HEAT DISPOSITION
PHOTOVOLTAIC	PHOTOVOLTAIC	BATTERIES (OR INDUCTION)	H_2O STORAGE AND RADIATION
THERMIONIC	THERMIONIC	BATTERIES (OR INDUCTION)	LiH STORAGE AND RADIATION
TELESCOPE (CONCENTRATOR)	BRAYTON, RANKINE, OR PISTON	BATTERIES OR INDUCTION	RADIATOR WORKING FLUID)
		FLYWHEEL/ GENERATOR	
TELESCOPE	TELEC	BATTERIES (OR INDUCTION)	LiH STORAGE AND RADIATION
TELESCOPE	ENERGY EXCHANGER WITH BRAYTON, RANLINE, OR PISTON	BATTERIES (OR INDUCTION) FLYWHEEI/ GENERATOR	RADIATOR (WORKING FLUID)

Preliminary Screening

A preliminary screening was performed which eliminated most of the concepts presented in Table IX. The preliminary screening indicated the following:

- Photovoltaic. The potentially high efficiency of the advanced technology photovoltaic devices for converting laser energy dictated that this should be evaluated.
- Thermionic. The low efficiency of this concept indicated that it should not be considered for real-time conversion. (Employed later as a topping cycle).
- Brayton, Rankine, or Piston (With or Without Energy Exchanger). The Brayton, Rankine, or Piston energy conversion concepts may be used either to generate electricity which is stored in batteries or induction circuits or to directly spin-up flywheels. The required high power and the short operating times required for real-time conversion result in very large units. Real-time laser power conversion is not an appropriate application for the rotating machinery conversion units.
- Thermoelectronic. The TELEC device had sufficient efficiency potential to warrant a more detailed evaluation.

Results of the Evaluation of Real-Time Conversion

The output requirements for the conversion systems were established at 34 kW for 3-hr, with a laser irradiation period of 108 seconds. These requirements were selected as being representative of the mission model.

Photovoltaic/Batteries. The results of the evaluations are illustrated in Figure 49. As shown, the efficiencies indicate that 10,070 kW of laser energy must be absorbed for a period of 108 s (1,087,560 kJ). The basic weight of this system is 13,340 kg.

Thermoelectronic/Batteries. The TELEC device requires a telescope to collect and direct the laser radiation. The waste heat from the TELEC device is stored in lithium hydride and then radiated. The required laser energy absorbed was 10,740 kW for 108 s (1,159,920 kJ). The weight of this system was 12,950 kg. The results are shown in Figure 50.

3.2.5.2 Evaluation of Real-Time Conversion to Electrical Energy Plus Bottoming Cycle With Delayed Conversion

The real-time conversion presented in the previous section results in waste heat which potentially could be stored and subsequently used in another conversion system as dictated by the satellite electrical power requirements. The possible approaches are shown in Table X.

As in the case of the previous evaluations, the requirements were based upon 34-kW output for 3 hr, with a laser irradiation time of 108 s. The efficiencies of the topping cycles and the bottoming cycles result in the split between the power outputs of each.

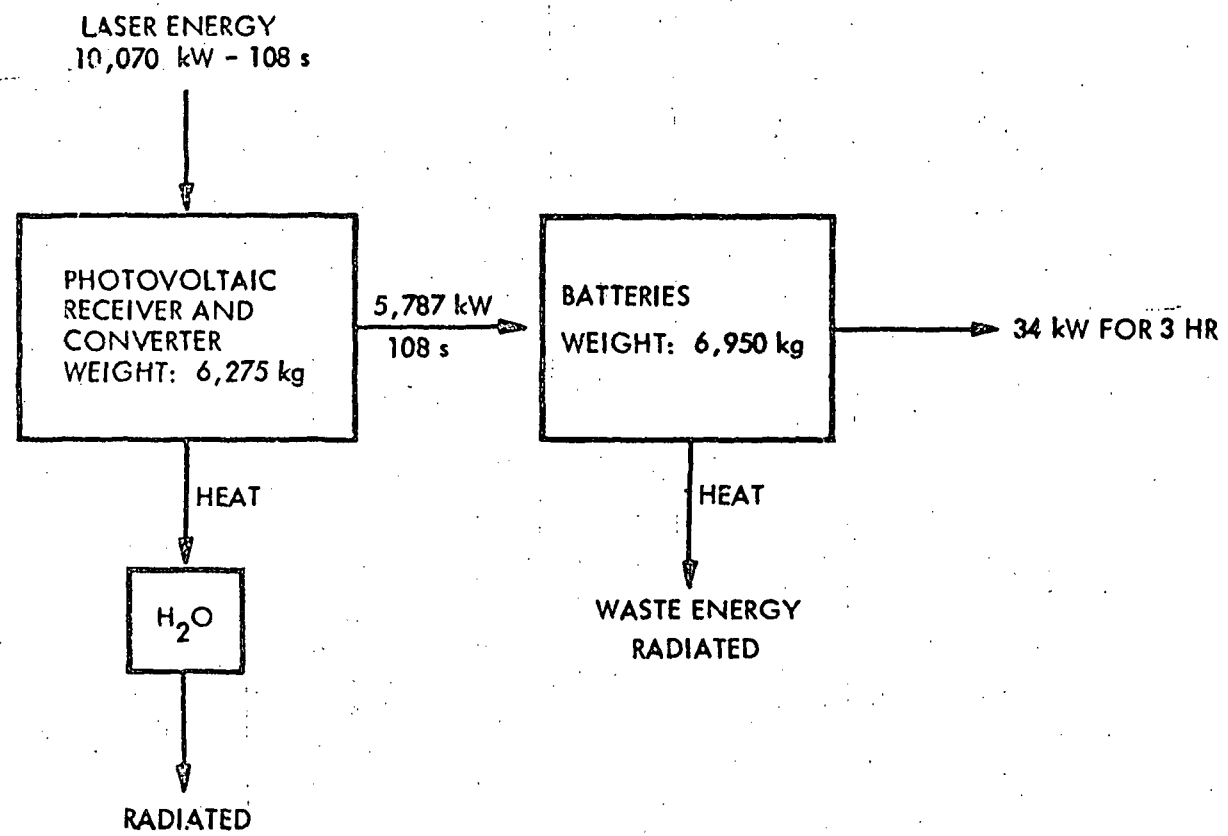

Figure 49. Photovoltaic (receiver-converter)/batteries

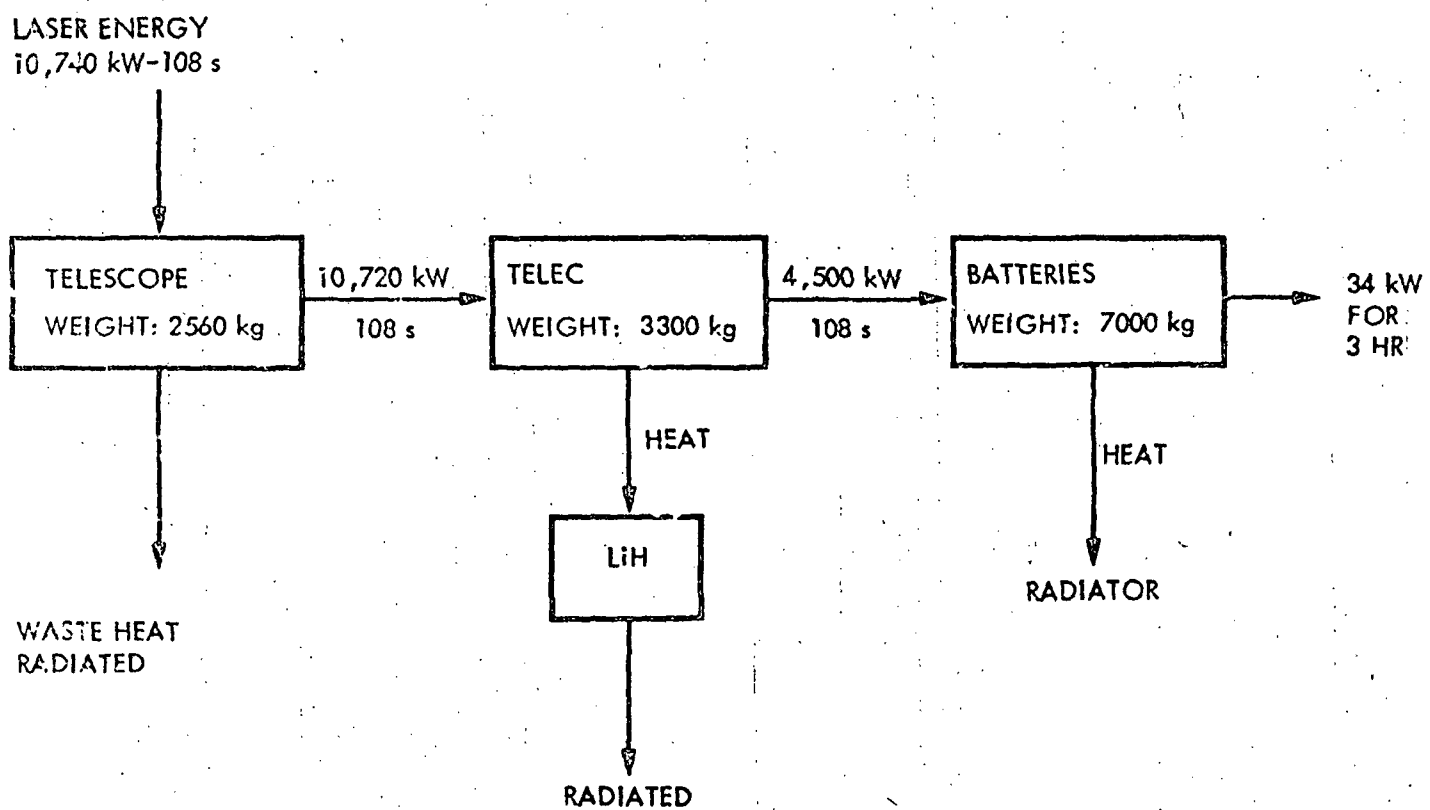

Figure 50. Telescope/TELEC/batteries

TABLE X. REAL-TIME CONVERSION TO ELECTRICAL ENERGY PLUS BOTTOMING CYCLE WITH DELAYED CONVERSION

RECEIVER	TOPPING CONVERTER	TOPPING ENERGY STORAGE	RESIDUAL ENERGY STORAGE	BOTTOMING CONVERTER	BOTTOMING ENERGY STORAGE	WASTE HEAT DISPOSITION
PHOTOVOLTAIC	PHOTOVOLTAIC	BATTERIES (OR INDUCTION)	H_2O	STEAM ENGINE/ GENERATOR	NONE	RADIATORS
THERMIONIC HEAT EXCHANGER	THERMIONIC	BATTERIES (OR INDUCTION)	LiH	BRAYTON, RANKINE, OR PISTON	NONE	RADIATORS
TELESCOPE	TELEC	BATTERIES (OR INDUCTION)	LiH	BRAYTON, RANKINE, OR PISTON	NONE	RADIATOR

Topping: Photovoltaic/Bottoming: Rankine

It was concluded that this system should be eliminated from the evaluation since the water temperature was too low to produce an efficient system.

Topping: Thermionic/Batteries/Bottoming: Brayton/Generator

This concept resulted in a substantial portion of the power being generated in the bottoming cycle because of the low efficiency of the thermionic cycle. The evaluation results are presented in Figure 51. The required laser input was 11,400 kW for 108 s. This system was the least efficient evaluated, but the weight was moderate at 4,294 kg.

Topping: TELEC/Batteries/Bottoming: Brayton/Generator

Since the TELEC device is relatively efficient, the major portion of the power is produced from this. The evaluation results are shown in Figure 52. The required laser energy input is 7610 kW for 108 s (821,380 kJ), making this a relatively efficient system. However, the system weight is 9777 kg.

3.2.5.3 Evaluation of Energy Storage With Delayed Conversion

As discussed in previous sections, the storage of the laser energy as heat, with conversion to electrical energy upon demand, appears to be one of the more viable approaches. In these evaluations, the same requirements for power and irradiation time were employed as for the previous evaluations (34 kW for 3 hr, 108 s of laser irradiation). The potential approaches are presented in Table XI. The difference between the two systems is that the addition of an energy exchanger allows the use of higher temperature gas in the thermodynamic cycles and also results in potentially more efficient cycles.

Receiver (Heat Storage)/Brayton Cycle/Generator

The previous discussions regarding the Brayton cycle indicated that the maximum turbine inlet temperature allowed by material limitations is approximately 1400 K. The most likely material for use with this maximum temperature is silicon, which melts at 1700 K and would provide a good temperature differential for heat transfer to the working gas. If the turbine inlet temperature is lower, in the range of 1100 K, then lithium fluoride is a possible heat storage material.

The results of the evaluation are summarized in Figure 53. The required laser input is 9930 kW for 108 s. The basic weight of the system if 2,660 kg.

Receiver (Heat Storage)/Energy Exchanger/Brayton/Generator

The cycle which was assumed for the analyses is that presented in a previous section in Figure 42, with the energy exchanger temperature lowered to 2100 K. The heat storage at this high temperature is accomplished in a mixture of beryllium oxide and

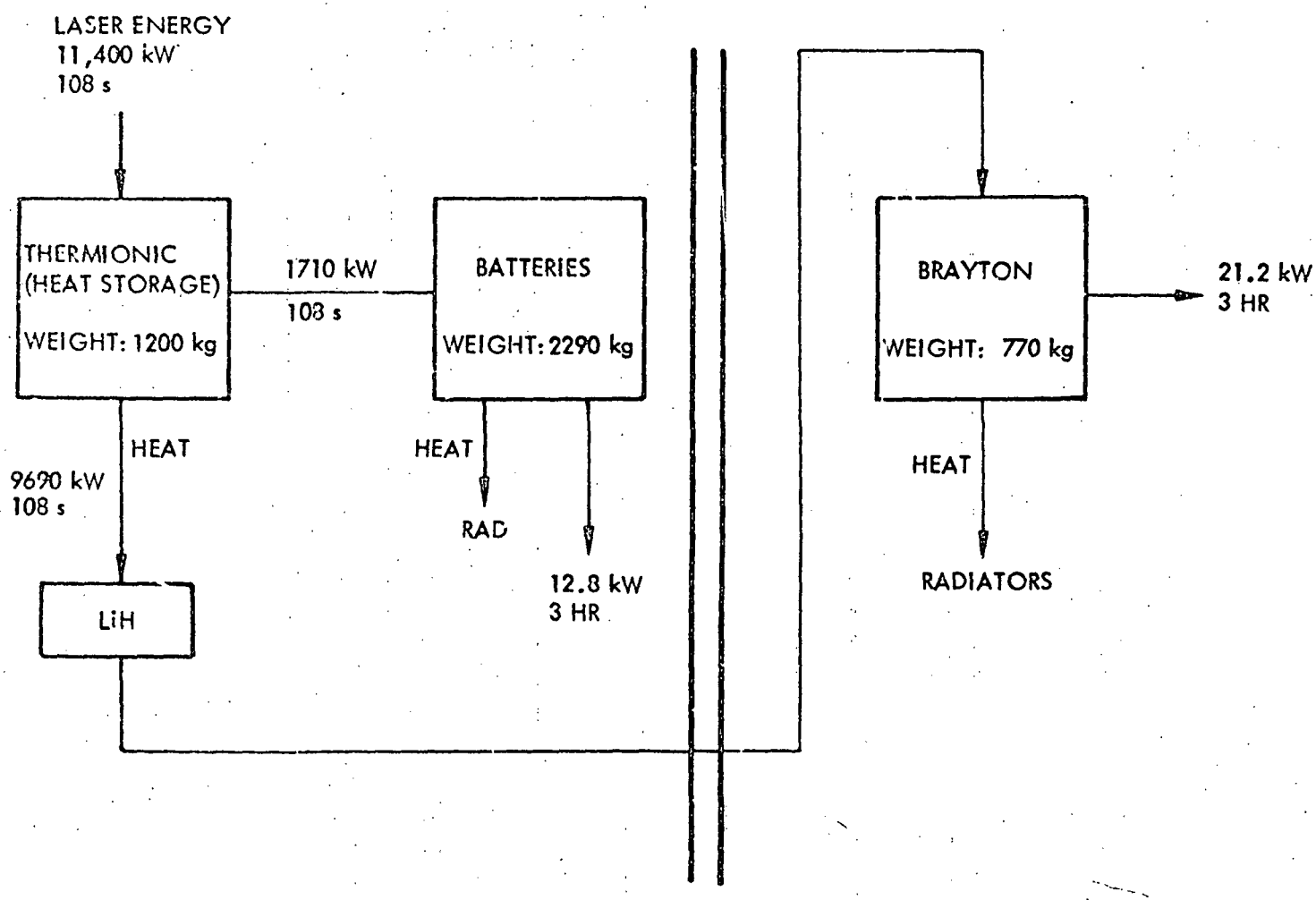

Figure 51. Topping: thermionic/batteries/bottoming: Brayton/generator

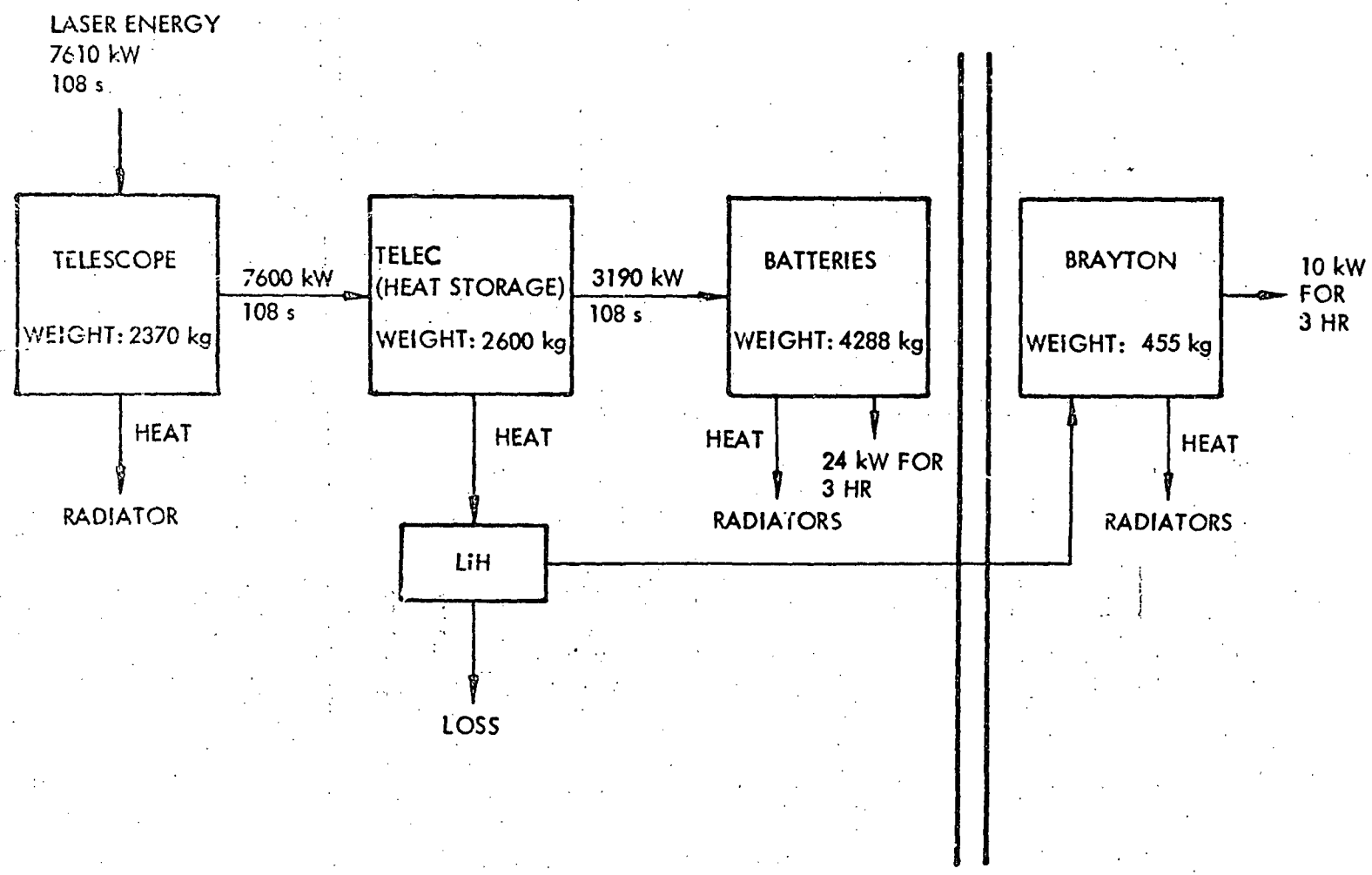

Figure 52. TELEC/batteries/bottoming: Brayton/generator

TABLE XI. ENERGY STORAGE WITH DELAYED CONVERSION

RECEIVER	ENERGY STORAGE	CONVERTER	ENERGY STORAGE
HEAT EX-CHANGER	SILICON (LiF) FUSION	BRAYTON, RANKINE, OR PISTON	DIRECT USE (LIMITED BATTERY)
HEAT EX-CHANGER	BeO + MgO FUSION	ENERGY EXCHANGER PLUS BRAYTON, RANKINE, OR PISTON	DIRECT USE (LIMITED BATTERY)

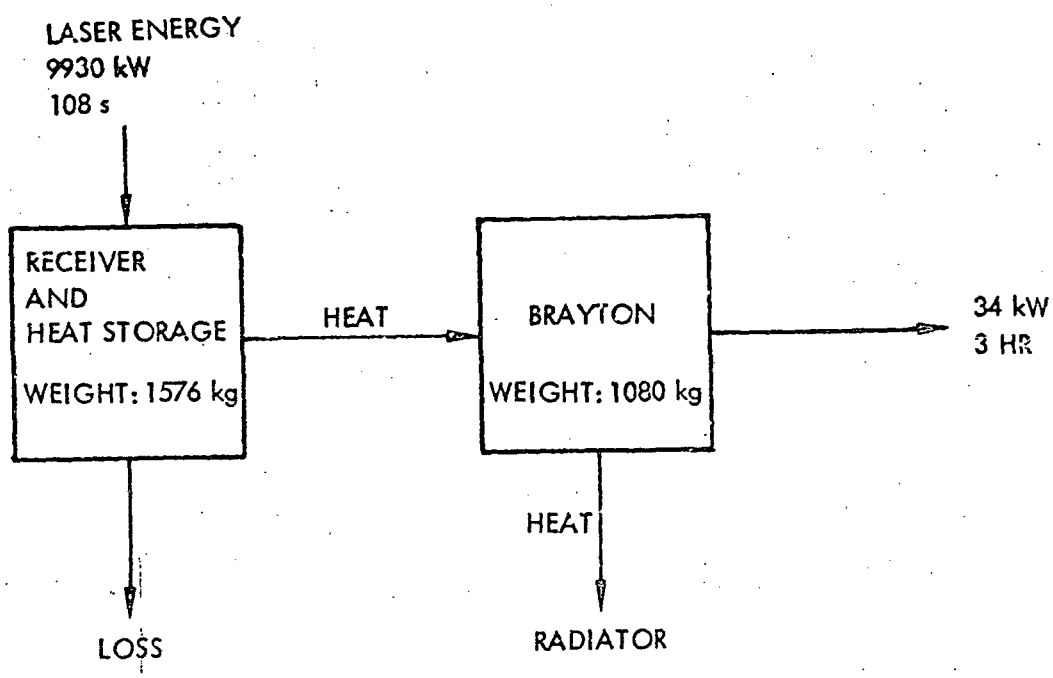

Figure 53. Receiver (heat storage)/Brayton/supply

magnesium oxide, which melts in the range from 2100 to 2200 K. Because of the high temperatures and the efficiency of the energy exchanger, this is the most efficient system evaluated. The required laser input energy is 6800 kW for 108 s (734,400 kJ). The system is illustrated in Figure 54.

3.2.5.4 Summary of Power Conversion System Evaluations

The results of the power conversion system evaluations are summarized in Table XII. The results indicate the following conclusions:

- The real-time conversion systems appear to be the least desirable. Their heavy weights result principally from the requirement to store the generated electrical energy rapidly.
- The systems involving real-time conversion plus a bottoming cycle for delayed conversion are in the moderate range with regard to weight. The system involving the TELEC device has a relatively high overall efficiency, but a rather high weight. The thermionic device with a bottoming cycle has a low overall conversion efficiency.
- The conversion systems which store all the laser energy as heat and then convert this to electrical power at the demand rate present the best approaches. The system which includes an energy exchanger has the highest efficiency.

3.2.6 System Effects

To determine the system effects and synthesize concepts toward optimization, the previous subsystem analyses must be evaluated relative to the impact that one subsystem or variation thereof may have on other subsystems. The Laser Power Conversion System Analysis is ultimately seeking feasible systems that can replace current satellite electrical power subsystems so that a more efficient and cost-effective system can replace the expensive and inefficient solar array electrical power subsystems used on today's satellites. To establish a baseline from which the new concepts could be compared, an existing computer program was exercised to provide details of the mission satellites established in Task I. Table XIII gives the satellite dimensions, average power, and electrical power subsystem (EPS) weights. Various costs are also shown for later comparison with the new concepts. Figure 55 graphically shows the EPS weights for satellites designed for a 5-year life at synchronous equatorial orbit where the time in shadow (t_s) is equal 5%. This set of curves is for the newer, lightweight, flexible solar arrays. With these data, new laser power conversion systems can be evaluated.

The operation of the laser power conversion concepts differs from the conventional solar array EPS regardless of the energy conversion technique or the type of receiver used. The solar array generates electrical power during the major portion of each satellite orbit ranging from about 66% to 100% of the orbit period depending upon the orbital parameters. For the laser power conversion concepts to operate for similar periods during each orbit, almost one laser would be required for each satellite, i.e., two lasers could handle three satellites for those missions charging 66% of the time with the ratio reaching 1 to 1 for satellites in sun synchronous and synchronous equatorial

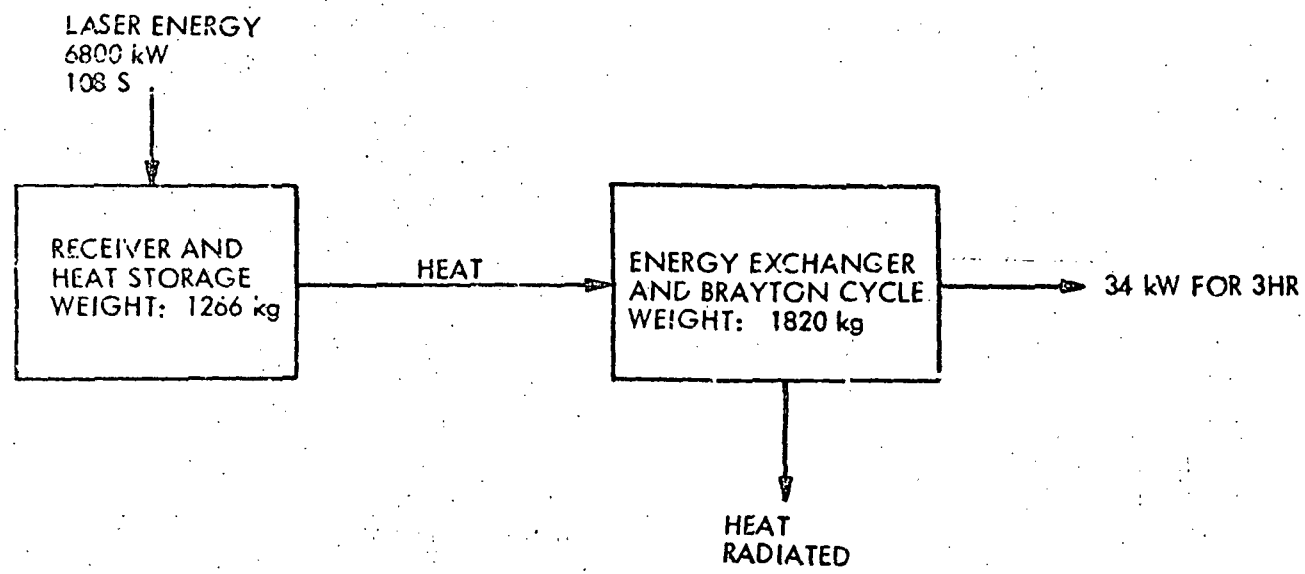

Figure 54. Receiver (heat storage)/energy exchanger/Brayton/supply

TABLE XII. SUMMARY OF POWER CONVERSION SYSTEM EVALUATIONS

34 kW – 3 hr
(Irradiated – 0.03 hr)

System	Weight (kg)	Absorbed Laser Energy (kW-hr)	Conversion Efficiency (%)
Photovoltaic (Receiver and Conversion)/Batteries	13,225 (+115)	300	34.0
Telescope/Telec/Batteries	12,860 (+90)	322	31.7
Telescope/Telec/Batteries/Brayton/Generator	9,713 (+64)	228	44.7
Thermionic/Batteries/Brayton Generator	4,260 (+34)	342	29.8
Receiver (Heat Storage)/Brayton/Generator	2,660	298	34.3
Receiver/Energy Exch./Brayton/Generator	3,080	208	49.0

TABLE XIII. LPCS – CONVENTIONAL POWER SPACECRAFT (FY '77$)

MISSION	SAT. WEIGHT (LB)	SAT. LENGTH (FT)	AVE. POWER (kW)	S/C UNIT ($M)	S/C R&D ($M)	S/C L.O. ($M)	EPS WEIGHT (LB)	EPS UNIT ($M)	EPS R&D ($M)
1 ANT. FARM	13,300	8.6	34.0	72.3	69.4	9.0	4,300	38.9	15.0
2 PERS. COMM	10,700	8.1	20.7	52.8	59.3	6.9	2,900	26.8	11.6
3 TV BROADC'T.	27,300	18.5	148.0	204.2	123.6	22.1	13,500	122.6	32.3
4 HOT LINE	2,000	5.9	0.9	12.1	24.3	1.9	340	3.3	2.7
5 EO/WEATHER (SM)	3,400	7.0	1.7	28.4	49.3	4.0	520	4.9	3.6
6 EO/WEATHER (BIG)	10,200	8.8	1.8	33.2	58.3	4.6	520	5.0	3.6
7 EL. MAIL	12,400	8.9	15.2	58.3	78.6	7.6	2,350	21.4	10.0
8 COAST RADAR	124,200	168.0	295.6	433.6	307.8	42.3	23,700	214.4	47.0
9 ASTRONOMY	11,000	11.0	14.9	50.5	69.1	6.6	3,700*	21.4	8.8
10 ENERGY MON.	10,600	8.0	22.7	60.8	72.6	7.7	3,600	25.6	10.9
11 SPACE PROCED.	22,900	20.4	34.2	96.8	102.6	11.6	5,900	47.8	15.8
12 ATMOSPHERE	5,700	8.0	4.0	29.3	40.8	4.1	2,400	12.0	6.9
13 SOLAR OBS.	30,900	24.3	48.6	141.9	124.8	16.1	11,900*	73.2	18.1
14 EOS (BIG)	81,400	87.9	48.8	207.0	205.0	22.3	22,300*	88.9	26.5
15 EOS (SMALL)	4,300	8.0	1.7	25.3	42.5	3.6	1,450*	7.3	4.5
16 OCEAN (SMALL)	3,600	8.6	1.2	21.7	40.1	3.2	930	5.2	3.7
17 OCEAN (BIG)	53,200	56.2	5.3	72.4	118.4	8.0	2,970	14.6	7.9
18 TRANSP/NV.	5,800	5.6	6.0	35.6	50.5	4.9	1,940*	11.5	5.8
19 WEATHER	3,800	5.4	1.8	26.1	43.9	3.7	930*	5.9	3.6
20 DOD (SMALL)	5,200	7.1	5.0	41.8	65.3	5.6	1,670*	9.9	5.2
21 DOD (BIG)	50,200	40.7	197.3	300.1	189.5	30.8	29,000*	164.7	33.9

*RIGID ARRAYS

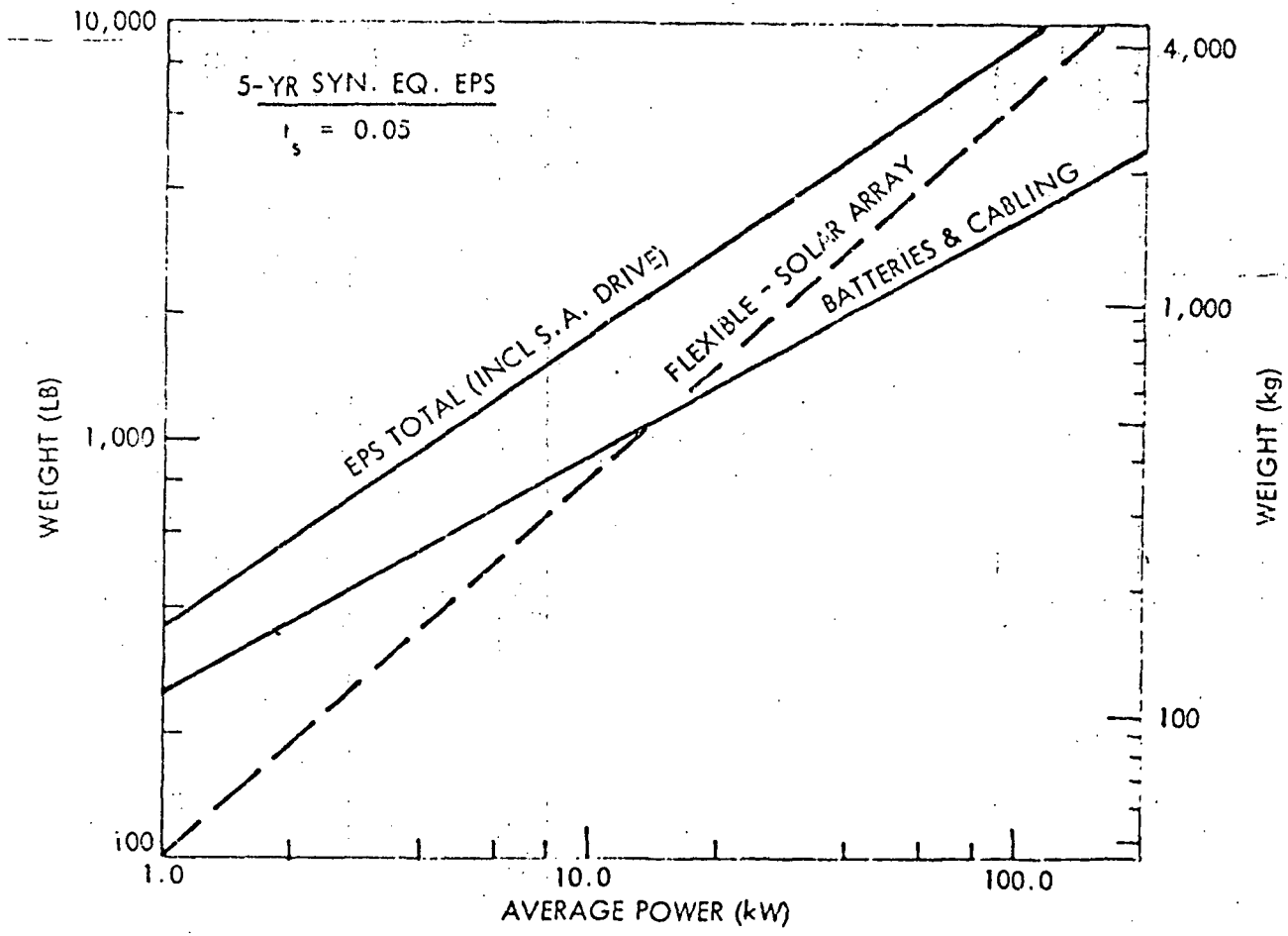

Figure 55. Solar Array Weights

orbits. Obviously, it would not be cost effective to put up a completely new laser satellite to provide electrical power for each mission satellite, particularly when one considers that the mission satellite EPS is not being eliminated but replaced with another system which may require a higher technology level. Table XIV shows some of the operating requirements for typical low-earth orbit mission satellites. For example, the space processing mission has transfer opportunities every 2.67 hr with a minimum transfer time of 0.63 hr (Figure 6). If the entire viewing time were used to recharge the energy storage system, only four satellites could be serviced with one laser. Table XIV evaluates the new EPS relative to the number of satellites (5, 10, 25, 50, and 100) serviced by one laser. Again refering to the space processing mission that has an average power requirement of 34.2 kW, if the entire mission model (~ 100 satellites) is to be serviced by one laser, then only 0.0267 hr can be spent in recharging the energy storage subsystem. Considering the losses in transmission, conversion, and storage, a laser power of 12,795 kW would be required. If the laser operates at 20% efficiency, then an electrical power subsystem of almost 64 MW would be required to drive the laser. However, the laser would not have sufficient power to service a satellite with a higher average power requirement as may be noted in Mission 13, Solar Observation, in Table XIV. In fact, a laser power of more than 110 MW would be required to service Mission 8, Coast Radar, (Table XIII) requiring 295.6 kW in the 0.0267-hr time period.

The laser power conversion concept operations also significantly effect the energy storage subsystem and the receiver. Because the mission satellite is operating a majority of the time on stored energy, the energy storage subsystem has to have a significantly larger capacity which can also be noted in Table XIV. The battery weights shown in Table XIV are for NiCd batteries and can be reduced by a factor of 3 if regenative fuel cells are used; however, the energy storage weight is still 66% of weight of the total electrical power subsystem it is replacing. The receiver weights shown in Table XIV are based on a photovoltaic power conversion system operating at 45% efficiency. The weights are only for the heat storage and radiator to reject the excess heat. The photovoltaic devices, power conditioning, and cabling are not included. Again, because of the laser power conversion concept operations, the energy must be stored in a relatively short period which makes it impractical to reject the excess energy (> 55%) in real time. The weights shown are for storage of the excess energy and radiating it to space during the entire cycle between charges. These weights cannot be reduced significantly and generally exceed the total weight of the electrical power subsystem being replaced.

In summary, even if the additional weights would not significantly affect the satellite's missions capability, transportation costs, and unit costs, the requirement to take to orbit more than two orders of magnitude more electrical power capability than required for all satellites combined cannot be shown to be cost effective. Table XV shows the electrical power required to drive both space-based and ground-based lasers. The number of space-based lasers servicing the mission model does not significantly affect the total electrical power requirements, but could vary the total cost significantly because each additional laser would be a complete space vehicle. The driving mission causing the high total electrical power requirements is the Coast Radar (295.6 kW_e average power), and 85% of the missions require 50 kW_e or less; therefore, Table XVI shows the electrical power requirements for all missions under 50 kW_e, which shows that more than an order of magnitude more electrical power is required for space-based laser systems and two orders of magnitude for ground-based laser systems.

TABLE XIV. TYPICAL MISSIONS

	CIRCULAR ORBIT ALT (km)	CIRCULAR ORBIT INC (°)		AVE PWR (kW)	BASE-LINE EPS WT		4-HR LASER ORBIT (6,395 km) CHG (HR)	CYCLE (HR)	LASER PWR (kW)	BATT WT	REC WT	PWR ON REC (kW)	BATT CAP (kWHr)
11. SPACE PROCESSING	555	28.5	5	34.2	5,900	5	0.0534	2.67	565	11,132	10,7-9	440	209
						10	0.267		1,216	12,523	11,623	946	235
						25	0.107		3,164	13,357	12,116	2,461	250
						50	0.053		6,476	13,638	12,263	5,038	256
						100	0.027		12,795	13,774	12,363	9,954	258
12. ATMOSPHERIC	1,110	90	4	4.0	2,400	5	0.648	3.24	66	1,580	1,547	51	30
						10	0.324		142	1,777	1,663	111	33
						25	0.130		370	1,896	1,733	288	36
						50	0.065		749	1,935	1,757	583	36
						100	0.032		1,532	1,955	1,763	1,192	37
13. SOLAR OBSERVATION	555	55	2	48.16	11,900	5	0.534	2.67	803	15,818	15,340	625	297
						10	0.267		1,728	17,796	16,510	1,345	334
						25	0.107		4,496	18,981	17,211	3,498	356
						50	0.053		9,203	19,381	17,448	7,159	364
						100	0.027		18,182	19,573	17,562	14,145	367
14. EARTH OBSERV (LG)	370	90	4	48.8	22,300	5	0.494	2.47	806	14,694	14,250	627	276
						10	0.247		1,736	16,531	15,337	1,350	310
						25	0.099		4,514	17,631	15,989	3,512	331
						50	0.049		9,246	18,003	16,209	7,193	338
						100	0.025		18,741	18,181	16,314	14,190	341
15. EARTH OBSERV (SM)	1,110	99	4	1.7	1,450	5	0.648	3.24	28	671	666	22	13
						10	0.324		60	755	716	47	14
						25	0.130		157	806	746	122	15
						50	0.065		318	822	756	249	15
						100	0.032		651	831	761	507	16

*ALL WEIGHTS IN POUNDS

TABLE XV. POWER REQUIREMENTS – ALL MISSIONS

(TOTAL SATELLITE POWER = 3,672 kW)

NUMBER OF LASERS	REQUIRED POWER (kW)*			
	SPACE		GROUND**	
	LASER	ELECTRICAL	LASER	ELECTRICAL
1	111,842	559,210	323,482	1,617,411
2	55,548	555,480	160,662	1,606,622
4	27,401	548,020	79,252	1,585,046
10	10,512	525,600	30,404	1,520,200
20	4,884	484,400	14,126	1,412,606

*BASED ON COAST RADAR MISSION (295.6 kW_e AVERAGE POWER)
**EACH GROUND SITE
FOR REFERENCE:
BOULDER DAM = 1,249,800 kW_e
GRAND COULEE DAM = 1,974,000 kW_e

TABLE XVI. POWER REQUIREMENTS: MISSIONS UNDER 50 kW_e

(Total Satellite Power = 1,383 kW_e)

Number of Lasers	Power Required (kW)			
	Space		Ground	
	Laser	Electrical	Laser	Electrical
1	14,686	73,430	42,477	212,383
2	7,282	72,820	21,062	210,620
4	3,579	71,580	10,352	207,040
10	1,363	68,150	3,942	197,100
20	620	62,000	1,795	179,500

3.3 REFERENCES

1 R. J. Stirn, "Overview of Novel Photovoltaic Conversion Techniques at High Intensity Levels," Proceedings of Third NASA Conference on Radiation Energy Conversion, Jan 1978

2 E. J. Britt and C. Yuen, "Thermoelectronic Laser Energy Conversion for Power Transmission in Space," Proceeding of the Third NASA Conference on Radiation Energy Conversion, 1978

3 ----- and -----, "Thermoelectronic Laser Energy Conversion," Monthly Progress Reports 4, 5, and 6, Aug – Oct 1976, NASA Contract NAS 3-20089

4 G. O. Fitzpatrick and E. J. Britt, "Thermionics and Its Application to the SPS," Proceedings of the Third NASA Conference on Radiation Energy Conversion, Jan 1978

5 NASA-SP-731 (1966), Space Power Systems Advanced Technology Conference

6 AIRMC-(2) (Sep 1964), Application of the Brayton Cycle to Nuclear Electric Space Power Systems

7 NASA-TM X-67835 (1971), Status of the 2 to 15 kW_e Brayton Power System and Potential Gains From Component Improvements

8 APL TDR 64-103 (1964), Closed Brayton Cycle Solar Power Unit Research and Development Program

9 NASA TN D-2487 (1964), Summary of Brayton Cycle Analytical Studies For Space Power System Applications

10 IECEC '68 (1968), The Influence of Heat Rejection Radiator Mars in Space Power Systems

11 IECEC 4 (1969), paper 699077, Closed Brayton Cycle Power System Applications

12 Journal of Spacecraft and Rockets, Vol. 1, No. 1 (Jan – Feb 1964), Thermodynamic Characteristics of Baryton Cycles For Space Power

13 NASA-TN D-2968 (1965), Thermodynamic and Turbomachinery Concepts for Radioisotope and Reactor Brayton Cycle Space Power Systems

14 NASA-TN D-5815 (1970), Effect of Operating Parameters on Net Power Output of a 2 to 10 kW Brayton Rotating Unit

15 NASA TM X-67846 (1971), Performance of a Brayton Cycle Power Conversion Unit Using Helium-Xenon Gas Mixture

16 NASA CR-133810 (1973), Preliminary Design of a Mini-Brayton Compressor Alternator Turbine

17 NASA TM-X-52824 (1970), Performance of the Electrically Heated 2 to 15 kW_e Brayton Power System

18 IECEC 10, Paper No. 759161 (Aug 1975), Space Power Application of the All Purpose Mini Brayton Rotating Unit (Mini-BRU)

19 AiResearch Div. of Garret Corp. — Brochures on Mini-BRU

20 Space Power Systems Engineering, Vol. 16, by Szego and Taylor, "Progress in Astronautics and Aeronautics"

21 IECEC '68 (1968), Paper 689053, The Organic Rankine Cycle

22 IECEC 4, Paper 699052 (1969), An Organic Rankine Cycle For Manned Space Applications

23 APL-TR-64-156 (1965), Investigation of a 15 kW_e Solar Dynamic Power System For Space Applications

24 IECEC 4, Paper 699003 (1969), Jet Condenser For An Organic Rankine Cycle Power Conversion System

25 NASA-TM X-1919 (1969), Study of a 300-Kilowatt Rankine Cycle Advanced Nuclear Electric Space Power System

26 NASA-CR-54334 (1965), Parametric Study of Large Rankine Cycle Nuclear Space Powerplants

27 Journal of Engineering for Power, Vol. 89, April 1967, "The Energy Exchanger, a New Concept for High Efficiency Gas Turbine Cycles

28 3rd NASA Conference on Radiation Energy Conversion (Jan 1978), Paper by Taussig et al., Energy Exchanger Technology Applied to Laser Heated Engines

29 3rd NASA Conference on Radiation Energy Conversion (Jan 1978), Paper by Taussig et al., Study, Optimization, and Design of a Laser Heated Engine

30 IECEC-4, Paper 699081 (Sep 1969), The Radioisotope Energized Stirling Engine For Spacecraft Auxiliary Electric Power in the 250 to 500 W_e Power Range

31 IECEC-8, Paper 739-35 (Aug 1973), Stirling Engine Design Studies of an Underwater Power System and a Total Energy System

32 IECEC-11, Paper 769257 (Sep 1976), The Stirling Engine — Engineering Considerations In View of Future Needs

Section 4

CONCLUSIONS

Orbit-to-orbit Laser Power Conversion Systems for supplying energy to satellites is not competitive with current satellite electrical power subsystems from either technological or economical standpoints.